INTEGRATED RESERVOIR CHARACTERIZATION AND MODELING

Mickaele Le Ravalec
Brigitte Doligez
Olivier Lerat

Chapter 5

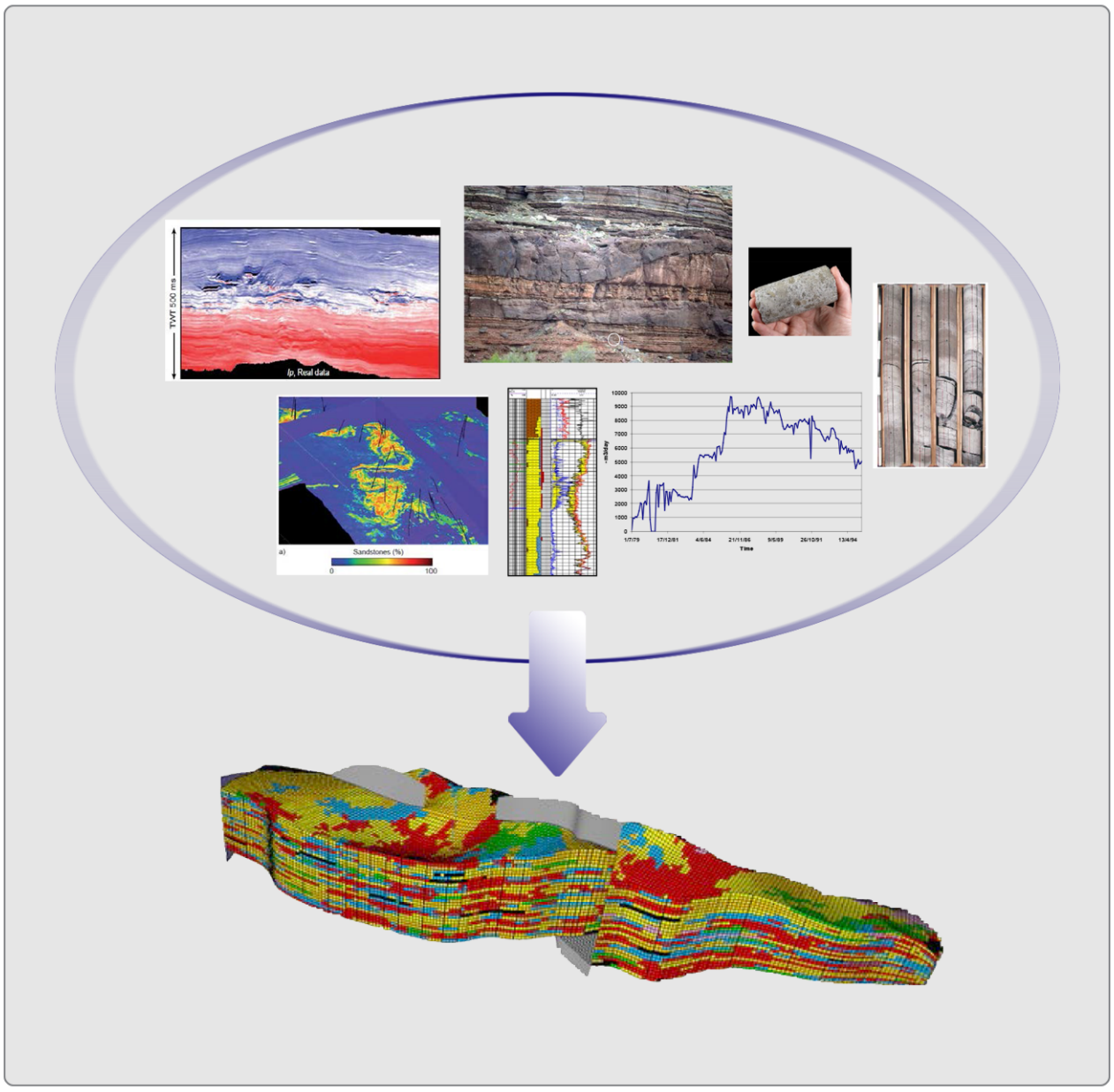

ISBN: 2-901638-15-5
EAN: 9782901638155

Book DOI: 10.2516/ifpen/2014001
Chapter 5 DOI: 10.2516/ifpen/2014001.c005

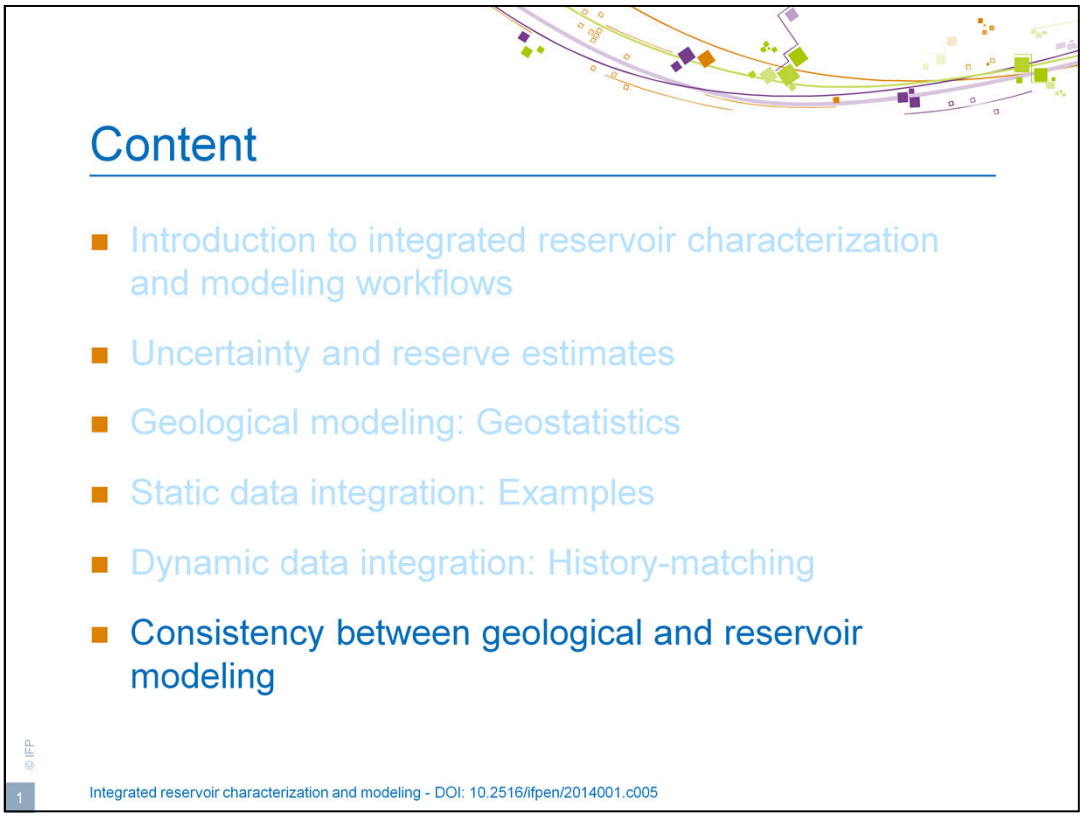

The previous chapter pointed out that sampling techniques based upon metamodels is a promising approach to estimate posterior probability density functions. This, of course, depends on the quality of the metamodels. In other words, such an approach can be used when the problem is not too non linear or irregular and when the number of parameters is small (usually less than a dozen).

However, history-matching problems are very complex with a very significant number of parameters. For instance, the petrophysical properties populating the geological model are very important parameters in terms of fluid displacement: they strongly influence the efficiency of sweeping or production. Unfortunately, there is only little information to describe how they spatially vary. If the reservoir model is built over a grid with millions of grid blocks, there are millions of unknown petrophysical values. These parameters are named stochastic parameters as they are generated from random draws. As explained in Chapter 2, the petrophysical properties that populate the reservoir model are realizations of random functions. They are specific parameters because of two essential features. They include a huge number of unknown values and they have a spatial structure.

This chapter focuses on the way to handle these very special type of parameters.

It is also worth mentioning that gradient-based optimization techniques are usually preferred to sampling techniques when dealing with these parameters.

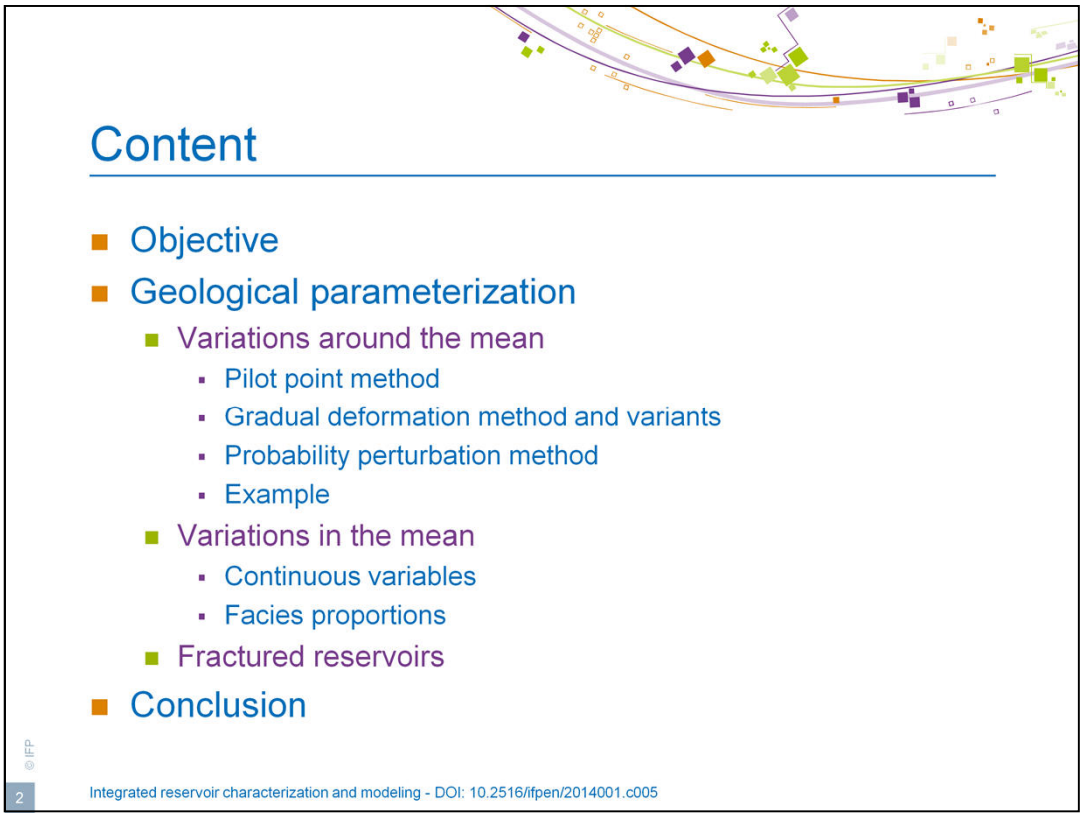

Distinct parameterization (or re-parameterization) techniques are introduced. They are distinguished depending on the way they impact petrophysical properties.

The list is clearly not exhaustive.

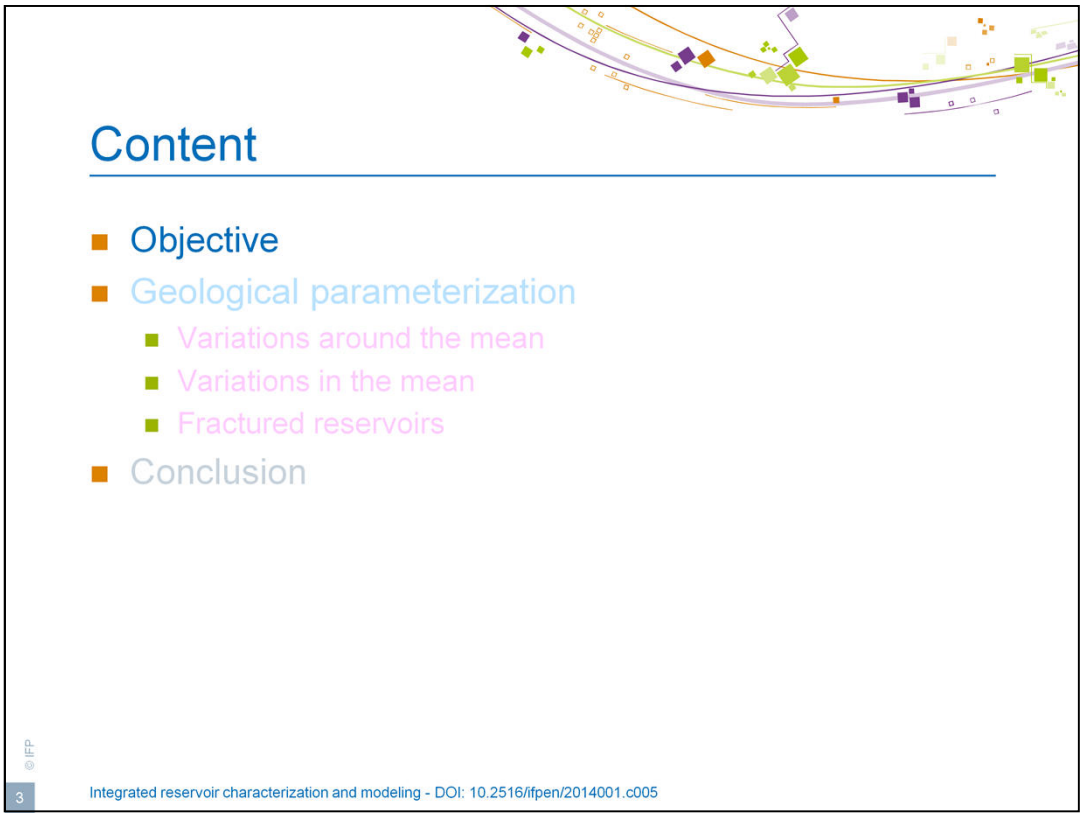

This chapter puts forward the two following questions. Why are we interested in petrophysical properties? How do we handle the uncertainties in their spatial distributions?

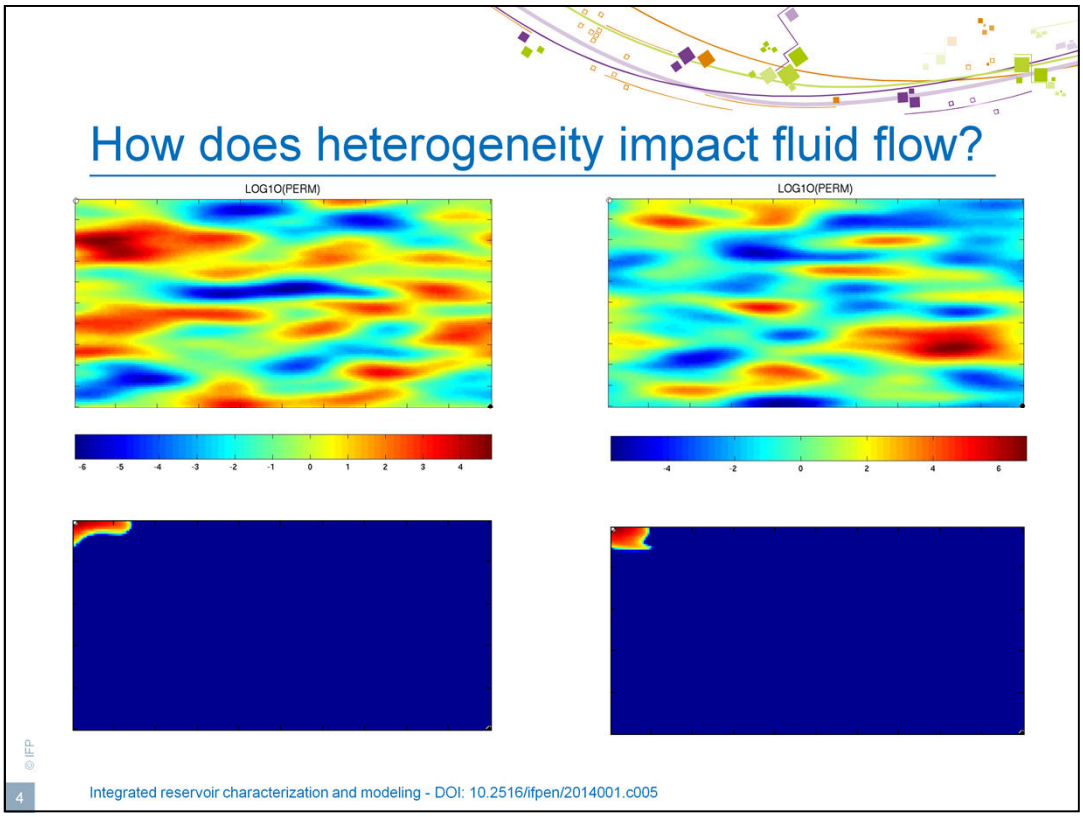

Permeability is one of the most heterogeneous and influential transport properties. High permeability regions form preferential flow paths, while low permeability regions form barriers to flow.

The two examples above stress the influence of permeability heterogeneity on fluid flow. The reservoir is assumed to be initially saturated with oil. The corresponding model is a horizontal grid populated by permeability values randomly drawn from the same random function. For simplicity, porosity is considered to be 0.20 everywhere. Water is injected into the reservoir (vertical injector at the top left corner, the well is perpendicular to the viewed cross-section) to displace oil towards the producer (vertical well at bottom right corner). The two log-permeability realizations shown above are characterized by the same mean, variance and variogram. The only difference is the seed used to initiate the generation process. The logarithm of permeability is displayed in the top raw. Permeability varies the same way, but the high/low values are not found in the same regions. The evolution of water saturation within the reservoir is shown in the bottom raw as a function of time. As expected, the way water moves into the reservoir strongly depends on permeability heterogeneity. At the end, the swept areas are not the same. This induces distinct volumes of oil produced and distinct breakthrough times.

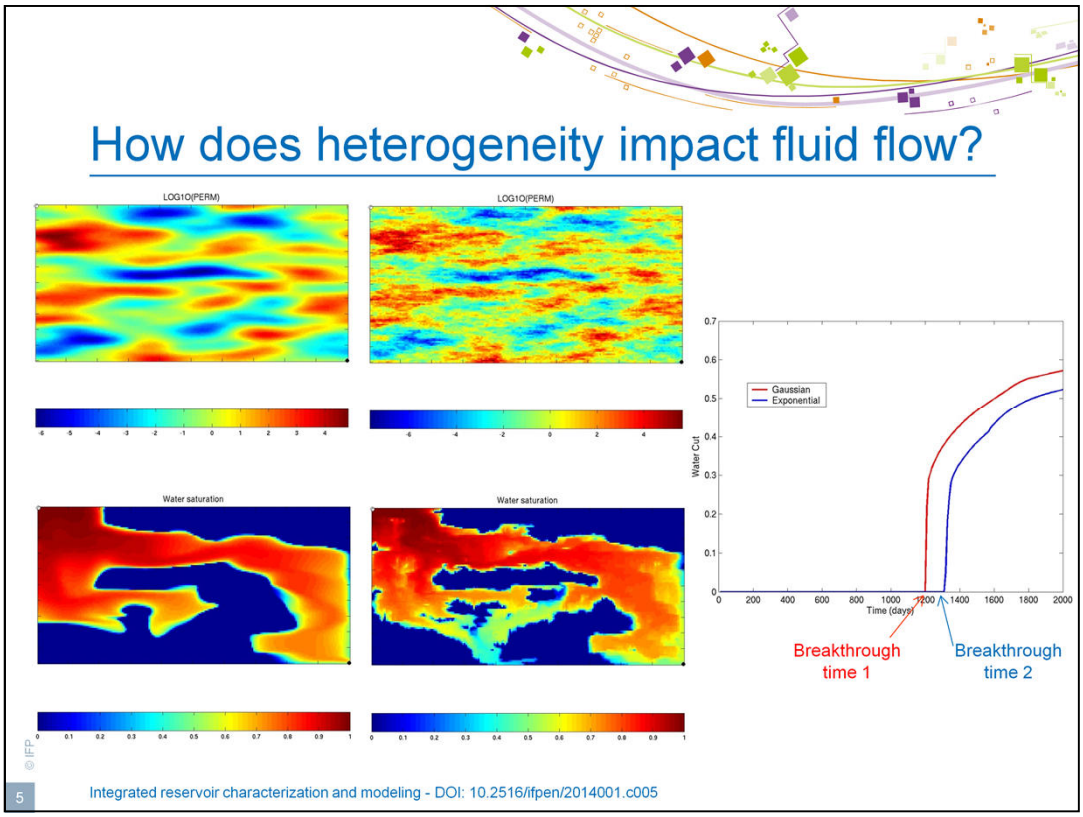

In the example presented in the previous page, we considered two realizations of the same random functions (same means, variances, variograms). The variogram is now considered as uncertain: it can be a Gaussian or an exponential variogram. The other parameters involved in the definition of the variogram are identical. In addition, the seed used to initiate the generation process is kept constant. Therefore, we obtain two permeability realizations with distinct smoothness (top raw). However, as the seed is unchanged, the high/low permeability values are located in the same regions.

Again, the reservoir model corresponds to a horizontal grid with a water injector in the top left corner and a producer in the bottom right corner. The reservoir is assumed to be initially saturated with oil and water is injected to favor the displacement of oil towards the producer.

Water saturation in the entire reservoir is displayed after 2000 days of injection for the two realizations (bottom raw). The swept areas are different. The plot on the right shows the corresponding simulated water cuts. The difference in the variogram type induces a difference in the breakthrough times of about 100 days.

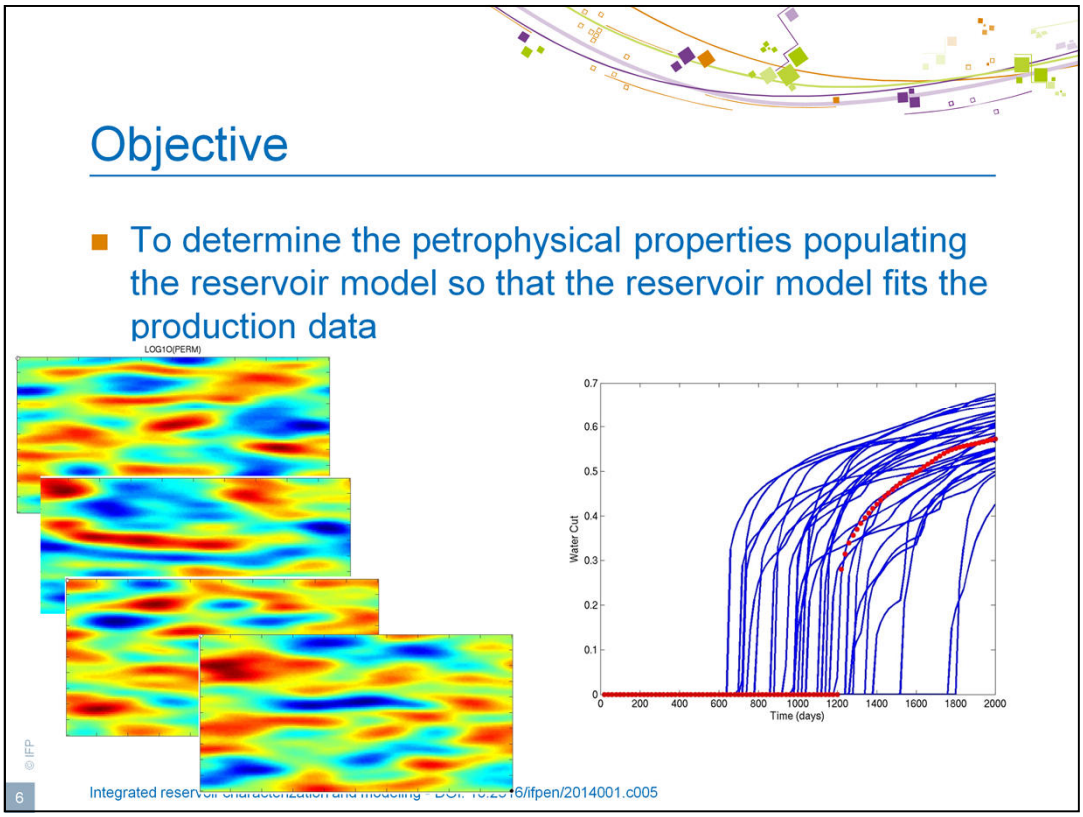

We consider the same production scheme as the one described on the previous page. The reservoir model is again a horizontal grid.

We assume that the mean, variance and variogram characterizing the log-permeability field are known. In addition, the water cut measured in the producer during oil production is known (red dots on the right plot).

The mean, variance and variogram are used to define a random function. Many realizations (see examples on the left) can then be randomly drawn that all respect the mean, variance and variogram. If considering static information solely, these realizations are equally likely representations of the reservoir. Flow simulation can be performed for a given number of these realizations to compute the output water cuts. The results are reported in blue on the right plot. We check that none of them reproduces the water cut data. We can also note the large dispersion in the simulated water cuts.

The problem to face is the conditioning to the measured water cut. These data are not linearly related to the log-permeability field and cannot be integrated through kriging or related techniques.

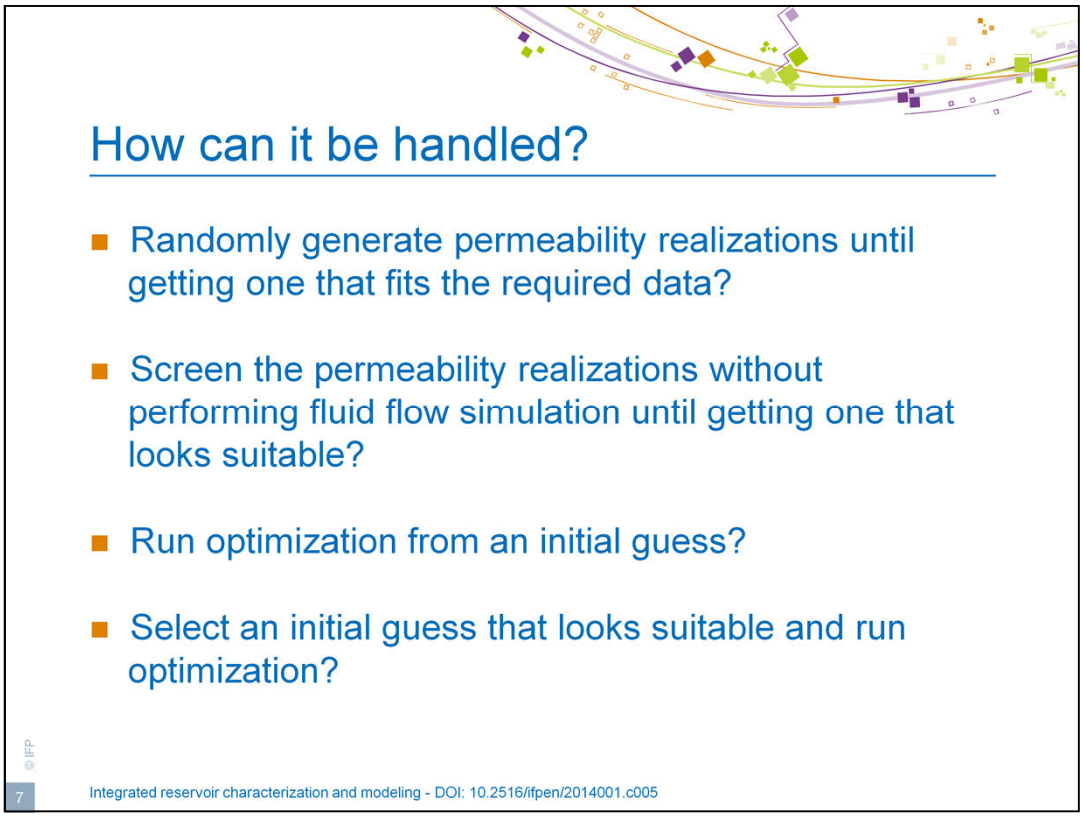

Different approaches can be envisioned to determine a permeability realization (or several) that replicates the dynamic data.

A first possibility consists in randomly generating permeability realizations, then in simulating fluid flow for each of them to see whether they reproduce or not the required data. The process is repeated until identifying a suitable permeability realization.

The second approach is pretty close. The idea behind is still to screen the permeability realization space, but without performing any fluid flow simulation to check the suitability of the realizations. This strongly depends on the definition of a meaningful criterion to characterize the dynamic behavior of permeability realizations without running flow simulations. The reason for avoiding/limiting flow simulations is their huge computational overburden.

We may also randomly generate a starting permeability realization and run an optimization process aiming to minimize an objective function by adjusting the permeability realization.

The last option combines both smart screening and optimization. You can first screen the permeability realization space from a given criterion that does not call for flow simulation. This yields a good starting realization that is adjusted in a second step to minimize the objective function.

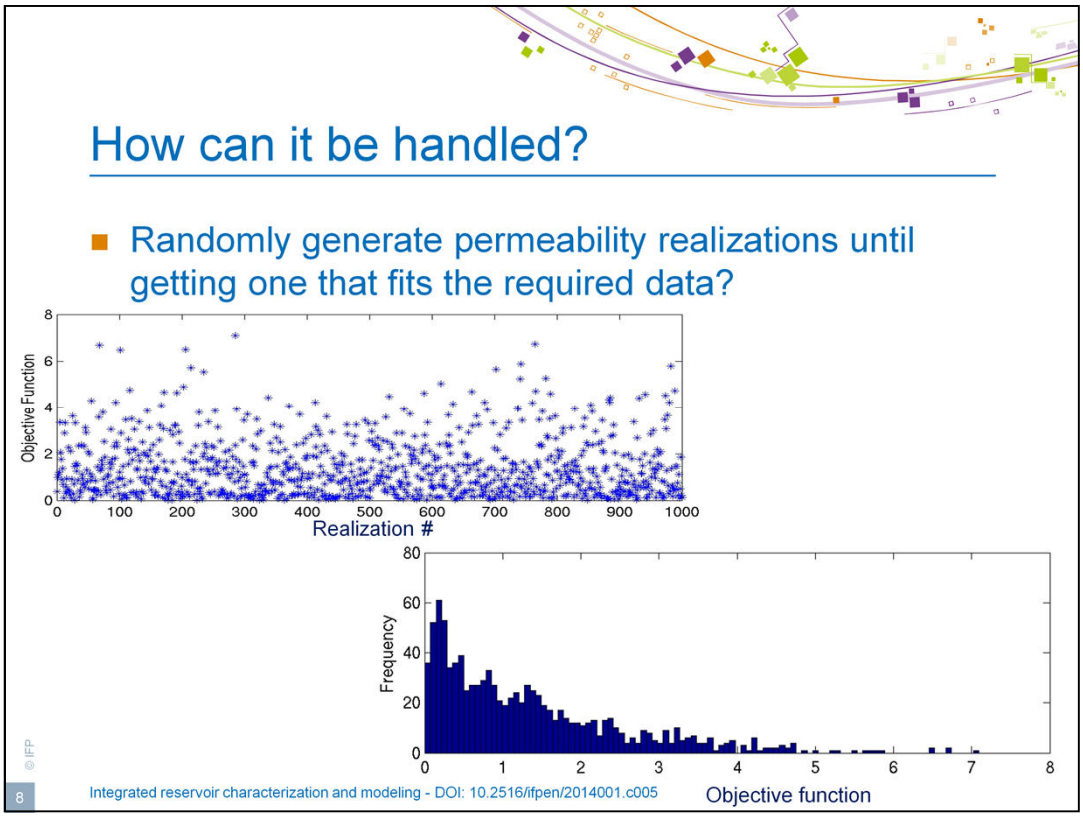

We investigate the first option. The problem under consideration is still the same as before: identify a permeability realization that makes it possible to retrieve the reference water cut measured in the producer. Of course, this is just a toy problem with a single set of data measured in a single well and we may assume that getting an appropriate permeability realization is not too difficult.

We take a random sample of 1000 realizations and simulate fluid flow for all of them. The resulting simulated water cuts are then compared to the reference one through the definition of an objective function.

The two plots above display the objective function value for every realizations as well as the corresponding histogram. A zero objective function means a perfect match. In practice, the perfect match is out of reach due to the complexity of the problem, the uncertainty in the data, in the modeling. However, for this toy problem, we may hope to identify suitable permeability realizations. 35 realizations over the sample of 1000 actually yield a satisfactory match. They provide very small objective function values (although slightly different from zero).

If considering a more realistic case, the chance of generating at random a permeability realization consistent with the production data is very close to zero. In addition, you must perform flow simulation any time you want to see whether a realization is acceptable or not. In other words, random sampling is not the solution.

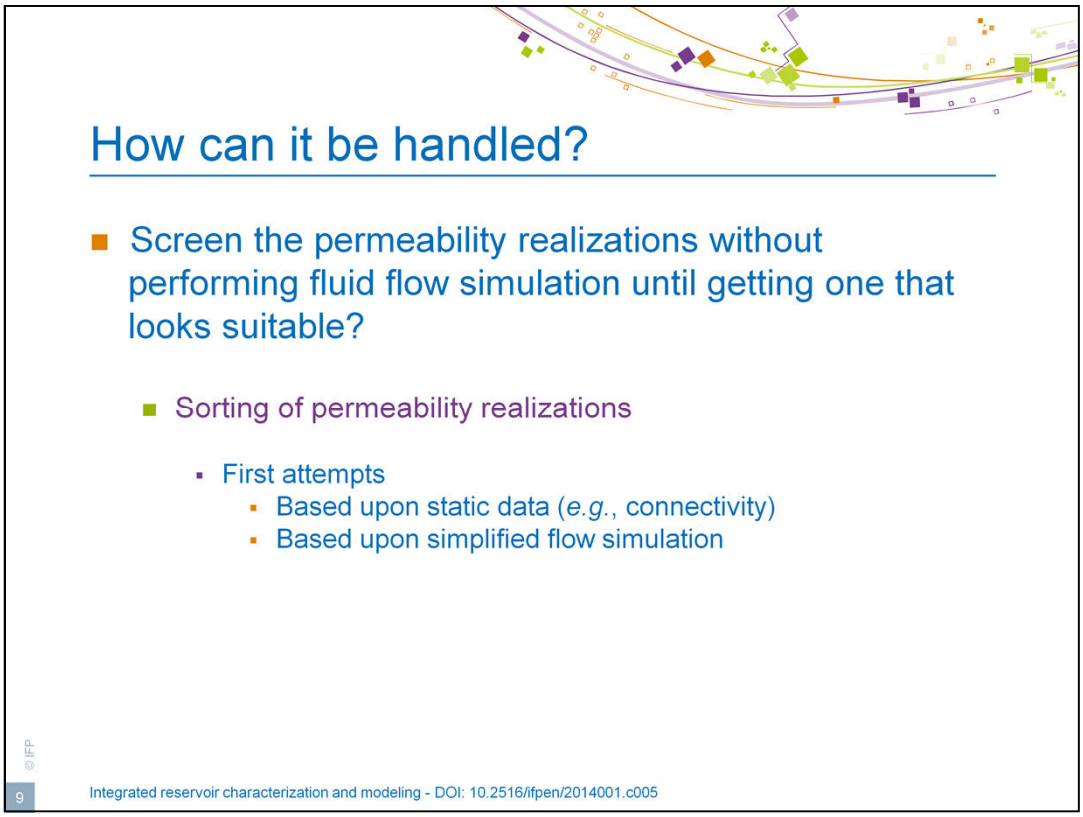

Geostatistical simulation techniques yield an infinite number of equiprobable realizations. In practice, estimating oil recovery for so many realizations is just infeasible: there is no way to perform a flow simulation for all of them.

Different ideas have been envisioned to screen and sort the permeability realizations without calling for flow simulation. A first possibility consists in identifying the ones that lead to extreme production behaviors. Budding *et al.* (1988) and Galli *et al*. (1990) proposed to proceed using connectivity analysis. Their approaches were simple and restricted to the analysis of static properties. Therefore, they were not able to properly capture the dynamic behaviors of the permeability realizations. Guerillot and Morelon (1992) referred to simplified flow simulations to evaluate the dynamic differences between permeability realizations: the pressure field, calculated assuming single phase flow, was assumed to be constant in time and was not updated at each time step. The multiphase character of flow was reflected by the saturation equation. This simplified flow simulation requires less computation time than the full-physics one and was run for every generated realizations. Based on these results, Guérillot and Morelon (1992) selected a few permeability realizations for which the full-physics flow simulations were performed.

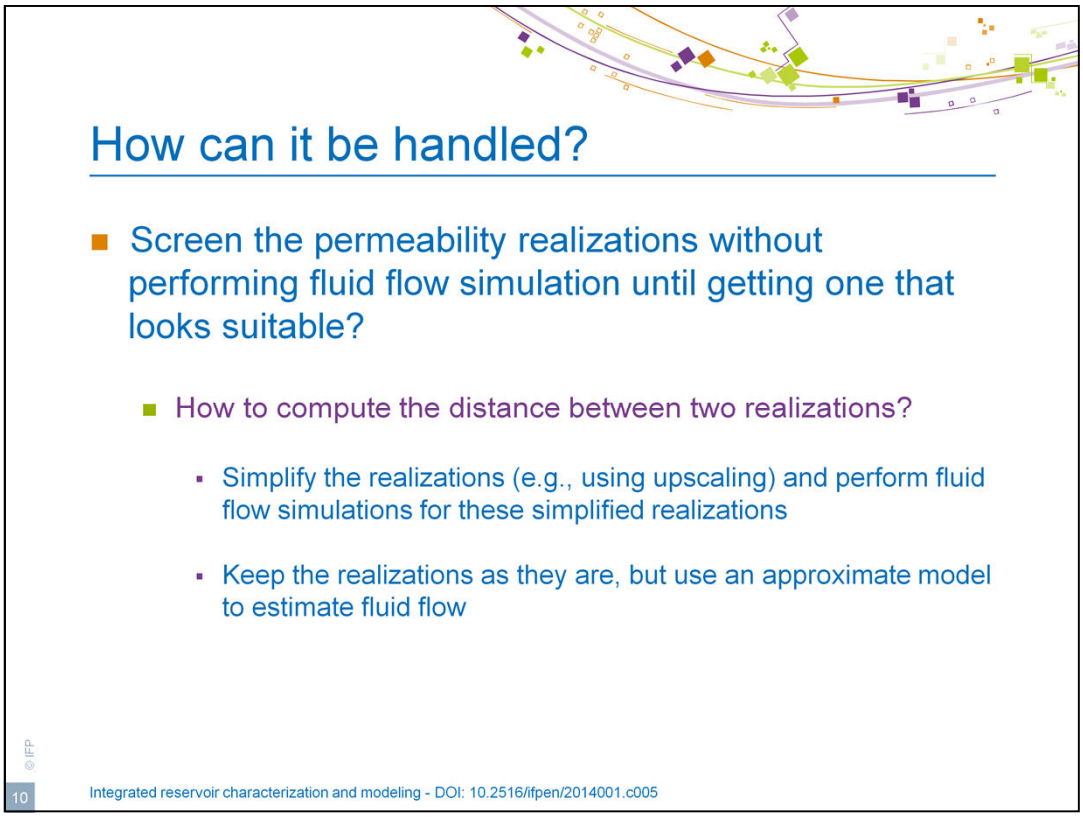

Since a few years, distance-based stochastic techniques have been proposed to elude this drawback (Scheidt and Caers, 2007). The leading idea consists in computing the distance between realizations from an appropriate metric. The distance is expected to indicate how similar two realizations are in terms of their associated response of interest. Clearly, the distance must be defined in order to have a good correlation with fluid flow.

A possibility may be to convert the permeability realizations (that may comprise millions of grid blocks) into very coarse realizations and to simulate fluid flow for these ones, which is obviously less computational time demanding (Scheidt *et al*., 2011). Then, the distance between two realizations can be derived from the squared difference between the two sets of dynamic profiles (*e.g*., water cuts) simulated for the coarse realizations. Another criterion can refer to the use of an approximate, but cheap fluid flow simulator instead of an expensive full physics one. Scheidt and Caers (2007) used a streamline simulator; Bouquet *et a*l. (2014) performed single-phase flow simulations to approximate the pressure behavior when CO_2 is injected into aquifers.

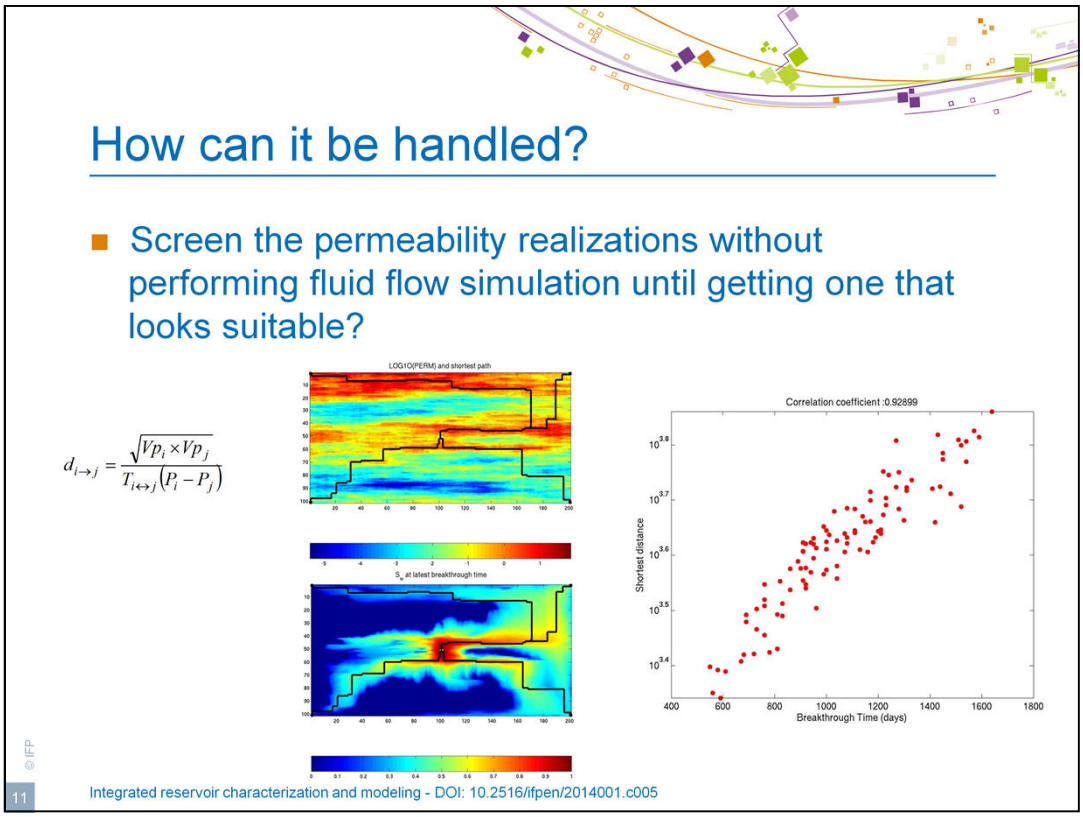

In the example presented above, we refer to graph theory to compute the lengths of the shortest paths between the water injector in the middle of the permeability field (top middle figure) and producers in the four corners. The length of the link between two adjacent grid blocks depends on transmissivity *T* (hence permeability) and pressure (Preux *et al*., 2013). The four shortest paths determined for the permeability realization of interest can be compared with the saturation map shown below. In addition, the plot on the right points out a clear correlation between the lengths of the shortest paths and the breakthrough times. This suggests that the lengths of these paths are relevant indicators of the dynamic behaviors of the realizations. As such, they can be used to quantify the dissimilarity between two realizations.

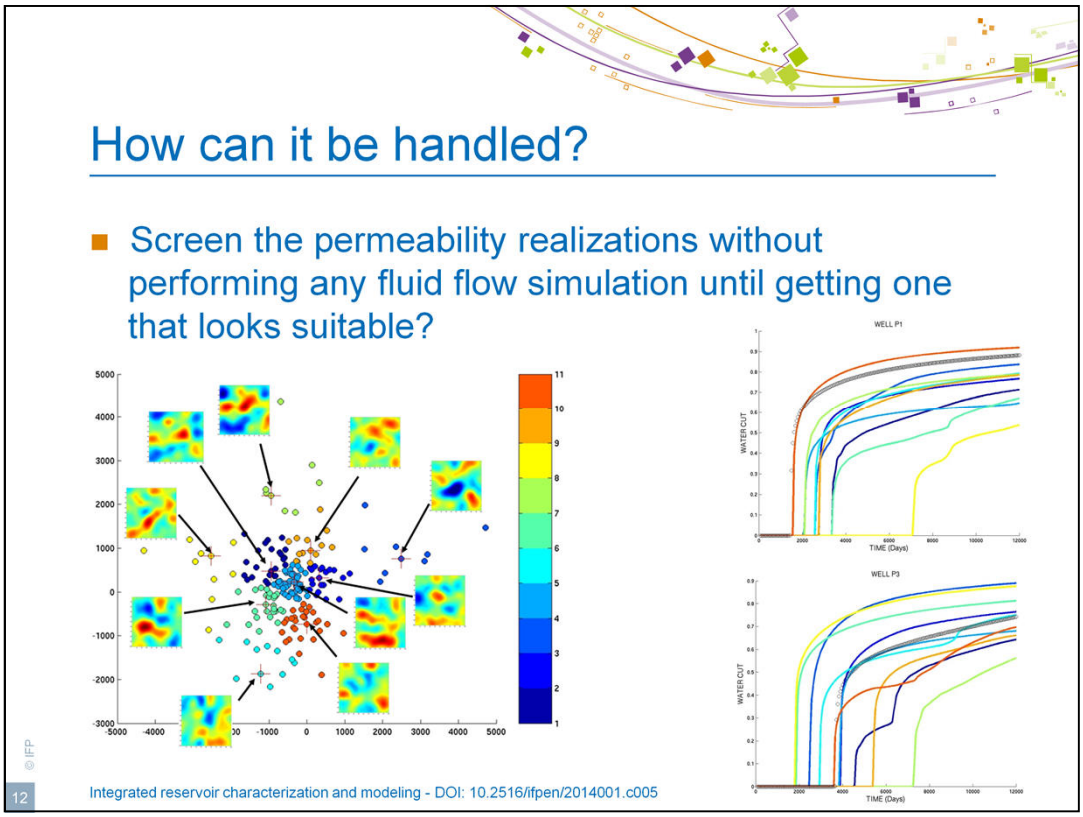

Therefore, we generate 100 permeability realizations, identify for each of them the lengths of the shortest paths. This step does not call for any fluid flow simulation and is very fast. Then, we map all realizations into an Euclidean space using a technique called multidimensional scaling (Scheidt and Caers, 2007). Each point in the left graph corresponds to a permeability realization. The following step consists in running a classification algorithm (k-means) to identify groups of points that are very close. These points represent realizations that are expected to behave more or less the same way in terms of fluid flow. Then, we select the realizations the closest to the centroids of the various groups and simulate fluid flow for these realizations solely. That way, we hope to cover the spread of possible production behaviors from a very limited number of fluid flow simulations (right plots). Last, we compare the simulated fluid flow responses to the available production data and identify the group of realizations whose behaviors look like the data.

Such approaches emerged a few years ago and research is still very active in this domain.

How can it be handled?

- Run optimization from a randomly drawn starting guess (or from a guess that looks suitable)?

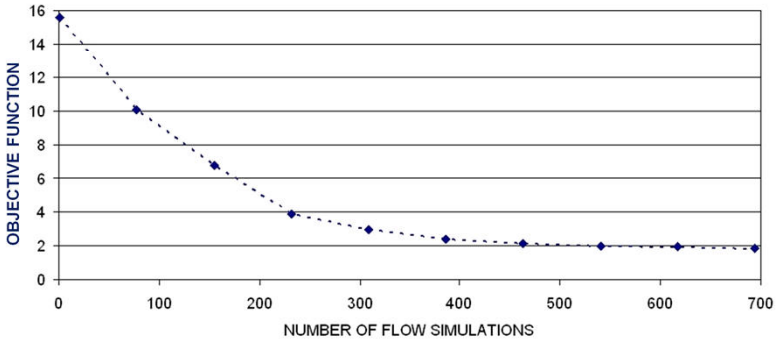

Integrated reservoir characterization and modeling - DOI: 10.2516/ifpen/2014001.c005

In fact, the easiest and most efficient way to determine a permeability (or porosity) realization consistent with production data is still history-matching. In other words, an initial permeability guess is generated, then adjusted step by step until honoring the required data (*i.e.*, minimizing the objective function). But how can we adjust a permeability realization (or any realization of another petrophysical property) when there are so many unknowns (each value in a cell is an unknown parameter) and how can we make sure that the adjusted realization still respects the mean, variance and variogram?

This is the issue addressed in this chapter.

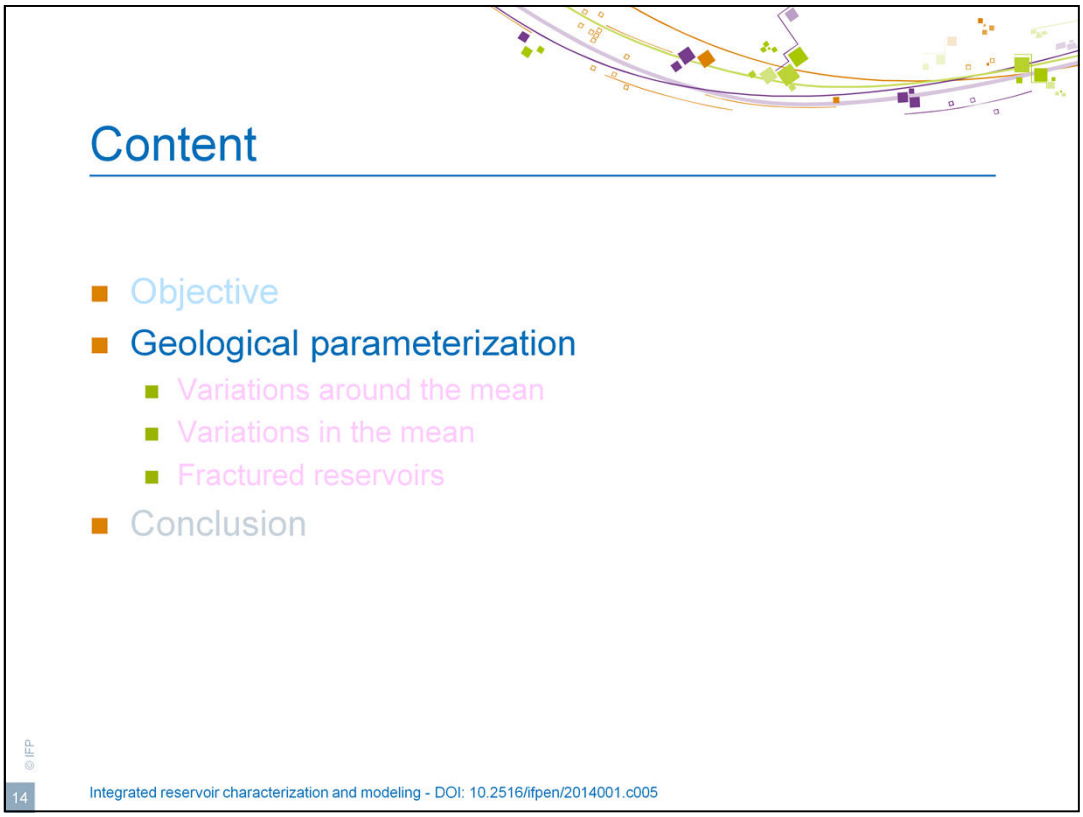

History-matching being the framework selected, how do we handle the parameterization of petrophysical properties?

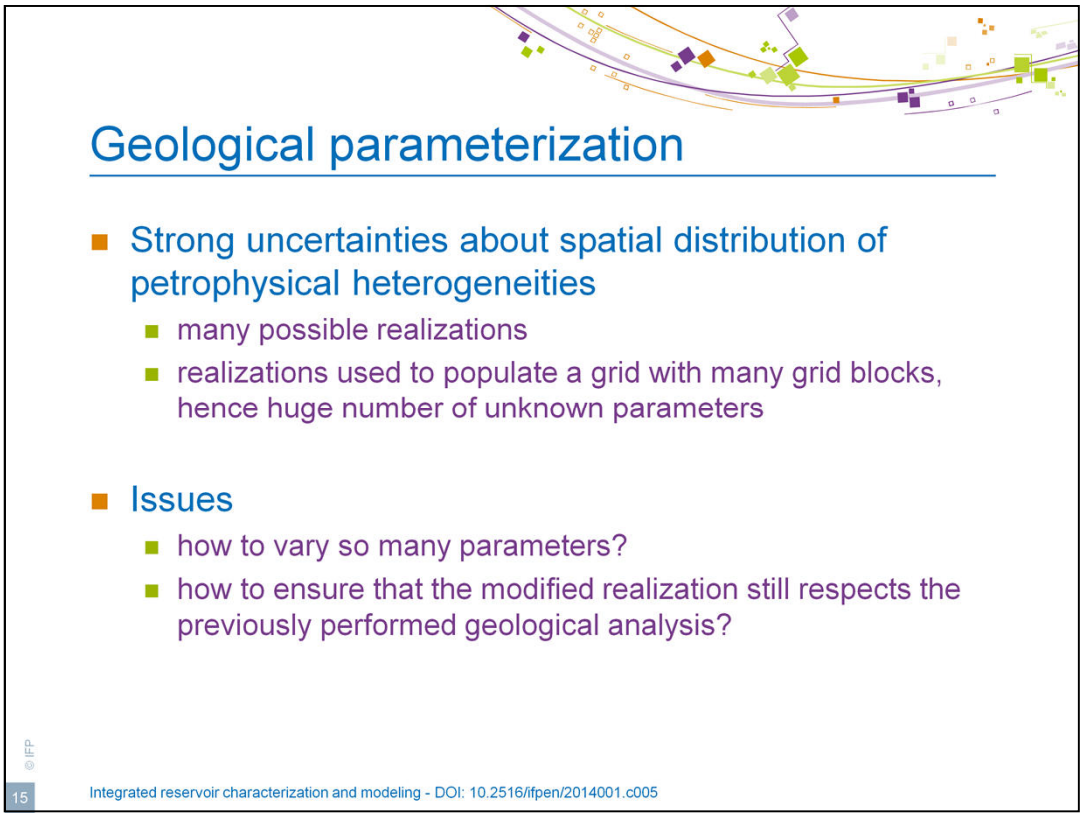

Many different realizations can be randomly drawn to populate the reservoir model. They usually encompass millions of values.

As already emphasized, two key issues are:

- how to adjust so many parameters within the history-matching process, but also

- how to ensure that the modified reservoir model does not depart from prior information?

An appropriate parameterization or reparameterization technique must answer these two questions. The word “reparameterization” can be preferred because by themselves all unknown petrophysical values are already parameters. The idea behind “reparameterization” is to define a set of intermediate parameters that drive the changes in the petrophysical parameters. A suitable “reparameterization” technique must first reduce the huge number of unknown petrophysical parameters to a manageable set of intermediate parameters. Second, it must ensure the preservation of the spatial structure of petrophysical properties whatever the modifications operated.

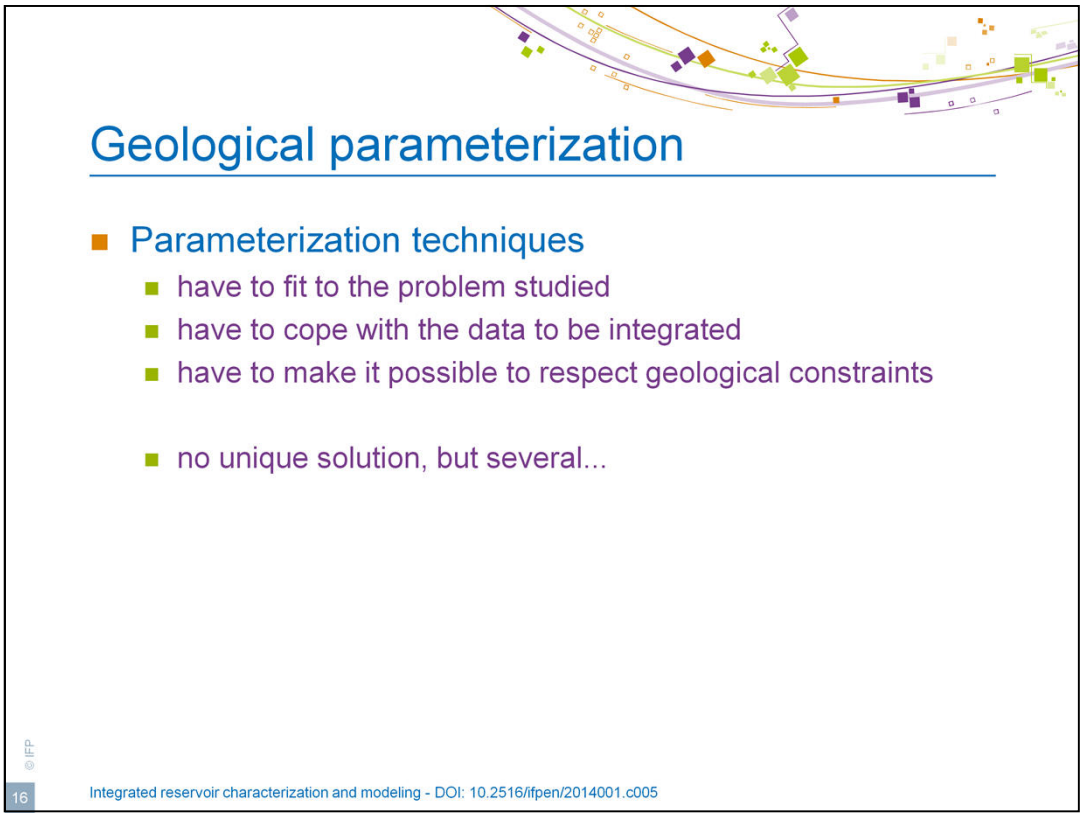

The parameterization (or reparameterization) technique to be used depends on the problem to be solved and the nature of the data to be incorporated within the reservoir model. A major issue is its ability to preserve the consistency between the geological and reservoir models.

This motivated many research works over the last 15 years, resulting in the development of several parameterization techniques. We propose to review some of them in the subsequent sections.

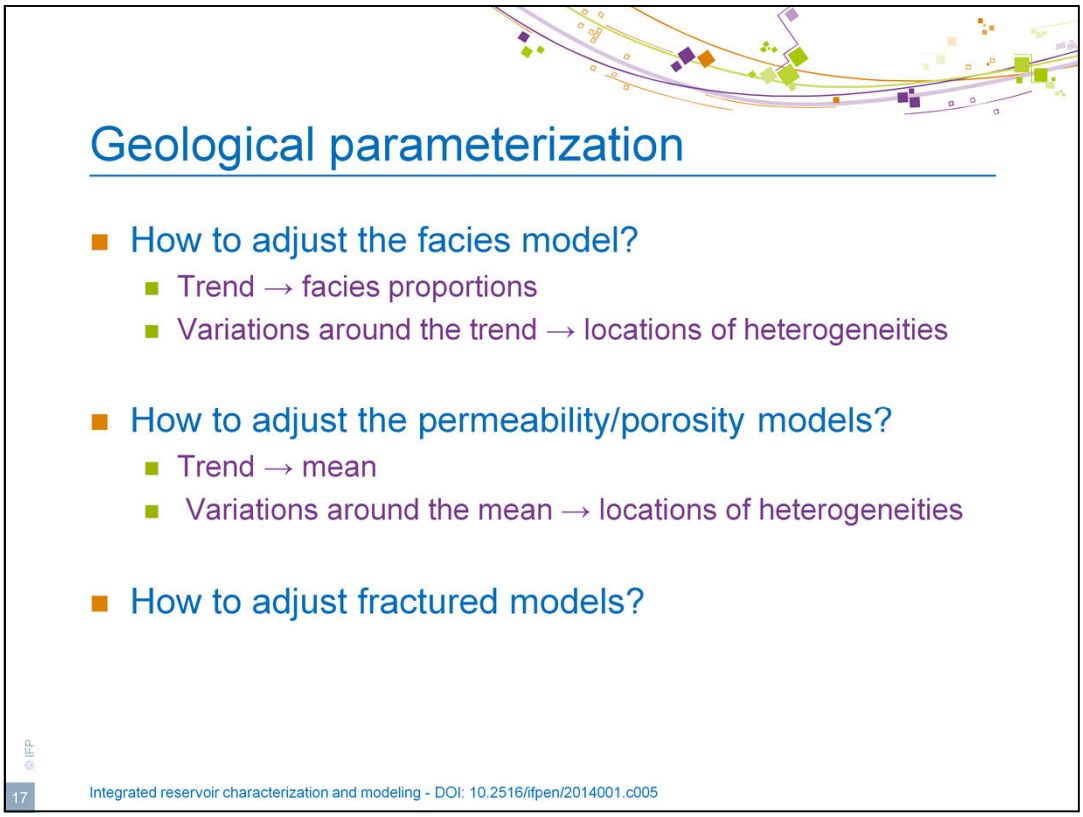

As explained in Chapter 3, the building of the reservoir model can follow a hierarchical approach with first the simulation of a facies realization, then the simulation of permeability/porosity realizations that populate the facies realization.

Therefore, a reservoir model can be changed by varying either the facies model or the permeability/porosity model. In addition, depending on the data to be matched, it may be suitable to vary either the trend or the variations around the trend. For instance, a well test helps evaluate the average permeability around the well whereas water cuts are sensitive to connectivity.

When focusing on the facies model, one may first proceed by adjusting facies proportions. This is more or less the same as varying the trend. Then, the facies proportions being fixed, one may also modify the spatial distribution of facies heterogeneities.

Likewise, for permeability or porosity, it may be required to first adjust their mean values before paying attention to their local variations around the means. In other words, one can change the mean or assume that the mean is known and change the spatial distribution of heterogeneities.

Last, we will also envision the case of fractured reservoir and will show how the spatial distribution of fractures or sub-seismic fractures can be modified in order to better fit some production data.

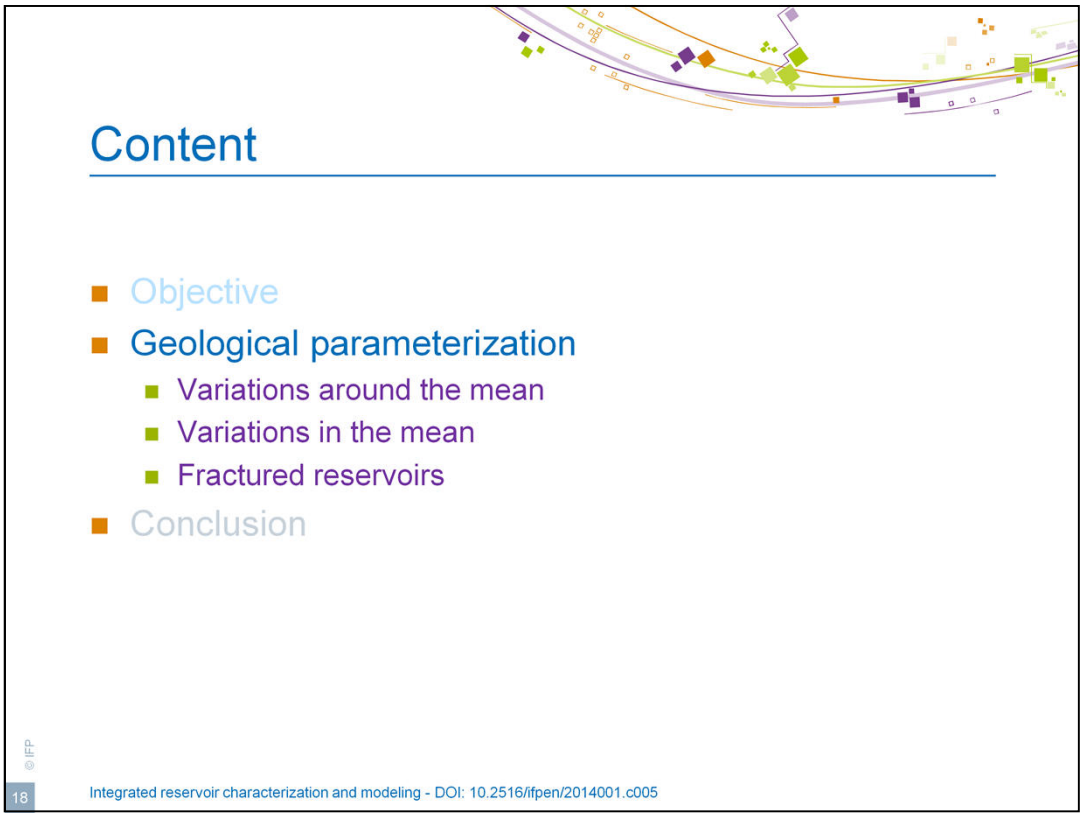

The following sections introduce various techniques that can be used to adjust the petrophysical property realizations. Broadly speaking, two main groups of techniques can be recognized: expansion-based techniques (expansion is truncated in order to end up with a basis of smaller dimension) and geostatistics-based techniques (make it easy to preserve the spatial structures).

We restrict ourselves to geostatistics-based techniques as they have known a growing interest over the last two decades. However, the reader interested in the first type of techniques can refer for instance to Gavalas *et al*. (1976), Oliver (1996) and Romary (2009) for Karhunen-Loève expansion, to Jafarpour and Mclaughlin (2009) for Discrete Cosine Transforms or Sahni and Horne (2005, 2006) for wavelet expansion.

Given this general context, we discriminate parameterization techniques suitable for varying the fluctuations of a realization around the mean, for varying the mean itself or for varying the spatial distribution of fractures.

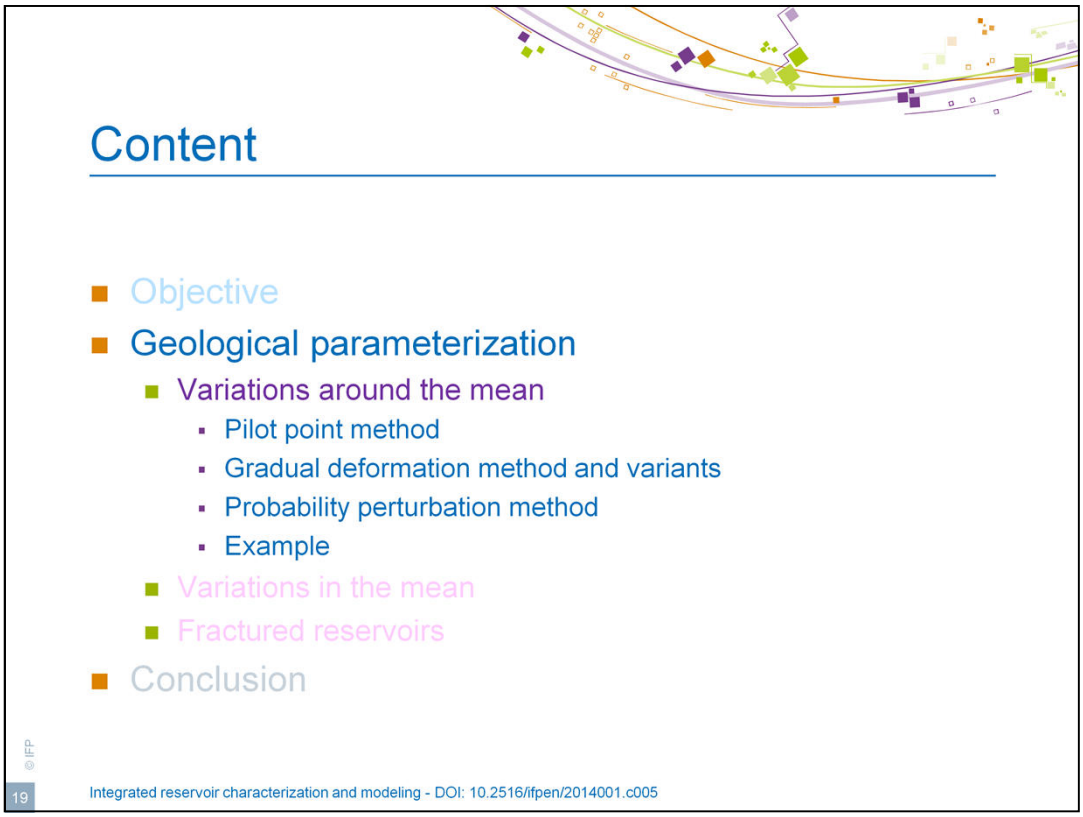

We first examine how to adjust the fluctuations of a given property around the mean. The case of pixel-based models only is investigated.

The concern about geological consistency when adjusting reservoir properties motivated the development of parameterization techniques inspired by geostatistics (Zimmerman *et al*., 1998). We distinguish three main approaches:

- the pilot point method,

- the gradual deformation method and its variants, and

- the probability perturbation method.

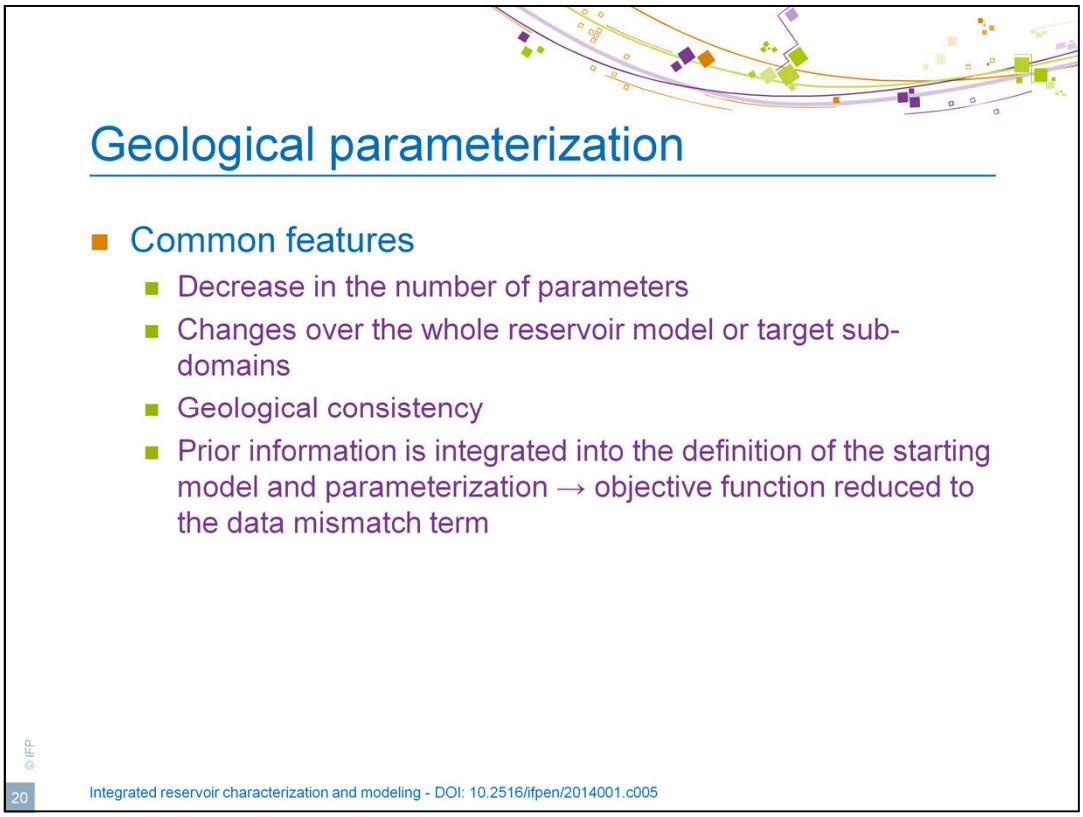

These different techniques share the following features.

1) They involve a drastic decrease in the number of parameters. For instance, if a permeability model is built over a grid with one million grid blocks, the number of parameters is decreased from 1 million to a few dozens.
2) They can be applied to modify the petrophysical properties under consideration over the whole reservoir grid or only part of it. The perturbation is said global when applied to the entire reservoir. Otherwise, it is local.
3) They ensure the preservation of the spatial variabilities of petrophysical properties despite the modifications.
4) The prior information is accounted for when building the starting reservoir model and within the parameterization technique itself. This makes it possible to restrict the objective function to the dynamic data mismatch term.

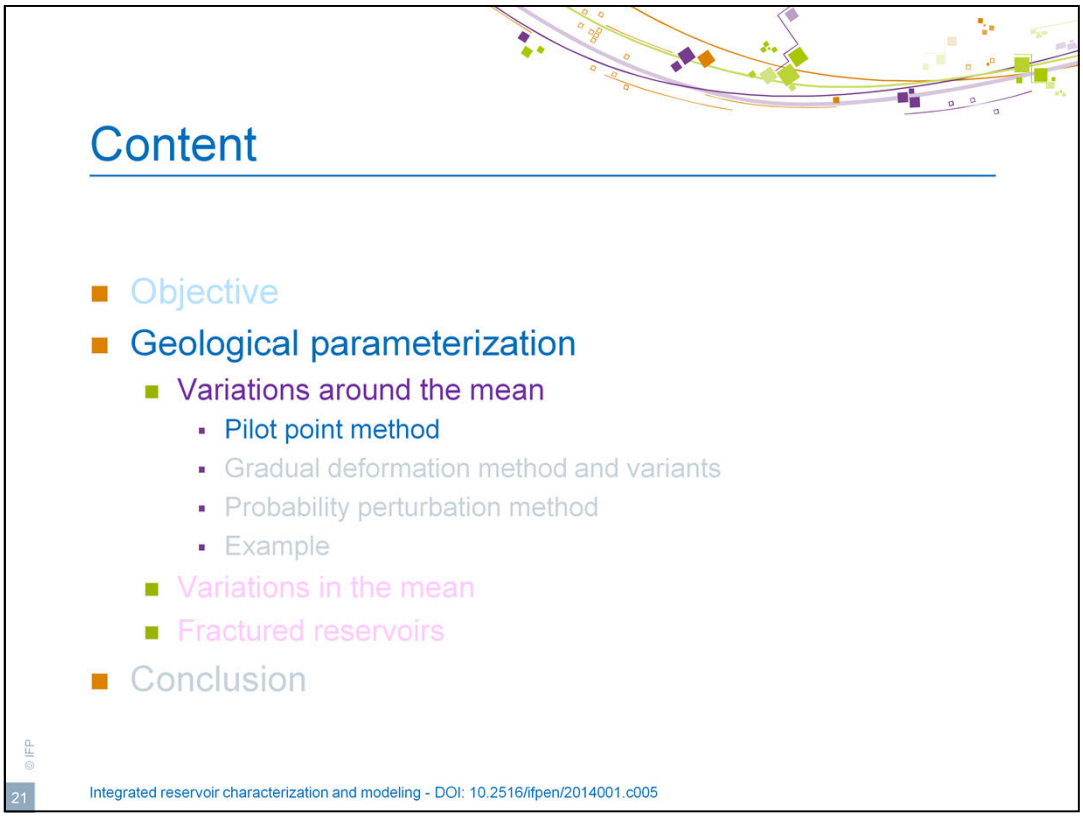

We first start with the pilot point method.

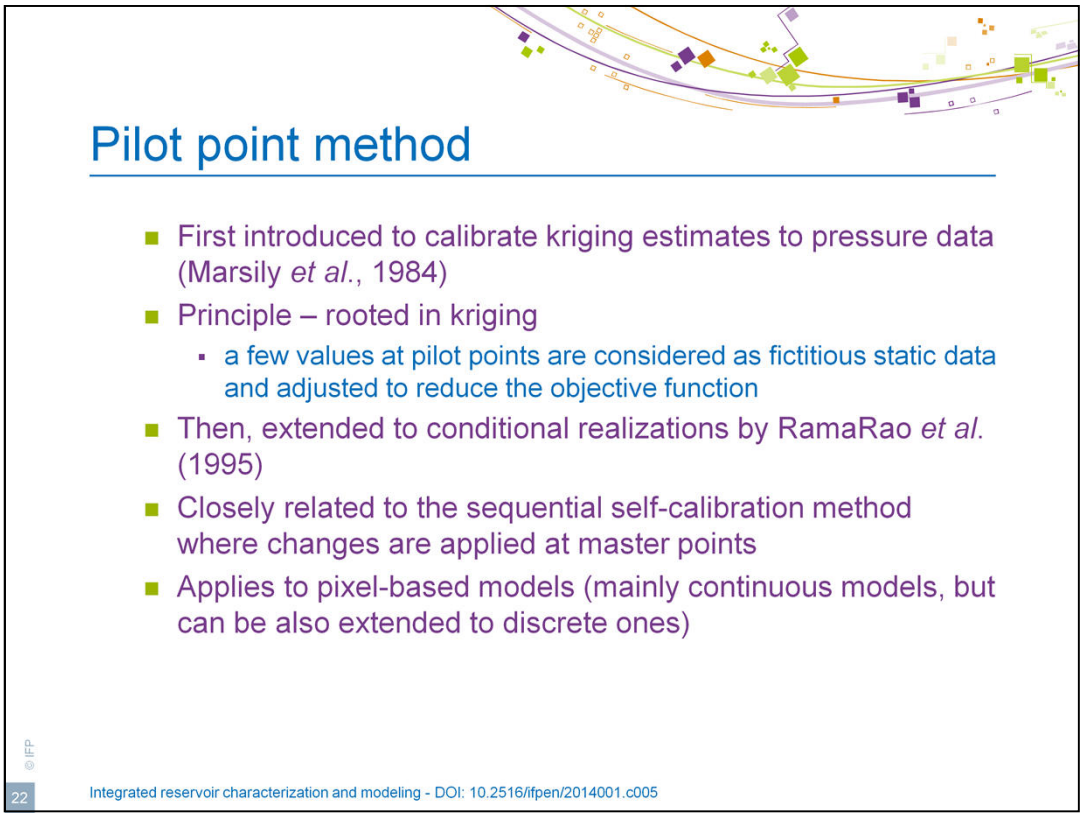

The pilot point method was originally introduced in hydrology, but it is also widely used in petroleum engineering. It has been devised by Marsily *et al*. (1984) to calibrate kriging estimates to pressure data. The values of the property of interest (permeability, porosity or transmissivity for instance) at a few points are considered as kind of fictitious static data, which are adjusted to reduce the objective function. These points are called pilot points.

Later on, the pilot point method was opened up to conditional realizations by RamaRao *et al*. (1995).

A closely related method, called sequential self-calibration method, was also proposed by Gomez-Hernandez *et al*. (1997) and Wen *et al*. (1999) for models generated from the Sequential Gaussian Simulation algorithm.

The pilot point method applies to pixel-based models. It better suits continuous models (porosity or permeability), but can be extended to discrete (facies) ones.

Pilot point method

- Basis = double kriging
- The realization is constrained to a value at a given location (this is the pilot point)
- The modification is local and centered around the pilot point. The radius of the modified region depends on the range

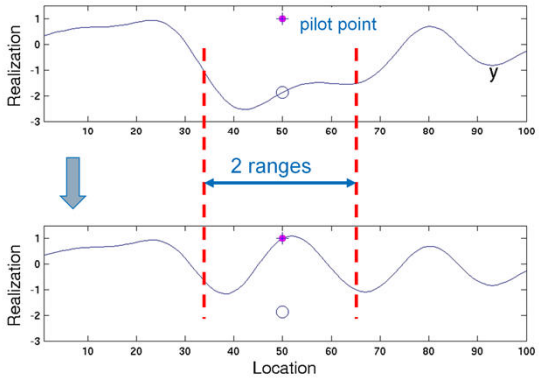

Integrated reservoir characterization and modeling - DOI: 10.2516/ifpen/2014001.c005

The pilot point method refers to kriging to constrain realizations to the values assigned to the pilot points (see Chapter 3, p. 22). As pilot points are considered as fictitious static data, the covariance model considered for kriging is the same as the one derived from static data. Static data and pilot points are handled the same way, the only difference is that the values of pilot points can change while those of data are fixed.

The figure on the right illustrates the basics of the pilot point method. The blue curve is a one-dimensional realization randomly drawn from the prior probability density function. This probability is assumed to be characterized by a mean, a variance and a covariance. The simulated realization is plotted against spatial position. A pilot point is then located at location 50 and assigned the value indicated by the pink dot. Initially, the realization does not respect this point (top figure). Then, kriging is applied twice to compel the realization to go through the pilot point (bottom figure). As expected, the influence of the pilot point is detected over an area with a radius roughly equal to the range.

The main idea behind the pilot point method is that the value of the pilot point is an adjustable parameter.

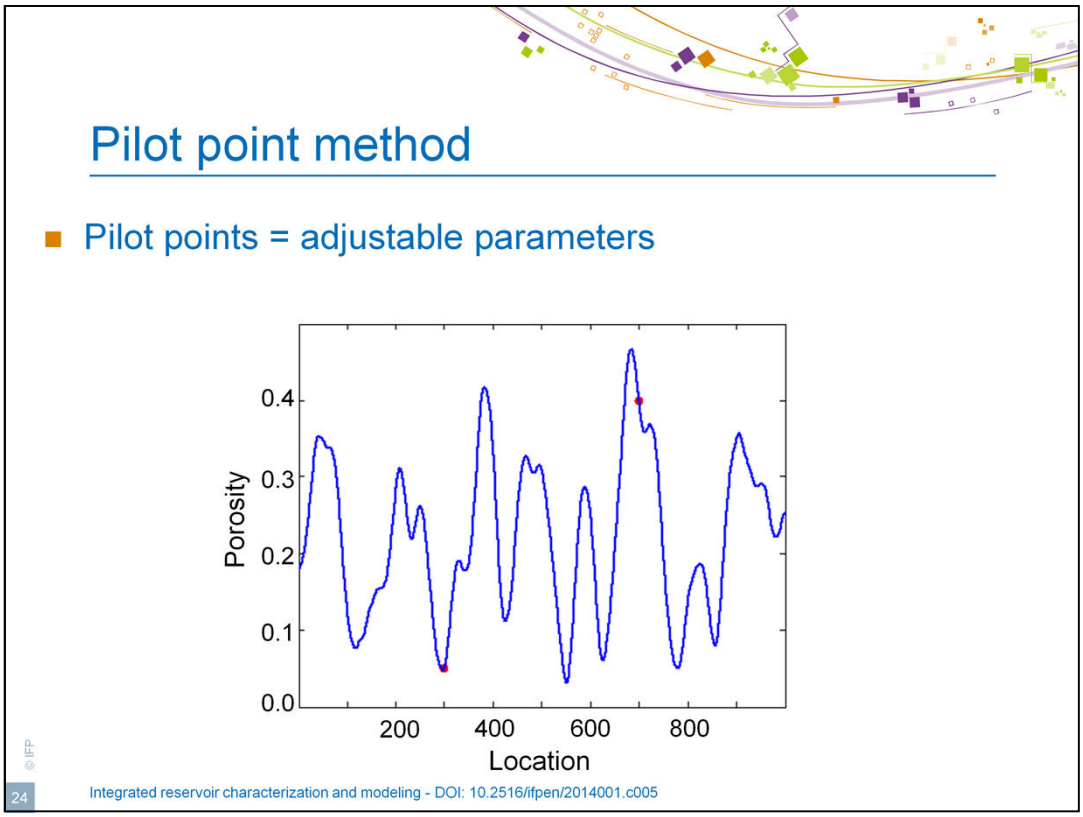

Variations in the pilot point values involve variations in the realization. The example above is a one-dimensional porosity realization with two pilot points: one at location 300 and the other one at 700. Their values can be modified at the same time or not. First, we increase the value of the pilot point at location 300 from 0.05 to 0.4. Then, we decrease the value of the pilot point at location 700 from 0.4 to 0.05. Last, we simultaneously change the values of the two pilot points. Each pilot point value is considered as an unknown parameter that can be adjusted to better honor a given constraint. When we modify two pilot points at the same time, the problem involves two parameters.

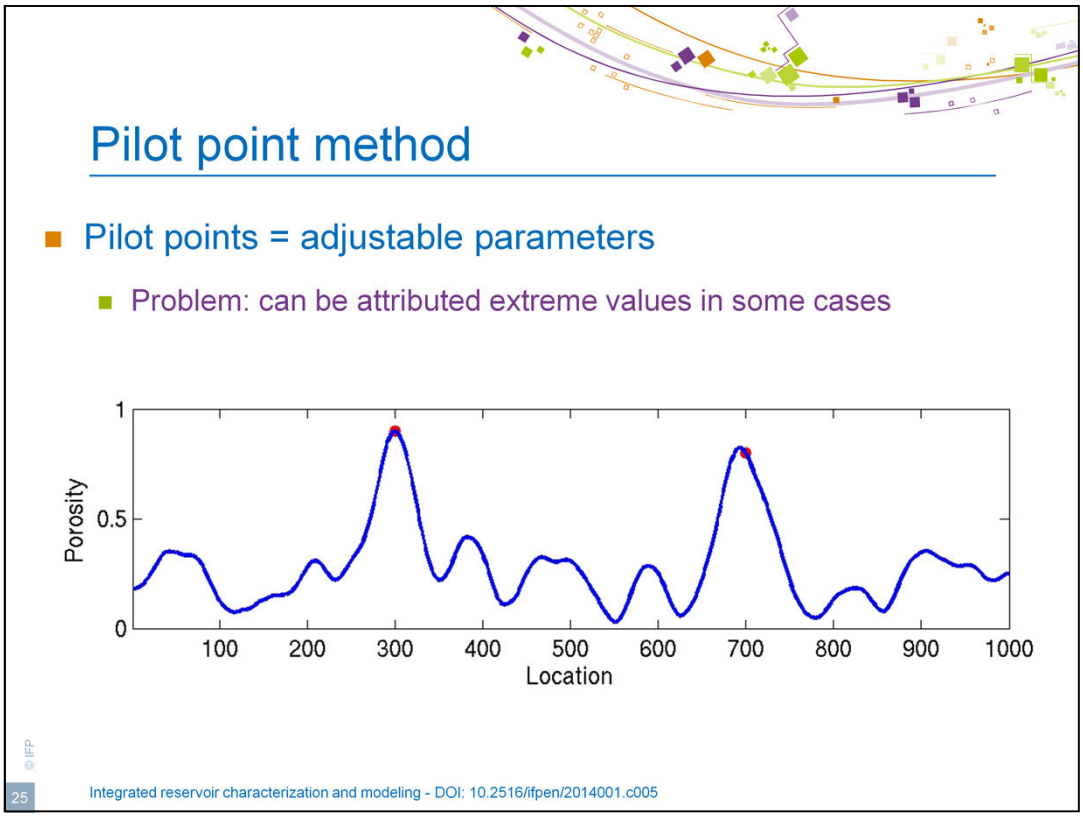

The pilot point method suffers from a few pitfalls (Cooley and Hill, 2000; Cooley, 2000). These ones can occur when neglecting sources of model inaccuracy (modeling errors) and over-parameterization.

Over-parameterization makes the optimization problem instable. Then, pilot points can be attributed extreme (unphysical) values during the matching process as the fluctuations are not bounded. For instance, when used to calibrate a permeability field, pilot points can generate strong permeability variations over very small distances.

Different strategies were investigated to elude this undesired effect. A first possibility consists in bounding the variations in the parameters (RamaRao *et al*., 1995; Gomez-Hernandez *et al*., 1997). However, this approach does not seem to improve the reliability of the solution (Alcolea *et al*., 2006). Other alternatives involve the decrease in the number of pilot points (this implies adding the pilot point sequentially until a satisfactory match is obtained) or the integration of prior information into the objective function (Alcolea *et al*., 2006).

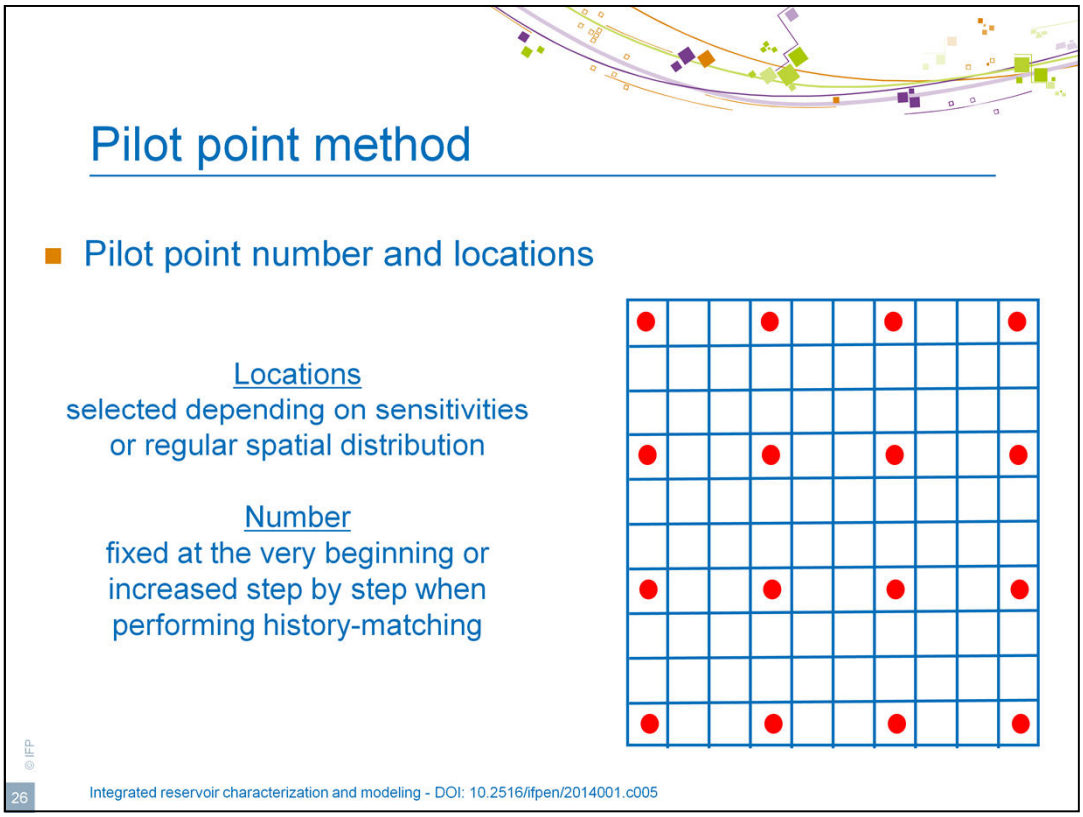

We can refer to two distinct approaches to locate pilot points.

Traditionally, pilot points are pre-fixed. They are often distributed so as to form a regular gridding. For instance, two pilot points are separated by a distance equal to the range along each direction. Another technique for selecting pilot point positions involves a combination of geological uncertainty and sensitivity to production data. Lavenue and Pickens (1992), Cuypers *et al*. (1998), and Mezghani *et al*. (2000) suggested to select pilot point positions depending on their ability to reduce the objective function. This approach relies on the computation of sensitivity coefficients. Of course, this can be time-consuming. It has to be stressed that history-matching is very sensitive to the locations of the pilot points.

Regarding the number of pilot points, it is also often pre-fixed by the engineer before starting history-matching. The idea is to use the number of points required to cover the whole reservoir model. Another possibility involves the sequential addition of pilot points. A first optimization process is then run with a given number of pilot points. Then, the values of these points is set to their optimal values and a new optimization process is run with new pilot points added to the grid. The procedure is repeated until achieving a reasonable match.

The use of pilot points to drive the variations in the petrophysical property of interest is expected to induce a significant decrease in the number of parameters, more especially if pilot points are added sequentially.

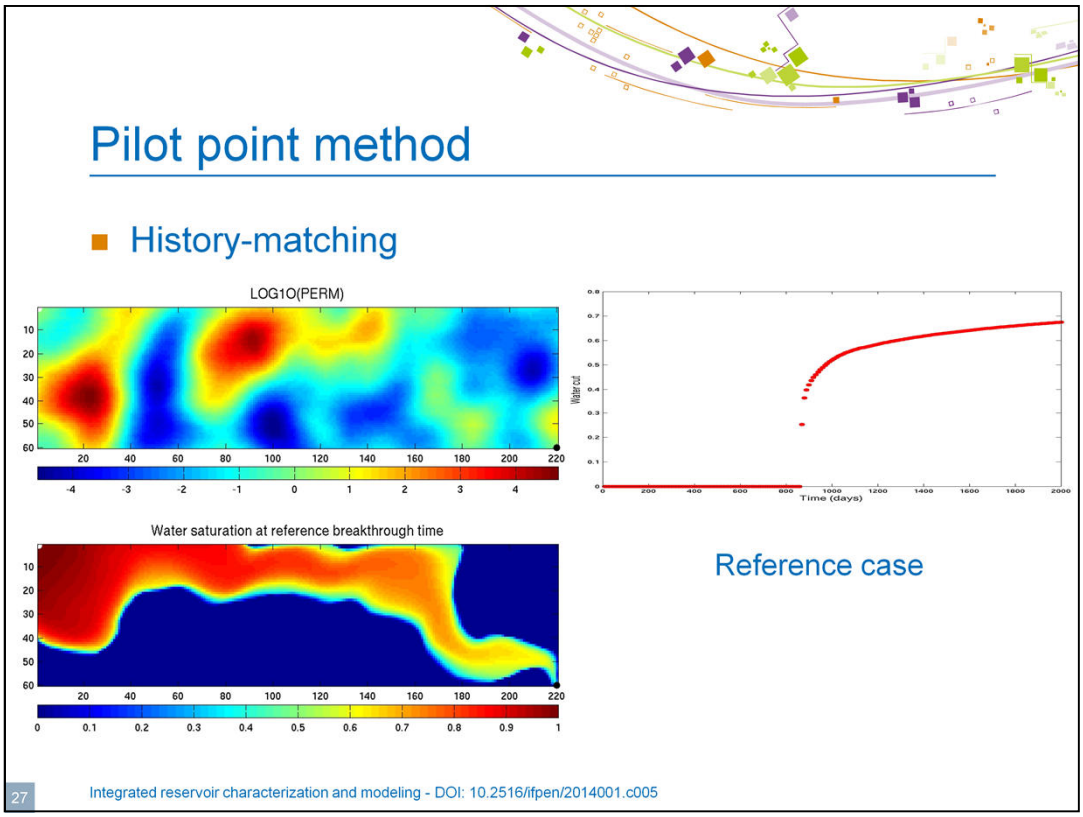

When the pilot point method is incorporated into optimization processes, the parameters to be adjusted to reduce the objective function are the values of the pilot points.

Let us consider the following two-dimensional case as a reference case. The reservoir model comprises 220 and 60 grid blocks along axes X and Y, respectively. The spatial variability of the log-permeability is described by an isotropic Gaussian variogram with a horizontal range of 30 grid blocks. The logarithm of permeability is shown on the top, left. There is one water injector in the top left corner and a producer in the opposite corner (bottom right). The water cut simulated at the producer is displayed on the right against time. The breakthrough time is about 900 days. Water saturation simulated at breakthrough time is represented on the bottom left.

For illustration purposes, we assume that the objective function quantifies the water cut mismatch.

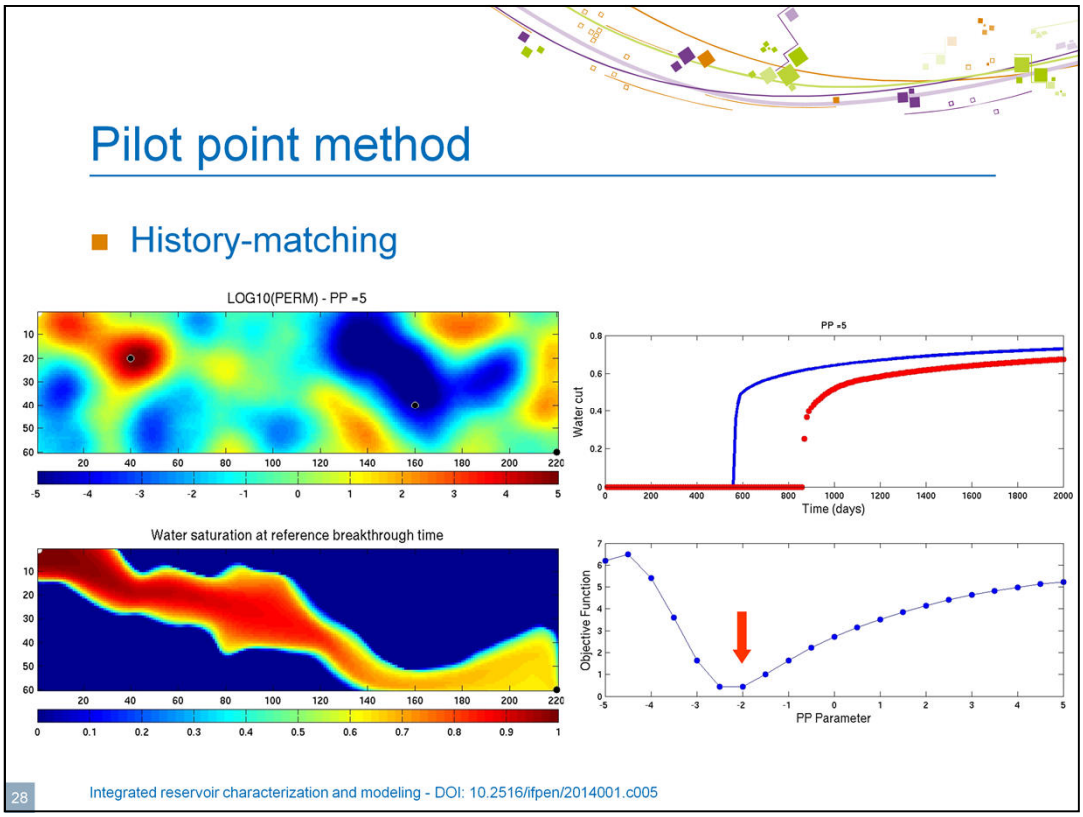

As explained before, the interest of the pilot point method when incorporated into a history-matching process is that it gives the possibility to vary the petrophysical realizations populating the reservoir model from a few parameters.

In this example, we vary a starting permeability realization (top left) from two pilot points (indicated by black dots): one at coordinates (40,20), close to the injector, and the other one at coordinates (160,40), close to the producer. Their values are driven by a single parameter evolving from -5 to 5. The value of the first pilot point is given by this parameter while that of the second one is just its opposite.

For each value of the parameter, we simulate the injection of water and compute the water cut at the producer (top right) and the water saturation map (bottom left) at the reference breakthrough time (*i.e.*, the breakthrough time determined for the reference model shown previously). The water cut (blue curve) obtained for the current model is compared to the reference one (red dots). The difference between the two of them provides the value of the objective function (bottom right).

At the very beginning, the values of the first and second pilot points are -5 and 5, respectively. Then, the value of the first one increases while that of the second one decreases. The breakthrough time computed for the starting model is larger than the reference one (1150 days instead of 900 days) and the objective function is about 6. Then, the increase in the parameter results in an earlier breakthrough time, which induces a decrease in the objective function. When it is -2.5, the breakthrough time is close to the reference one and the objective function is minimal. Then, increasing further this parameter still contributes to decrease the breakthrough time, leading to an increase in the objective function.

The pilot point method makes it possible to screen realizations that are modified at pilot points and to pick up the one, which better fits the reference data.

Pilot point method

- Example

Reference case

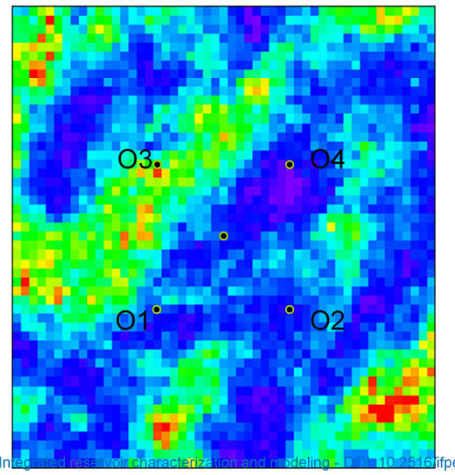

- 1 producer in the middle and 4 observation wells (O1 to O4) around
- Dynamic data: pressures in the 5 wells

(Roggero and Hu, 1998)

An application case (Roggero and Hu, 1998) is presented to illustrate the potential of the pilot point method. It is a simple synthetic case: a two-dimensional reference reservoir permeability model was built with a producer in the middle of the reservoir and 4 observation wells around labeled O1, O2, O3 and O4. This reference model was inputted into a flow simulator to simulate a well test and compute the pressures in the five wells. This yields the set of reference dynamic data.

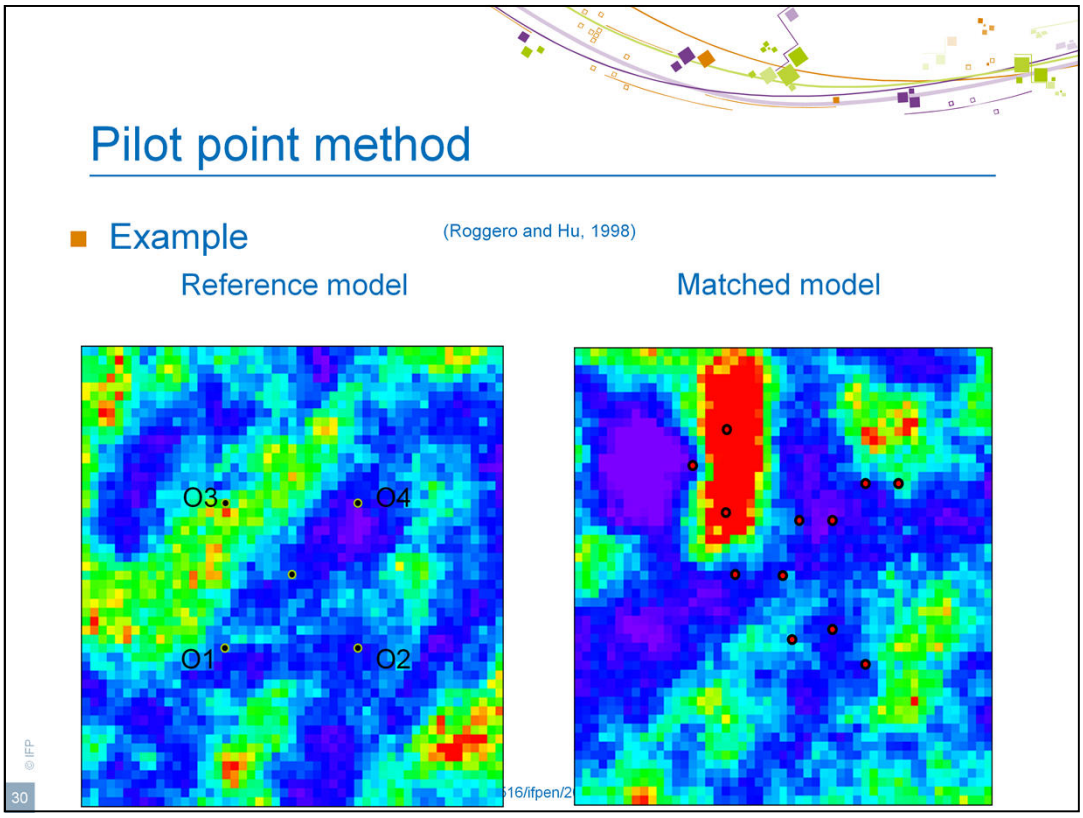

The reference model is kept on the left for comparison purposes. However, it is now assumed to be unknown. The only available data are the prior probability density function (pdf) and the reference pressures collected at wells.

We perform history-matching using the pilot point method to drive the changes applied to an initial permeability model (right) randomly drawn with respect to the prior pdf. Then, pilot points are sequentially added and their values are adjusted in order to reduce the misfit between the reference pressures and the pressures simulated for the currently modified model. This process is then based upon a sequence of optimization processes. Briefly, we add the first pilot point and optimize its value. Then, we fix its value to the optimal one and add two new pilot points. A second optimization process is then run varying the newly added pilot points and keeping the first one unchanged. This procedure is repeated until a reasonable match is achieved. Finally, 19 pilot points are added to obtain a matched model. This final constrained model captures the main trends of the reference model.

The number of pilot points incorporated into optimization processes can vary. It is decided by the engineer.

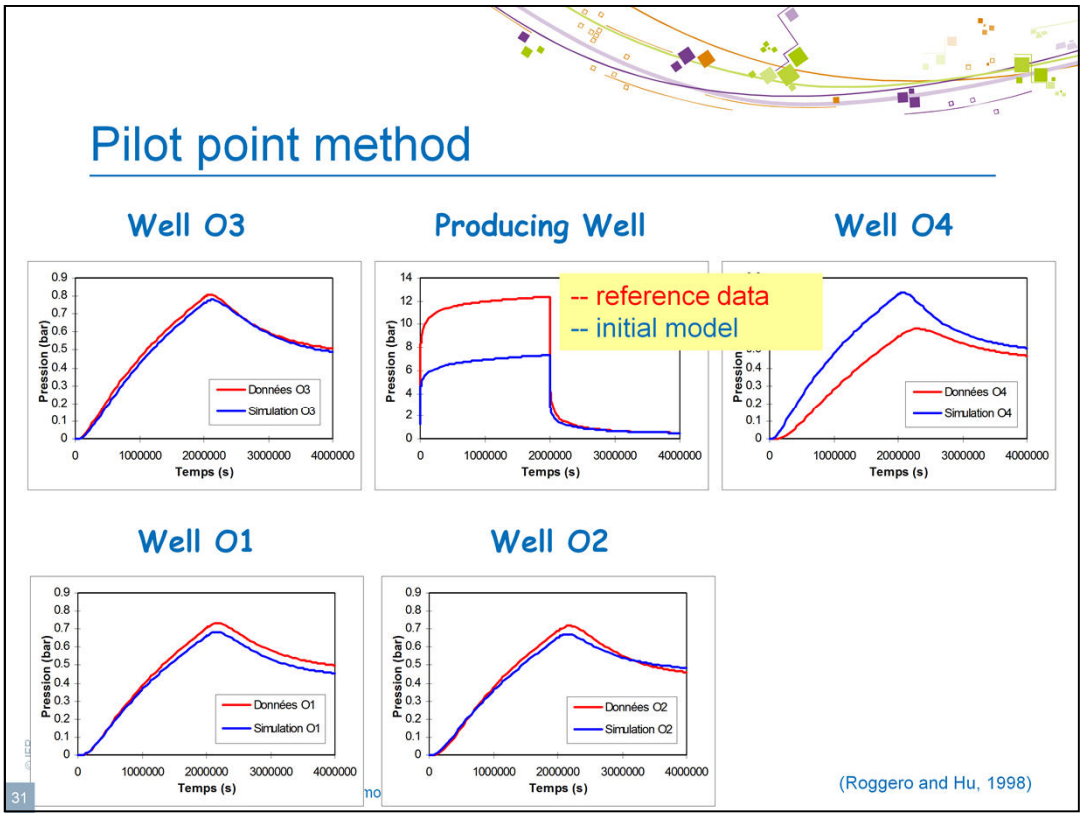

The pressures simulated at wells for the initial model (blue curves) are compared to the reference pressures (red). There are clear differences, especially for the producer and the observation well O4.

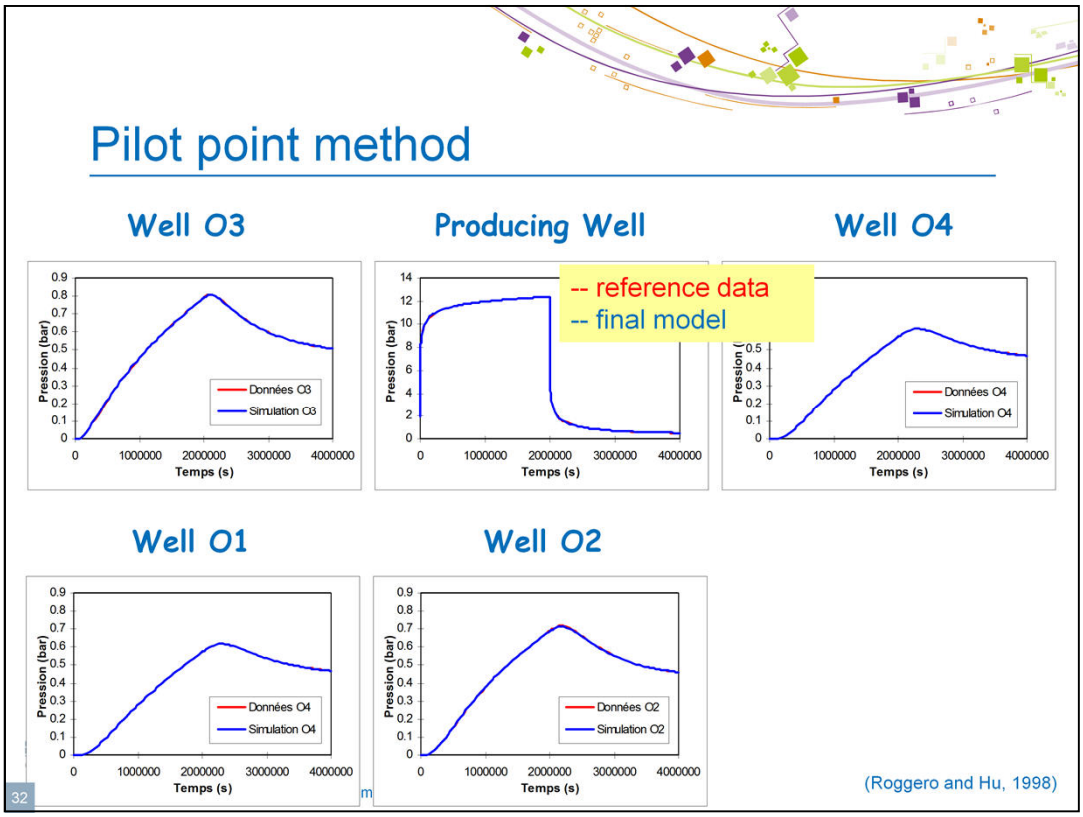

Now, we compare the pressures simulated at wells for the final model (blue curves) with the reference pressures (red). The final match is perfect.

This is of course a toy problem and we must not expect such a perfect result when history-matching a real field case.

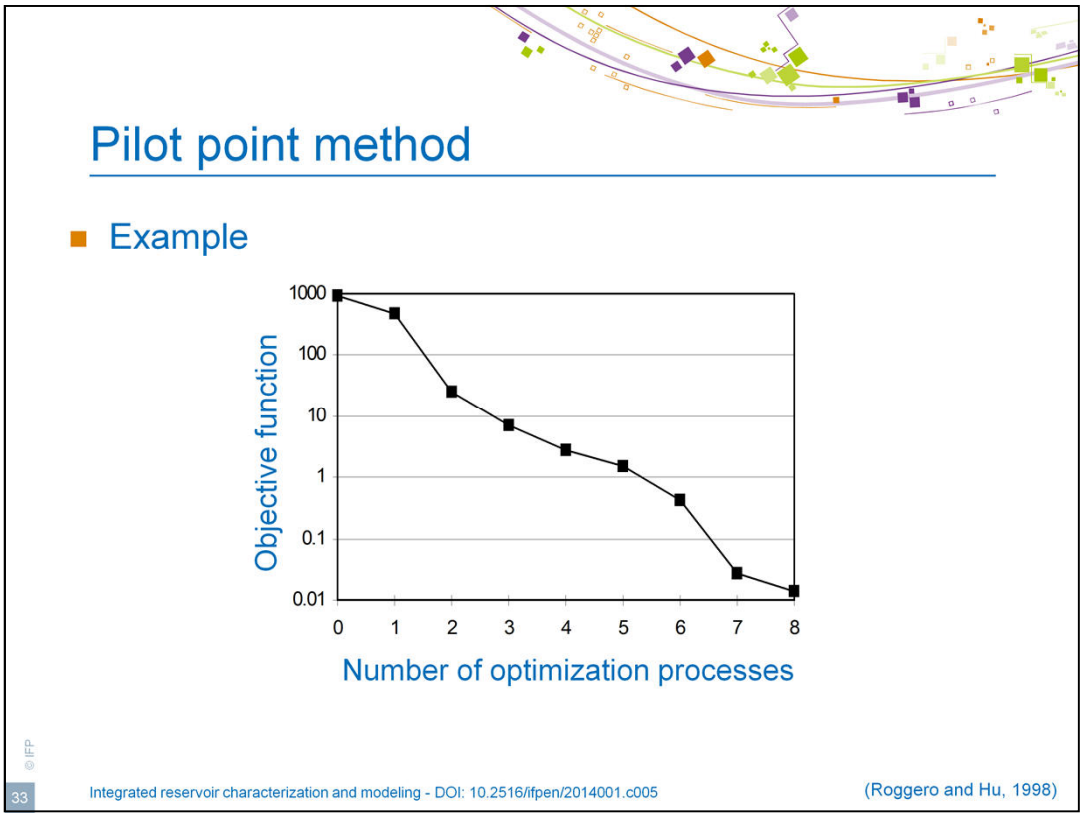

This graph shows the decrease in the objective function as more optimization processes are run. It goes from 1000 down to almost 0.01 with 8 optimization processes run one after another. Each optimization process is associated to newly added pilot points.

It is worth noting that one optimization process involves about 15 fluid flow simulations in the case studied.

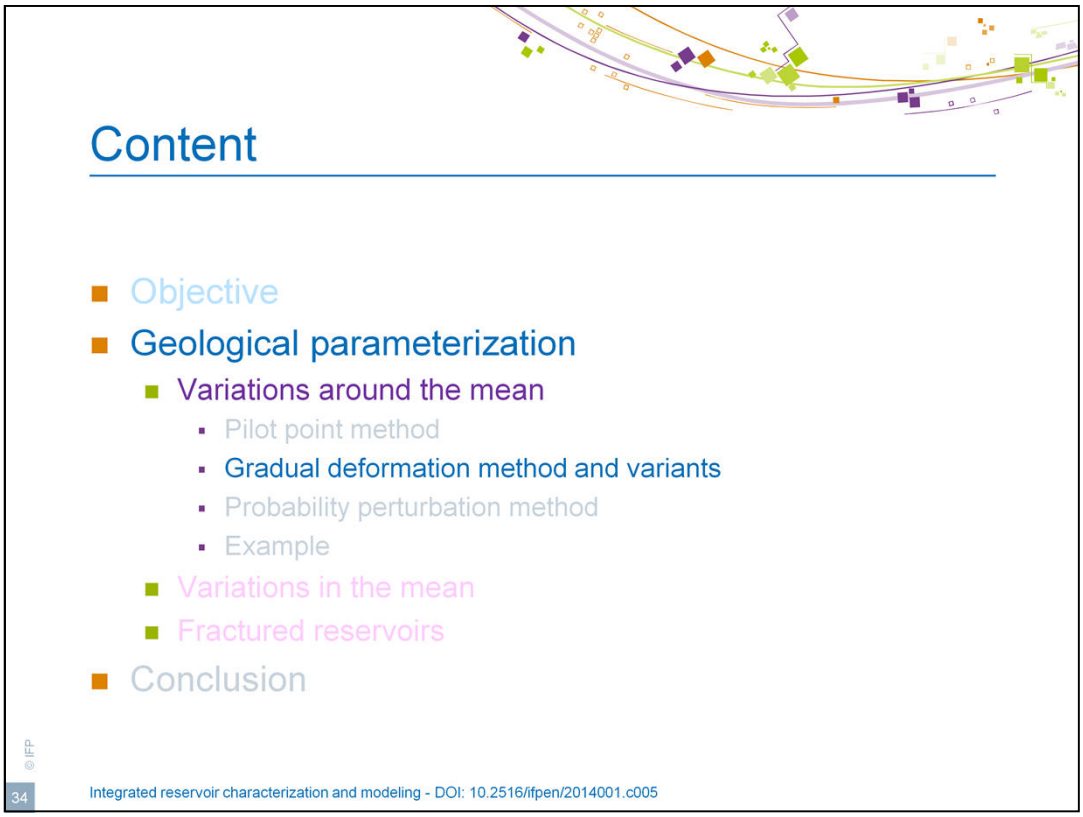

We now focus on the gradual deformation method and its variants. For simplicity, the acronyms GDM is used for gradual deformation method.

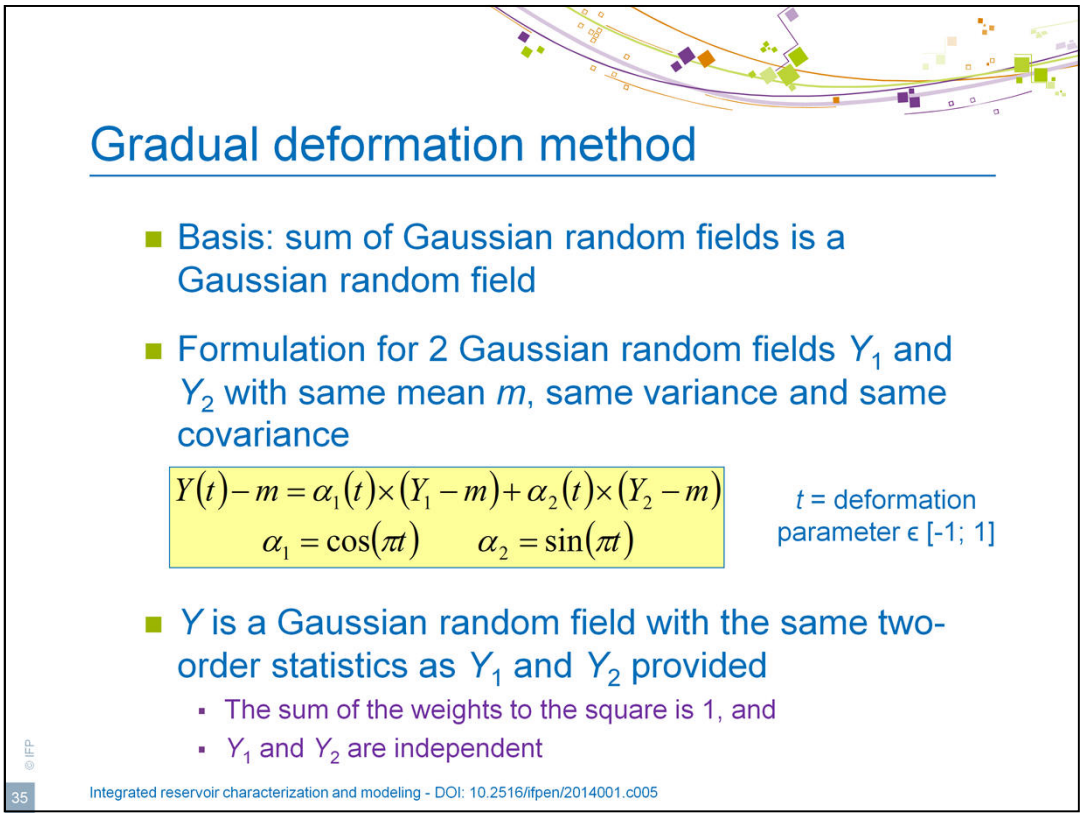

GDM is another geostatistical parameterization technique introduced in reservoir engineering for compelling reservoir models to respect production history (Roggero and Hu, 1998; Hu, 2000).

This method involves a linear weighted combination of Gaussian random fields. The weights can then be considered as parameters, which are adjusted to minimize the dynamic data mismatch. The underlying statistical theorem is that the sum of Gaussian random functions is also a Gaussian random function.

One of the simplest formulation of the GDM is shown above. It entails the combination of 2 independent Gaussian random functions Y_1 and Y_2 with same mean m, same variance and same covariance. The weights are cosine and sine functions of the deformation parameter t. This deformation rule is periodic and the deformation parameter belongs to the interval [-1; 1]. When it is 0, Y is the same as Y_1. When it is ½, Y is the same as Y_2.

Y is also a Gaussian random function with the same mean and covariance as Y_1 and Y_2 whatever the value of the t deformation parameter. This property holds because Y_1 and Y_2 are independent and because the sum of the combination weights to the square is 1 ($\cos^2(t)+\sin^2(t)=1$).

Gradual deformation method

- Gradual deformation parameter t = adjustable parameter

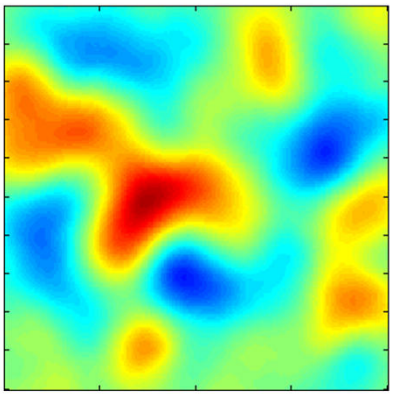

The whole model is modified when varying a unique deformation parameter.

The spatial variability is preserved.

Integrated reservoir characterization and modeling - DOI: 10.2516/ifpen/2014001.c005

The gradual deformation relationship makes it possible to modify a realization of a Gaussian random function by varying a single deformation parameter.

Whatever the deformation parameter used to change the realization, the spatial variability is preserved. The deformation is said global when the whole realization is modified.

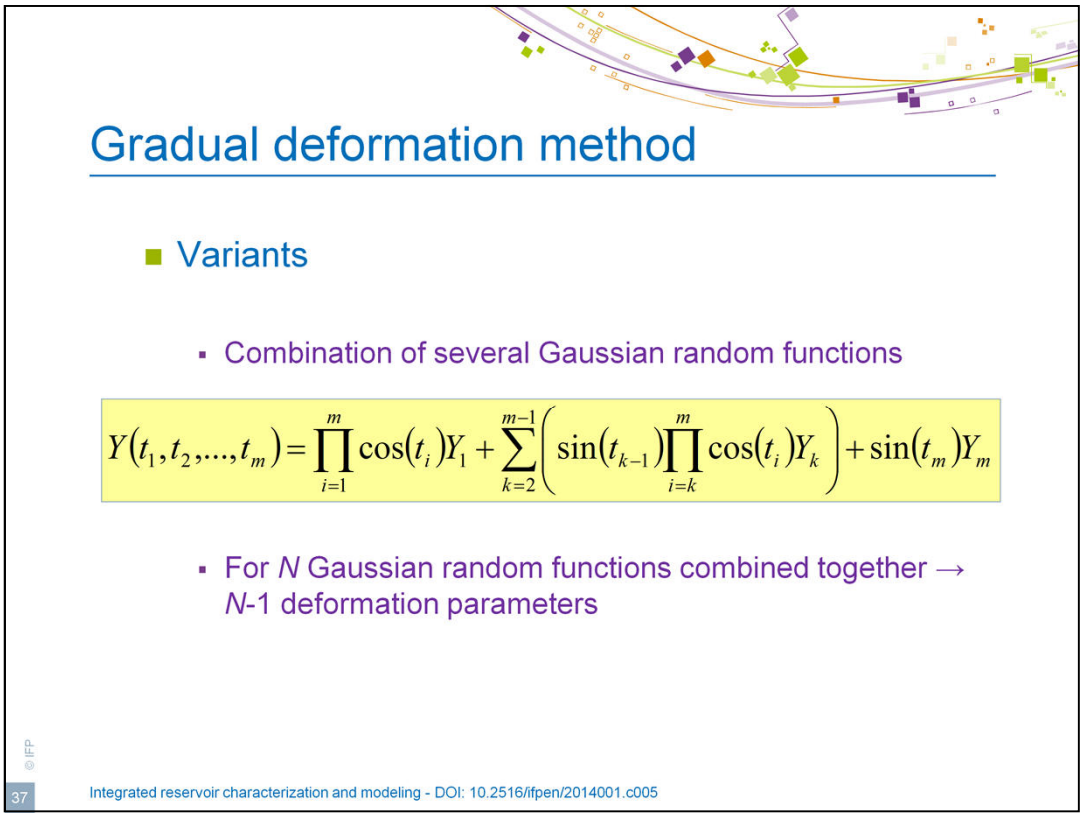

The gradual deformation scheme presented above can be extended to the combination of any number of Gaussian random fields with the same two-order statistics (Hu, 2000).

In this case, the combination of *N* Gaussian random functions entails *N*-1 deformation parameters. Increasing the number of combined functions provides more degrees of freedom, which is of interest when performing history-matching.

Heterogeneity distribution - Geostatistics

- Variants
  - Local deformation

$$Z(t) = Z_1 \cos(\pi t) + Z_2 \sin(\pi t)$$

Gaussian white noises

Key: combination of the random numbers used to generate the realizations instead of the realizations themselves

→ Ensures smooth transition between target region and embedding matrix

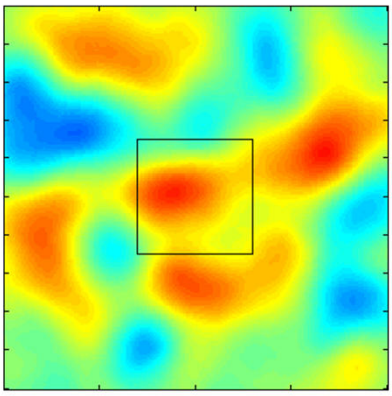

Deformation in 1 or several regions

Integrated reservoir characterization and modeling - DOI: 10.2516/ifpen/2014001.c005

Another variant of the GDM permitting local deformation has been developed for providing more flexibility (Hu, 2000; Le Ravalec-Dupin *et al*., 2001).

The key principle when addressing local gradual deformation is that the gradual combination is performed at the level of the random numbers used to generate the realizations instead of the realizations themselves. This prevents the occurrence of discontinuities between the modified area and the surrounding one. In this case the gradual combination formula reduces to the one displayed above where Z_1 and Z_2 are 2 independent Gaussian white noises. Again, it can be shown that Z is also a Gaussian white noise for any value of the t deformation parameter (because of the independency condition and because the sum of the weights to the square is 1).

The example on the right focuses on the gradual deformation of the field in the middle black square. Actually, changes are also evidenced in a transition zone all around the target square. The thickness of this zone is about a range. The transition zone ensures a smooth evolution between the modified area and the surrounding one.

This example describes the deformation of a unique sub-domain, but several sub-domains can be simultaneously considered with a distinct deformation parameter for each of them. In such conditions, t becomes a vector including all the local deformation parameters. When the local parameterization is incorporated into a matching process, the increased number of deformation parameters gives more flexibility to minimize the objective function. In addition, when some regions are well matched, the corresponding deformation parameters can be removed from the set of adjustable parameters.

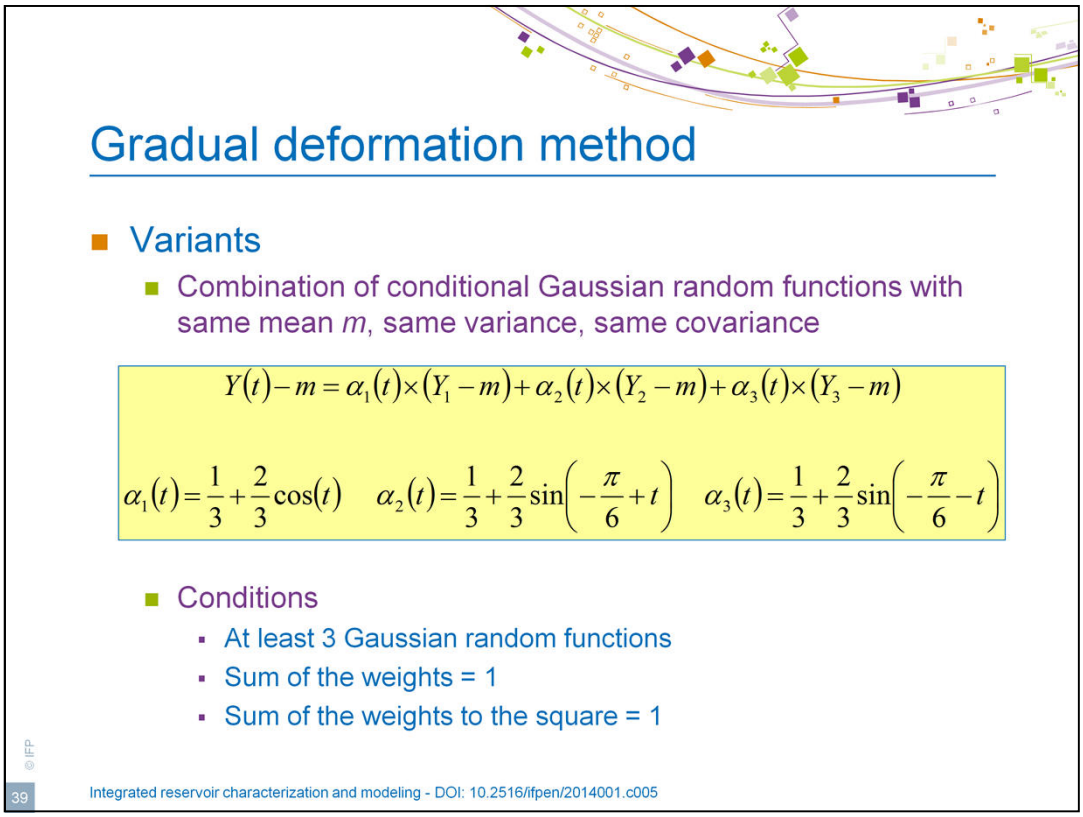

A variant of the GDM, called gradual conditioning method (GCM), was developed by Ying and Gomez-Hernandez (2000), Hu (2002) and Capilla and Llopis-Albert (2009). The main difference is that the combination involves conditional fields instead of unconditional ones as done with the GDM. A conditional realization is a realization that respects the static data.

Because the leading idea behind the GCM is to ensure that the modified field also respect the static data, the combination weights in the GCM variant are submitted to an additional constraint. Their sum has to be one.

In addition, the constraint already mentioned for the GDM according to which the sum of the weights to the square must be one is kept.

Since there is an additional constraint, the basic combination scheme involves 3 random fields with the GCM instead of 2 with the GDM. These 3 random fields are not independent because they all honor the static data. Given these conditions, the realization built from the 3 conditional realizations is also conditional. The 3 weights used to respect these constraints depend on a single deformation parameter *t*.

Note that the GCM does not cope with local deformation.

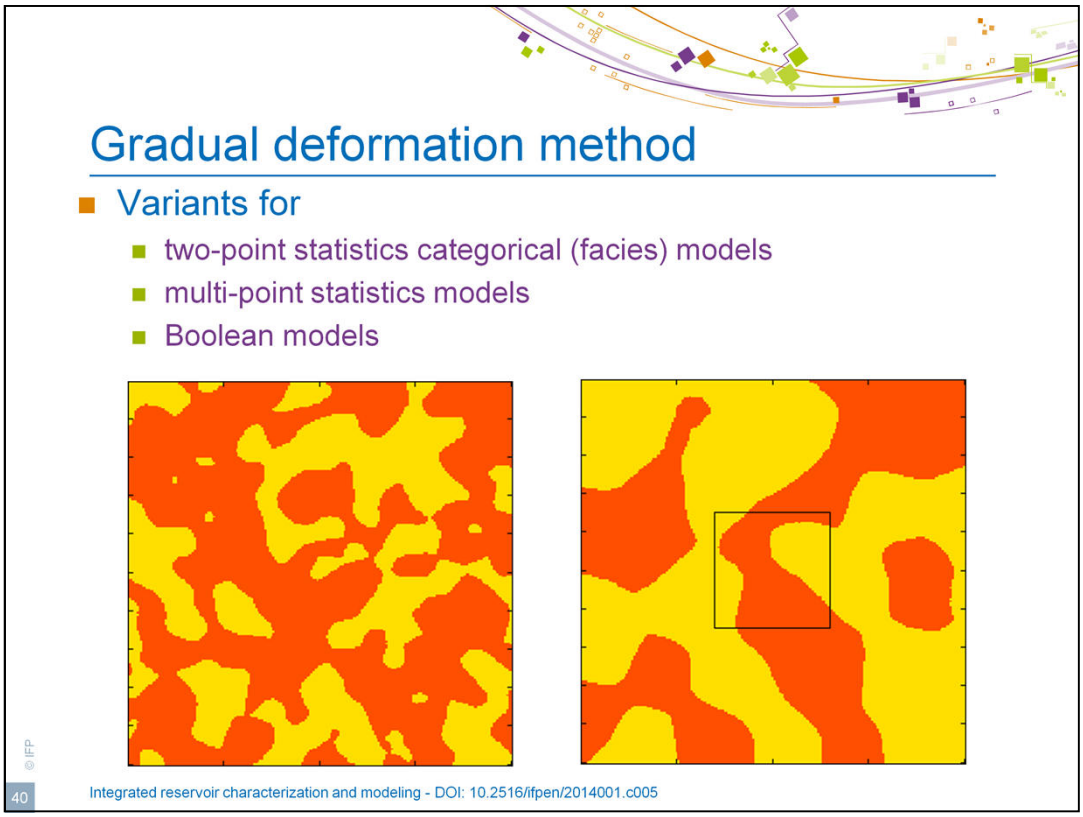

The GDM can be also used to modify two-point statistics categorical models, multi-point statistics models and even Boolean models as will be seen for fractures in a subsequent section (Hu *et al.*, 1999; Hu *et al.*, 2001a; Hu *et al.*, 2001b; Hu and Jenni, 2005; Jenni *et al.*, 2007; Hu and Chugunova, 2008).

The two examples displayed above describe the global (left) and local (right) gradual deformation of facies realizations.

Last, it has to be mentioned that cosimulation can be envisioned as a tool to modify a realization. Varying the correlation coefficient relating two realizations actually boils down to varying a gradual deformation parameter (Le Ravalec-Dupin and Da Veiga, 2011).

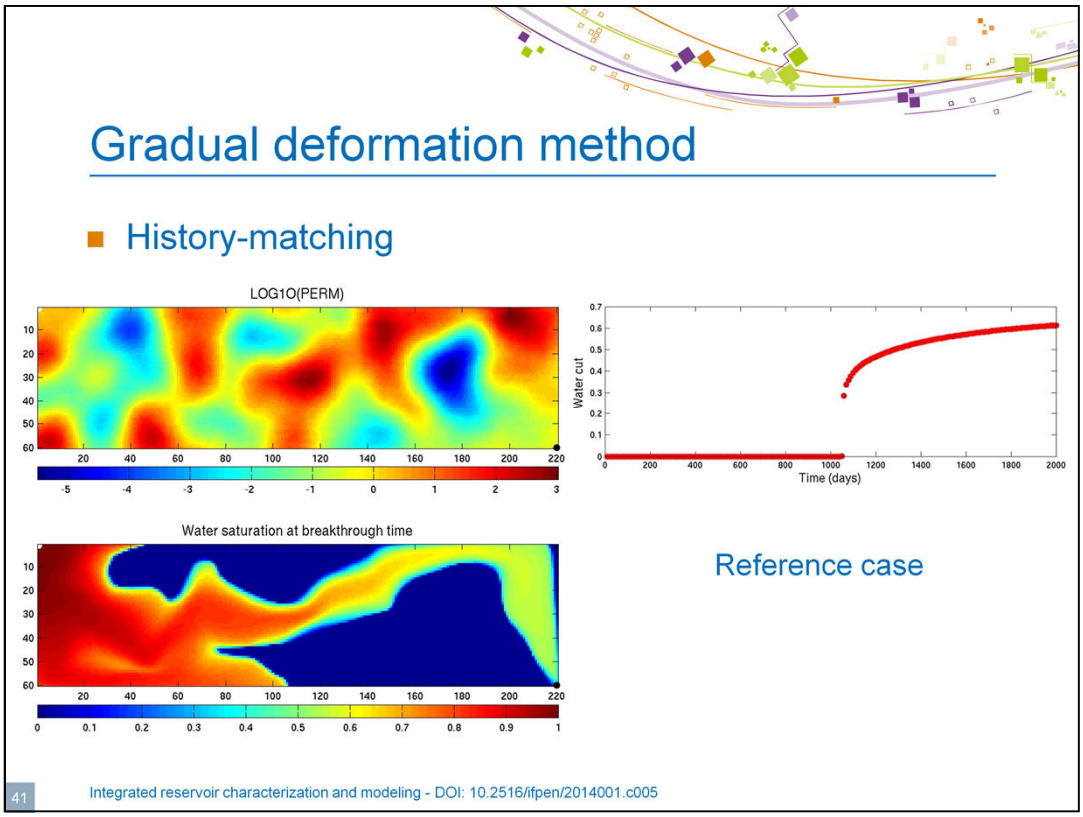

When the GDM is incorporated into optimization processes, the deformation parameter becomes the parameter to be adjusted to reduce the objective function.

Let us consider the following two-dimensional case as a reference case. The reservoir model comprises 220 × 60 grid blocks. The spatial variability of the log-permeability is described by an isotropic Gaussian variogram with a range of 30 grid blocks. The logarithm of permeability is shown on the top, left. There is one water injector in the top left corner and a producer in the opposite corner (bottom right). The water cut simulated at the producer is displayed on the right against time. The breakthrough time is about 1100 days. Water saturation simulated at breakthrough time is then represented on the bottom left.

For illustration purposes, we assume that the objective function quantifies the water cut mismatch.

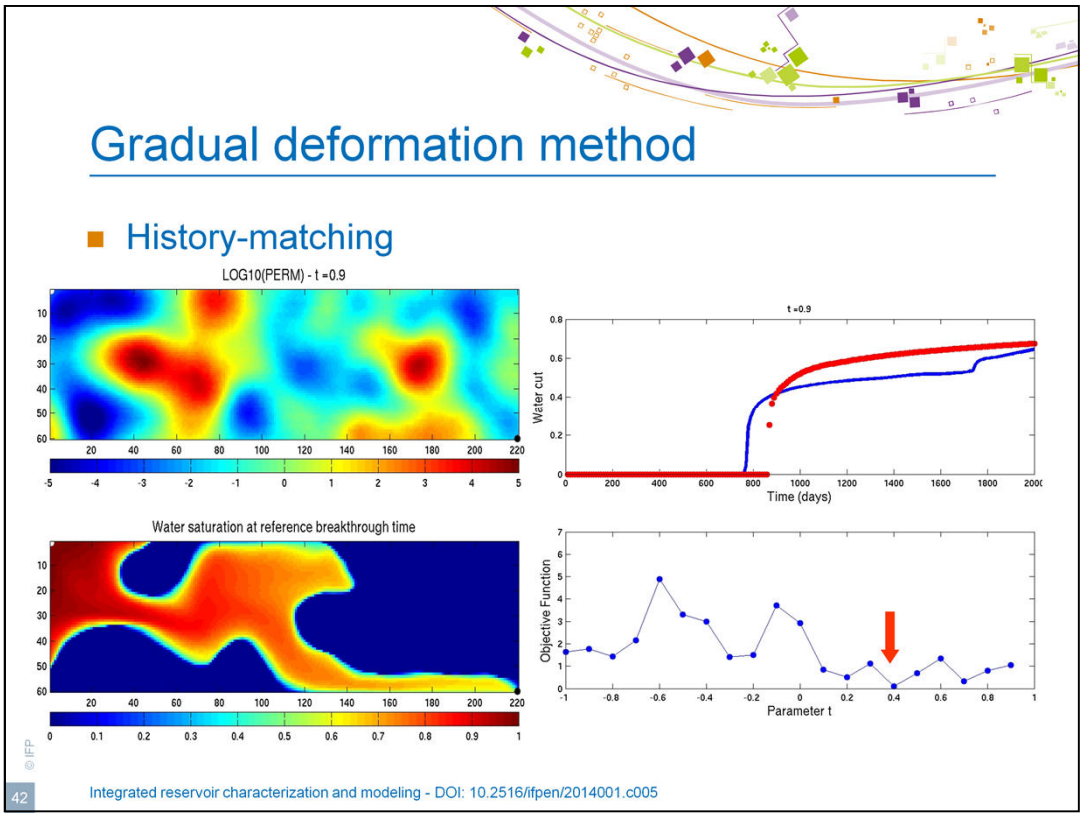

The GDM can be used to vary the petrophysical realizations populating the reservoir model from a limited number of deformation parameters.

We consider a given starting permeability realization (top left). It is associated to a *t* deformation parameter of -1. The simulation of water injection to push oil towards the producer (from top left to bottom right) provides the water cut at the producer and water saturation over the whole reservoir at the breakthrough time known for the reference permeability case (previous page). The water cut (blue line) is displayed as a function of time (top right figure) and is compared to the reference water cut (red dots). The water saturation map is shown on the bottom left. The objective function that measures the water cut mismatch is plotted on the bottom right graph.

The deformation parameter is varied from -1 to 1. This results in a gradual deformation of the entire permeability realization. Again, a flow simulation is run for each deformed realization, thus providing the water cut and the water saturation map. Although the deformation is gradual and smooth, the water cuts and saturation maps are clearly impacted. When the deformation parameter is -1, the simulated breakthrough time is larger than the reference one and the objective function is about 2. When the deformation parameter is -0.9, the breakthrough time increases, and the objective function too. The gradual variations in the permeability field produce significant variations in the flow behavior.

When this approach is applied for history-matching purposes, the idea is 1) to screen the chain of realizations by varying the deformation parameter and 2) to select the realization, which better fits the reference data. In this case, it is the one obtained with a deformation parameter of 0.4. However, even though this *t* value gives an objective function value close to 0, the corresponding permeability and saturation fields are quite different from the reference ones. The information content in the data is not enough to identify a single solution.

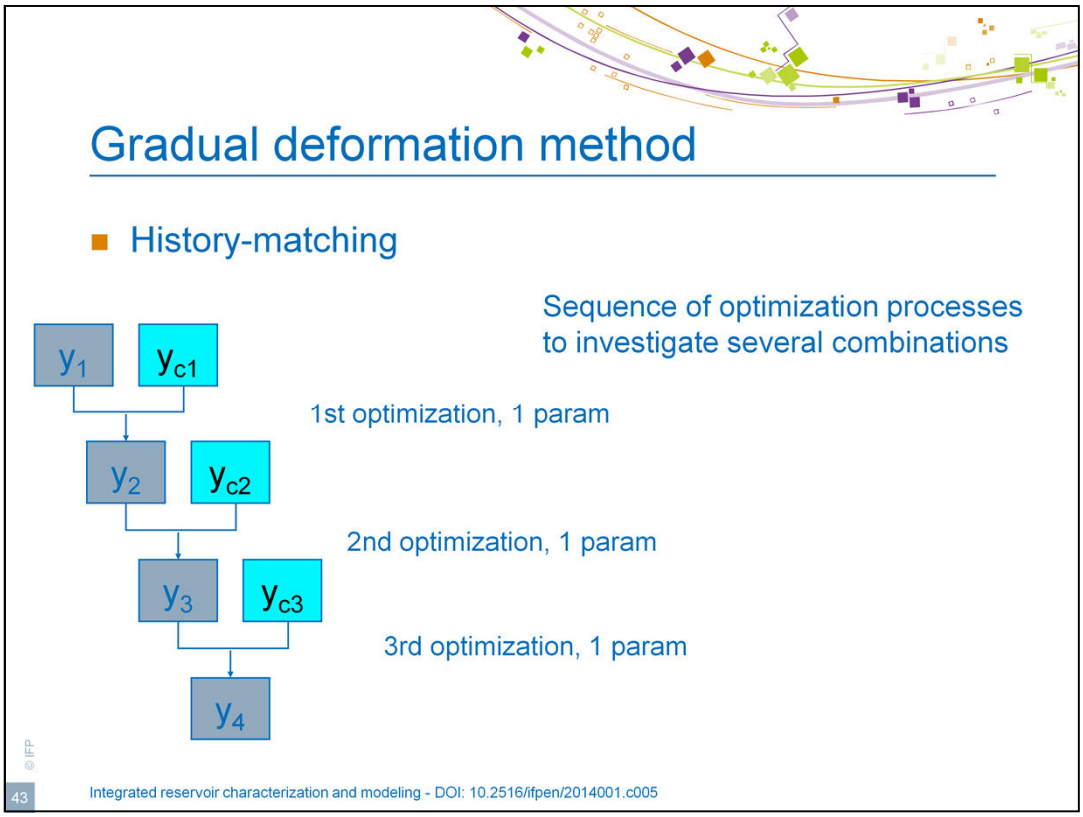

The combination of two realizations creates a path in the search realization space, but it represents only a very tiny part of it. Investigating this path solely can help reduce, but not minimize the objective function. The overall method is made more efficient by iterating the search process.

First, two realizations, randomly drawn from the prior pdf, are combined to create a path. A first optimization process is run to determine the “best” realization along this path (the one, which reduces the objective function as much as possible). Second, we start from this "best" realization and combine it with a new realization drawn again from the prior pdf. This yields a new path in the search space. Investigating also this path can provide a realization decreasing further the objective function. Then, paths are successively built and scanned until the data misfit is small enough. A GDM-driven optimization entails a sequence of optimizations.

Gradual deformation method

- History-matching

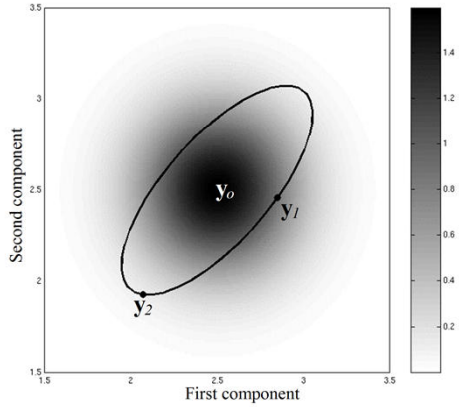

$\mathbf{y}_o\,(y_o, y_o)$

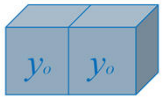

Likeliest reservoir model

$$y(t) - y_o = \cos(\pi t)(y_1 - y_o) + \sin(\pi t)(y_2 - y_o)$$

Integrated reservoir characterization and modeling - DOI: 10.2516/ifpen/2014001.c005

For simplicity, we focus on a reservoir model with two grid blocks populated by two values independently and randomly drawn from the prior pdf N(2.5,0.3).

The values assigned to the two grid blocks are plotted on a two-dimensional graph. The abscissa gives the value of the first grid block while the ordinate gives the second one. The prior pdf is shown in black: it is centered around the likeliest prior realization y_o.

Let y_1 and y_2 be two independent realizations representing the reservoir model. Combining these two realizations on the basis of the gradual deformation scheme yields an ellipse. Each point of this ellipse is associated to a given value of the deformation parameter

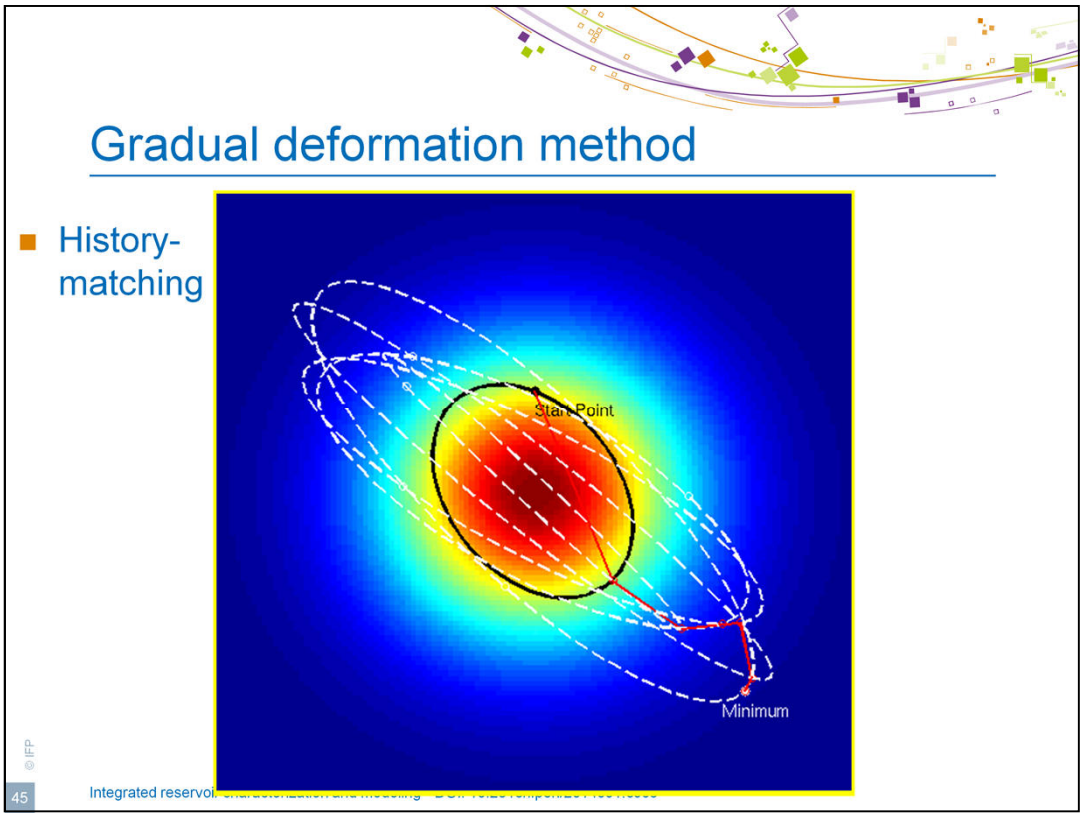

Incorporating the GDM into a history-matching process is then equivalent to the building of a sequence of ellipses (or hyper ellipses for dimensions greater than 2) to investigate the search space (Le Ravalec-Dupin *et al*., 2000). We come back to the previous example with a reservoir model made of two grid blocks and assume that the minimal objective function value is reached for a point far away from the likeliest prior value. Are we able to reach it with a GDM-based optimization process?

We scan the initial ellipse and identify the deformation parameter associated to the realization the closest to the minimum. Then, we consider this realization as the new starting one and we randomly generate a new complementary realization from the prior probability density function. These two new realizations are used to build a new ellipse that we scan again to identify a realization still closer to the minimum. The process is repeated until reaching or getting close enough to the minimum.

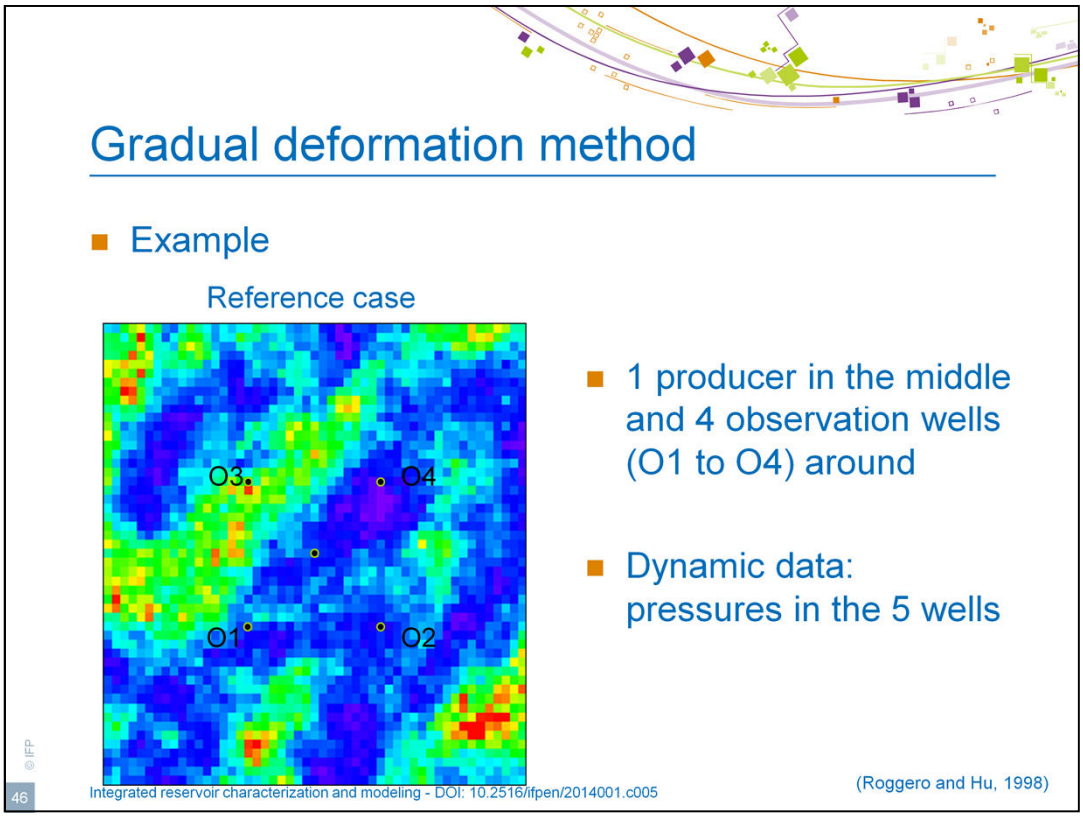

We focus on the application case already considered for illustrating the potential of the pilot point method (Roggero and Hu, 1998).

This is a two-dimensional reference reservoir permeability model (see figure above) with one producer in the middle of the reservoir and 4 observation wells around, labeled O1, O2, O3 and O4. This reference model was inputted into a flow simulator to compute pressures in the five wells. This is the set of reference dynamic data.

We now run a gradual deformation based history-matching process in order to determine a model respecting the reference set of pressures.

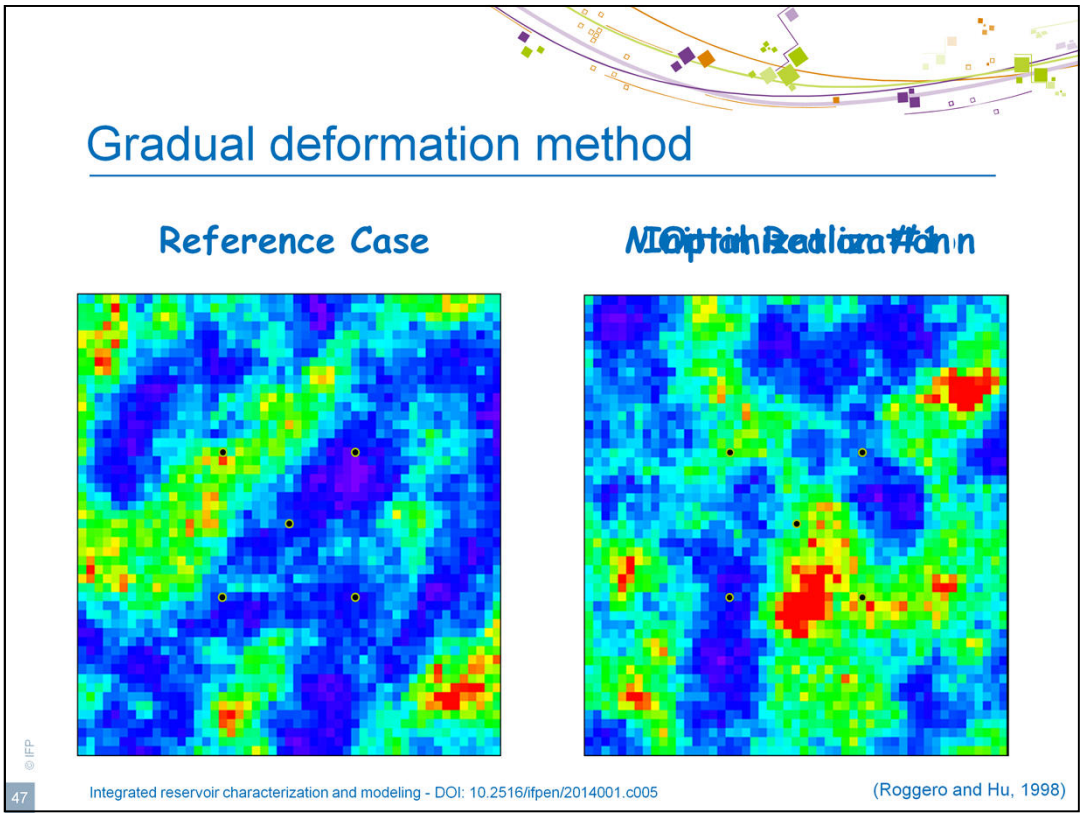

The reference model is kept on the left for comparison purposes, but it is assumed to be unknown. The only available data are the prior probability density function and the pressures collected at wells.

We perform history-matching with the GDM to drive the changes applied to an initial permeability model (right) randomly drawn with respect to the prior probability. In the test performed, the gradual deformation process involves the combination of 10 realizations from 9 deformation parameters. The deformation is applied to the entire model. Four matching processes are run one after another, each time starting from the best model previously achieved. The first optimization leads to a “best” model, the second one to an improved “best” model, the third one too. The fourth matching process actually provides the final “best” model. At this point, the search process is stopped because the objective function is small enough.

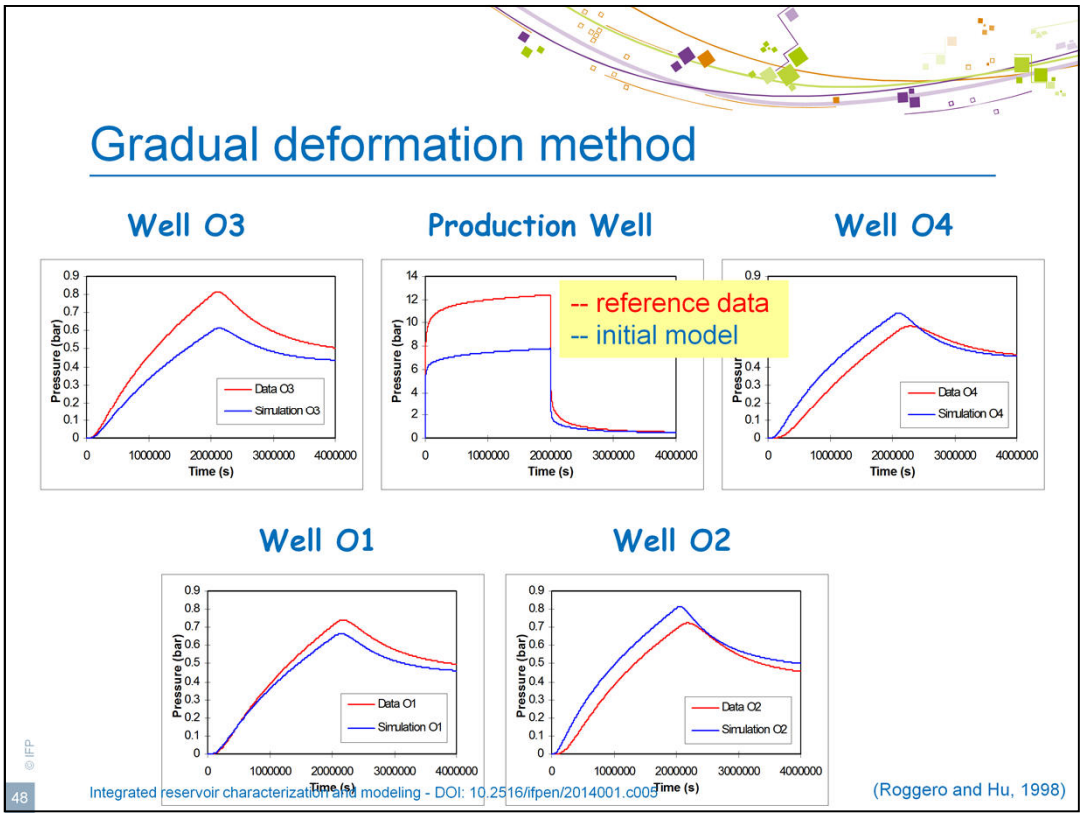

The pressures simulated at wells for the initial model (blue curves) are compared to the reference pressures (red). There are clear differences for all of the wells.

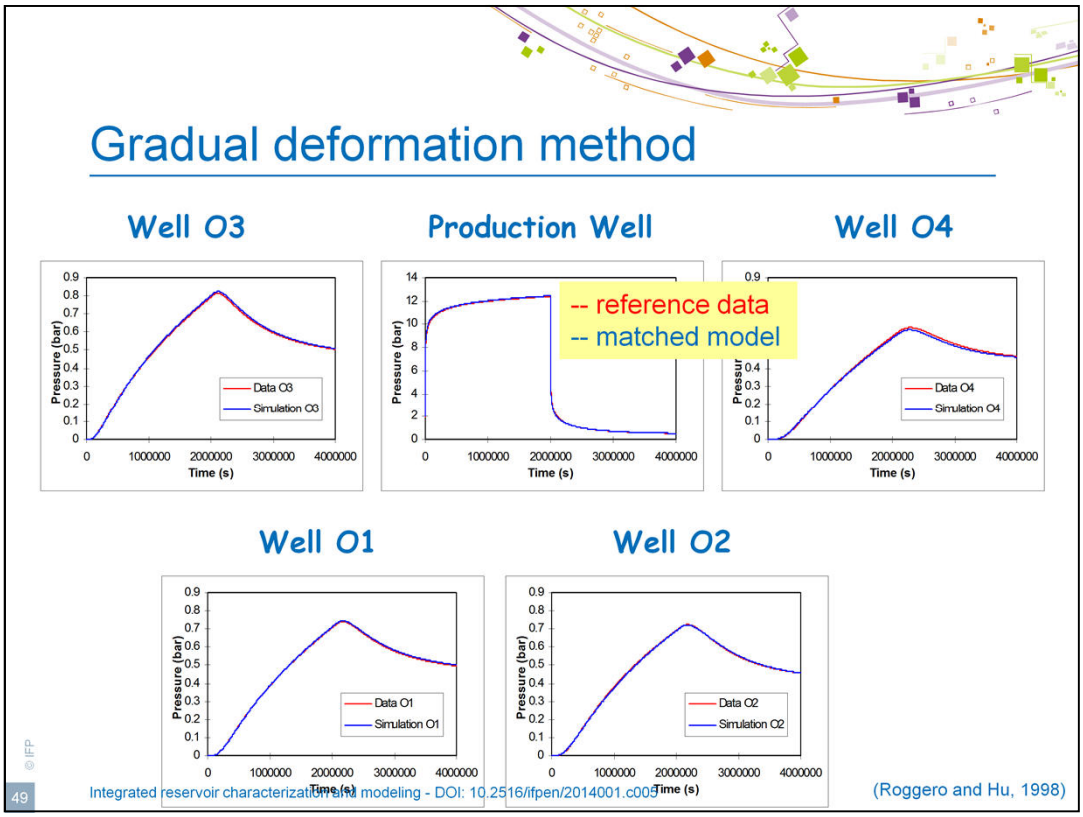

Now, we compare the pressures simulated at wells for the final matched model (blue curves) with the reference pressures (red). The final match is perfect. Such a result can be achieved because the problem is quite simple.

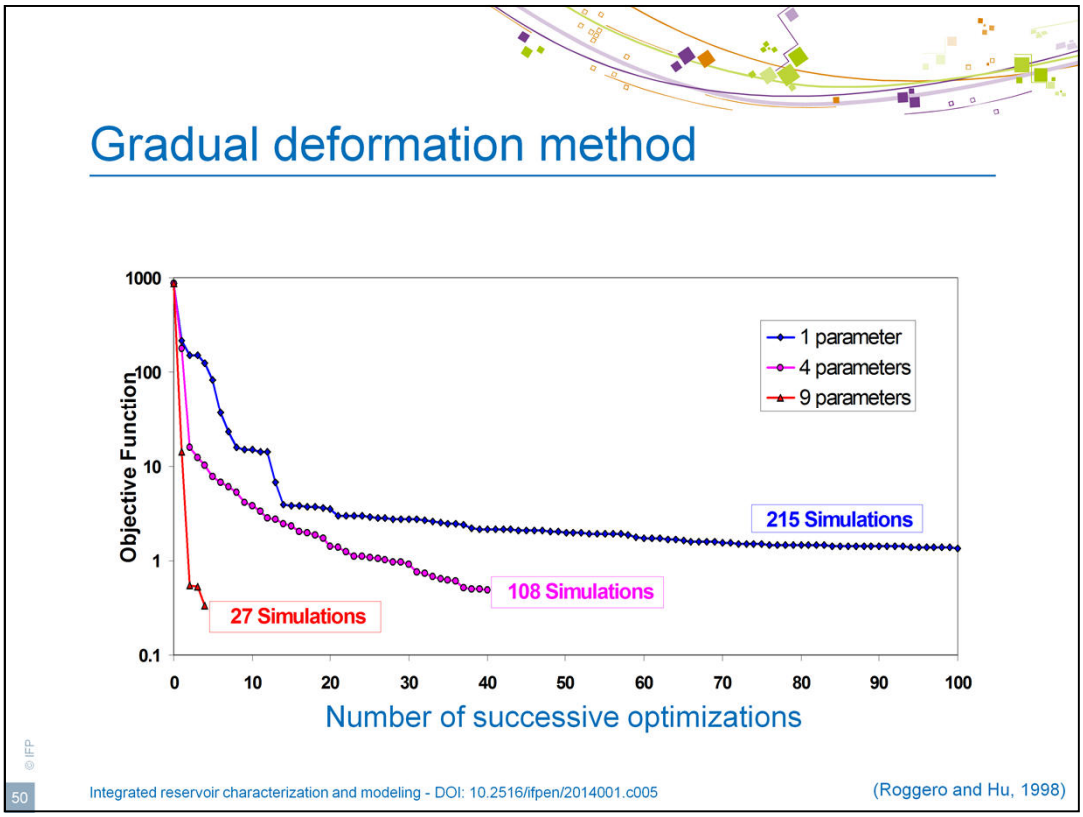

Three matching tests were performed for the application case previously described. The first one involves 1 deformation parameter, the second one 4, and the last one 9. They correspond to the combination of 2, 5 and 10 realizations, respectively. The graph above shows the evolution of the objective function against the number of successive optimizations performed. For every tests, we mention the total number of objective function evaluations (*i.e.*, the total number of flow simulations performed).

Two features are stressed.

1) Increasing the number of parameters accelerates the objective function decrease. This behavior is expected as an increase in the number of parameters provides more degrees of freedom, *i.e.*, more flexibility to investigate the search space.

2) Even though the objective function significantly decreases, especially during the very first iterations, it reaches kind of a plateau at some point. This behavior is explained as follows by Capilla and Llopis-Albert (2009). As more realizations are combined during the sequence of optimizations, the chances of significantly modifying the current realization from the new realizations added to the combination decreases. Thus, after a few iterations, the *t* deformation parameter remains close to zero. In other words, the current realization carries more and more information while the added random realizations are likely to depart more from the production data included into the objective function.

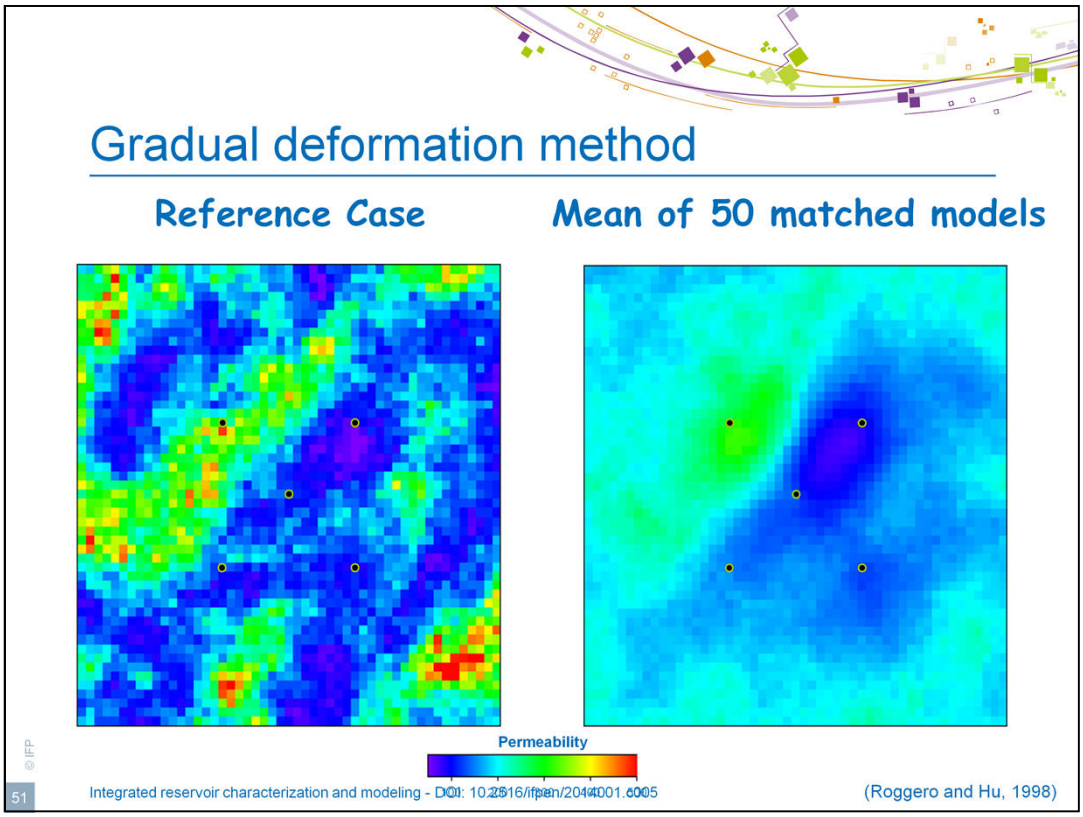

Another test was carried out by Roggero and Hu (1998) based upon the same study case. These authors actually run the matching process 50 times starting from 50 distinct initial permeability realizations. Therefore, they obtained 50 distinct final matched realizations. The mean of these 50 matched realizations is shown on the right and can be compared to the reference permeability case on the left. We observe that the mean of the 50 matched models captures the main features or trends of the reference model.

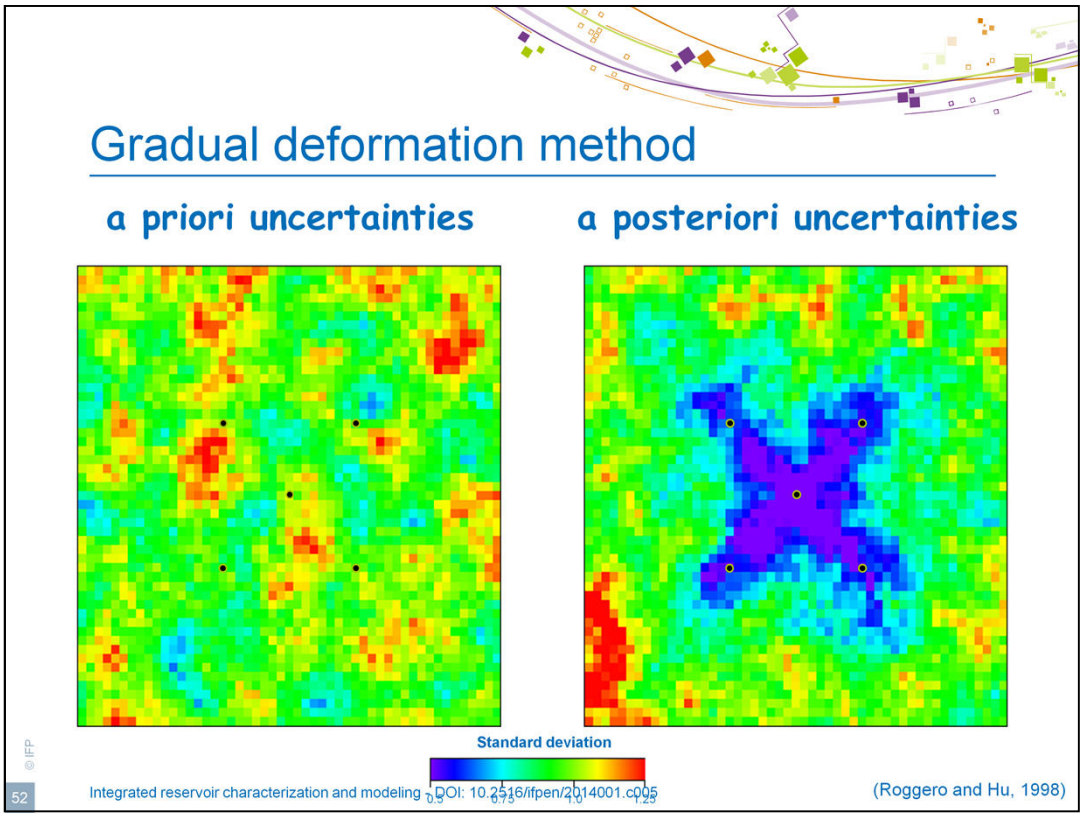

The variance was also computed for the 50 initial permeability realizations (left) and for the 50 final matched permeability realizations (right). For the initial realizations, the variance is about 1 everywhere (it would be 1 for an infinite number of initial realizations). For the matched realizations, the purple cross linking the wells highlights the uncertainty decrease due to the integration of pressure data into the model.

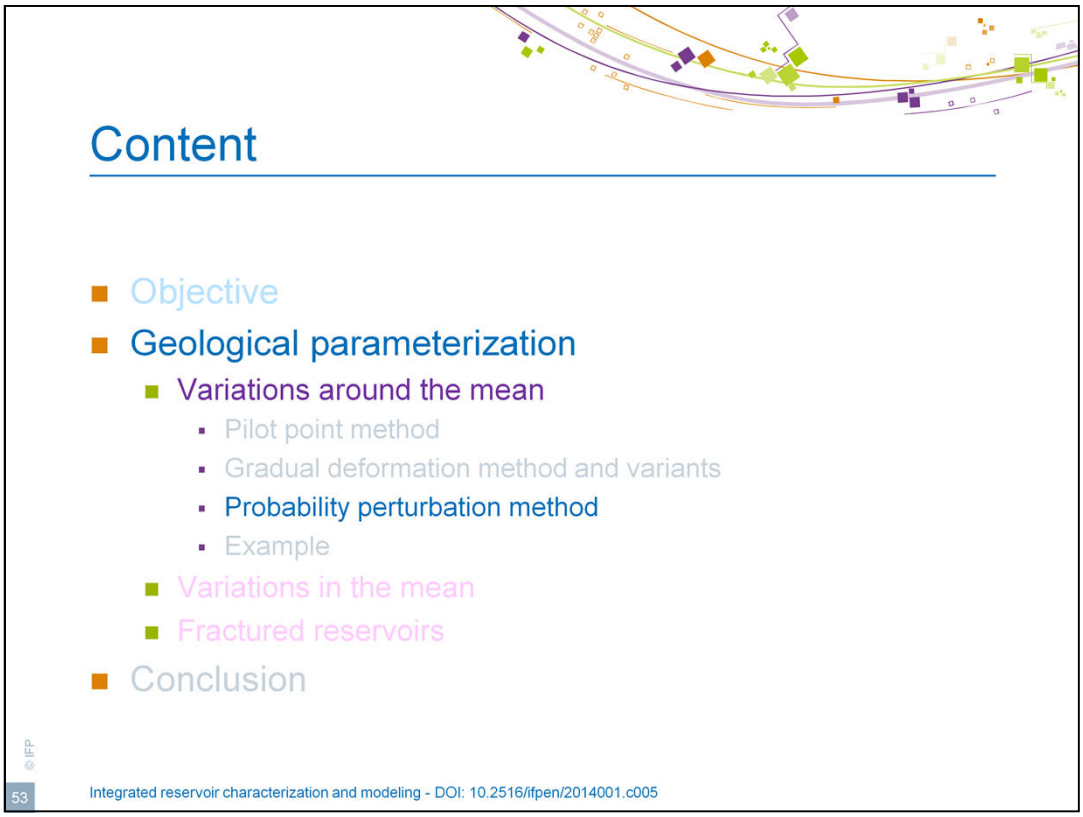

Another method to modify the fluctuations of a realization around the mean is the probability perturbation method, which was introduced by Caers (2003).

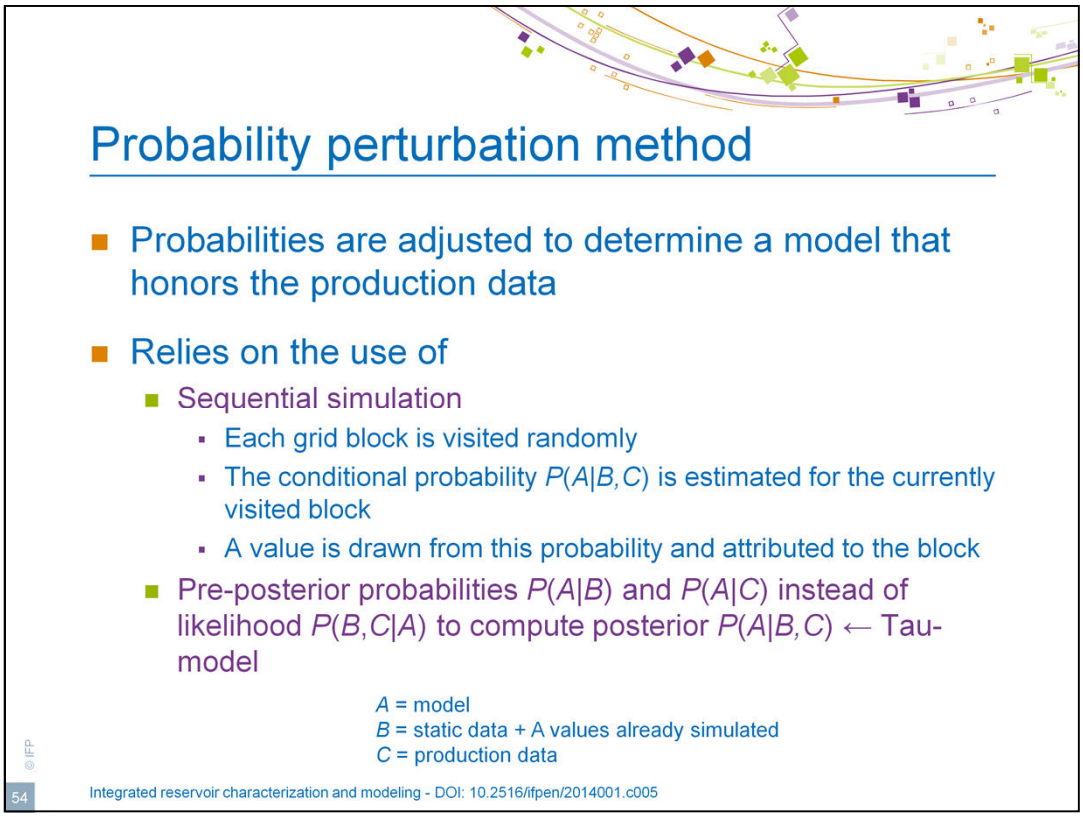

The probability perturbation method (PPM) is an alternative to the gradual deformation method, but it focuses on the perturbation of probabilities instead of realizations.

The method relies on two main principles (Caers and Hoffman, 2006):

1) the use of sequential simulation: a given joint probability can be written as the product of a series of univariate conditional distributions. Thus, each block of the grid is visited randomly. For each of them, a value is drawn from the conditional probability $P(A|B,C)$ to be attributed to that block. $P(A|B,C)$ is the probability of A occurring given information B and C. B includes the hard data and the values simulated for the blocks previously visited. C represents the production data. The difficulty consists in estimating the conditional probability. A is the variable at the grid node visited.

2) the use of pre-posterior probabilities instead of likelihoods within the decomposition of the posterior probability $P(A|B,C)$. This is performed referring to the Tau-model (Journel, 2002).

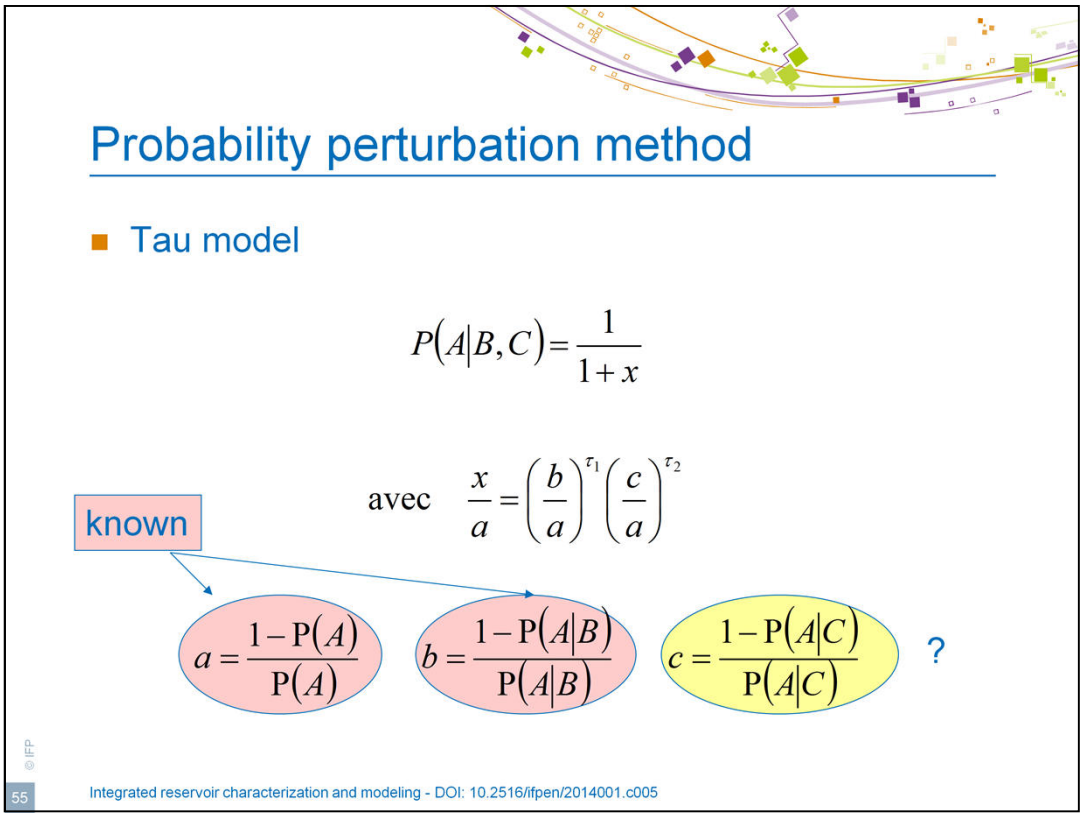

The Tau-model (Journel, 2002) involves the following expressions to combine $P(A|B)$ and $P(A|C)$ into $P(A|B,C)$. $P(A)$ is the prior probability. $P(A|B)$ is the probability of A occurring given B, where B is the set of hard data plus the A values attributed to the grid blocks previously visited. $P(A)$ and $P(A|B)$ can be estimated. The main difficulty is the determination of $P(A|C)$, that is the probability of A occurring given the production data.

The τ coefficients are usually set to 1. This amounts to a form of conditional independence.

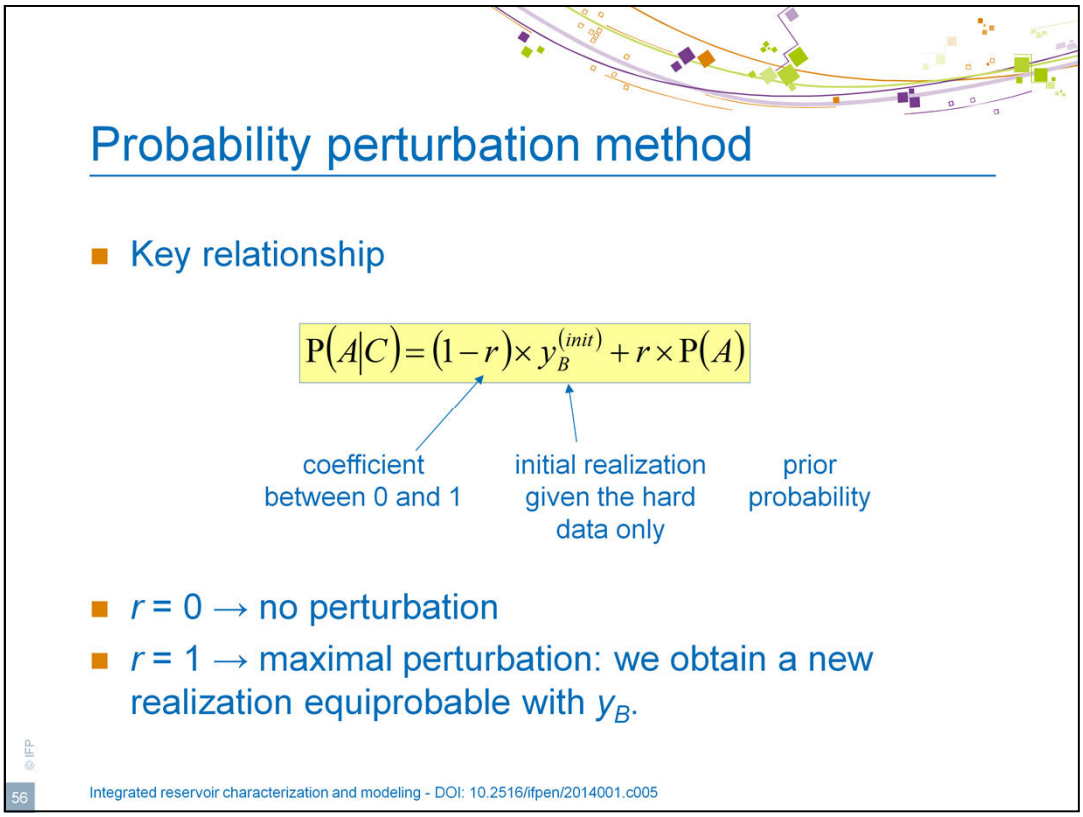

$P(A|C)$ is unknown. The probability perturbation method key idea is to perform a stochastic search for these unknown probabilities (for every grid blocks) in order to achieve a realization matching the production data C.

The method relies on the perturbation relation shown above that depends on the initial realization y_B simulated conditionally to the static data solely and the prior probability $P(A)$. The r perturbation parameter that belongs to the [0; 1] interval, controls how much the model parameters vary in the iteration process. This relation applies locally, meaning that y_B is the value of the initial realization in the grid block currently visited. This relation changes the problem. Instead of searching for probabilities $P(A|B,C)$ (hence $P(A|C)$), we search for a single r parameter that finally yields a realization matching the C production data.

When $r = 0$, the realization y is unchanged. When it is 1, $P(A|B,C) = P(A|B)$: we obtain a new realization equiprobable with the initial one (y_B). This is the maximum perturbation step.

This search process must be repeated in order to better explore the parameter space.

In addition, the underlying spatial structure is also maintained through all perturbations.

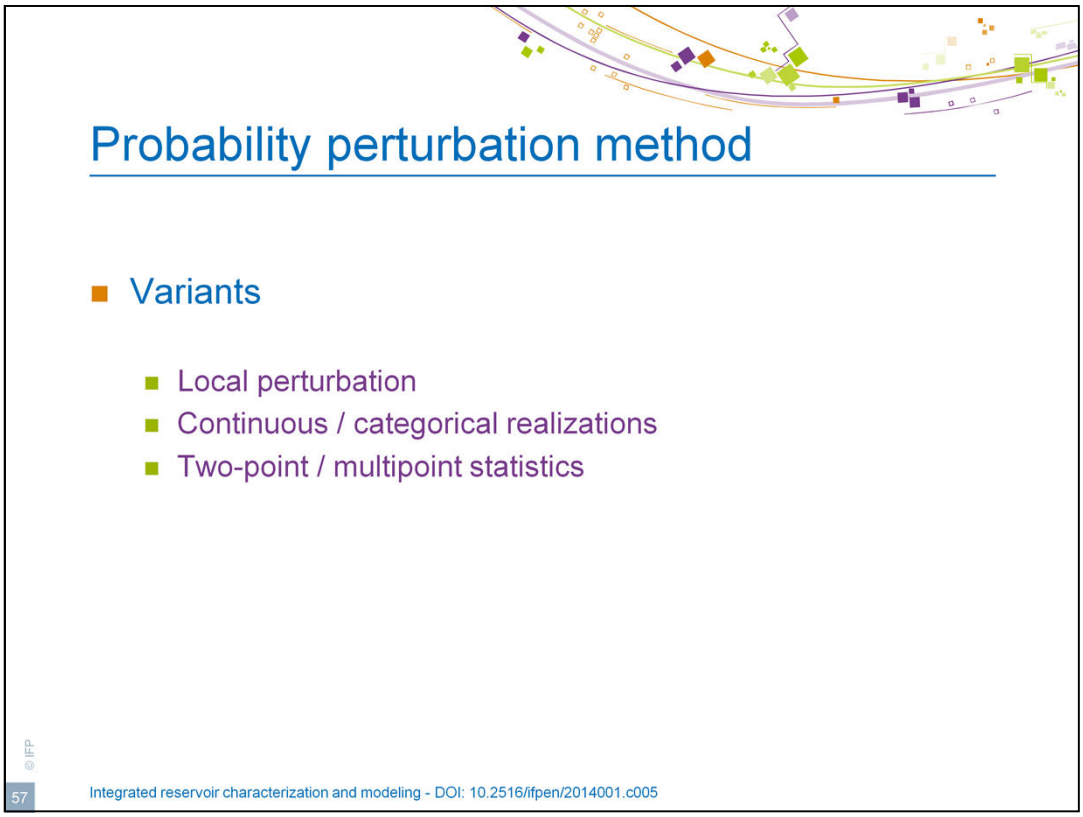

Just as the gradual deformation method, the probability perturbation method has been extended to cope with various cases.

Intrinsically, it is closely related to the sequential paradigm. Thus, it can be used with any of the sequential simulation techniques to produce continuous or categorical realizations, referring either to two-point or multipoint statistics.

In addition, it can be applied to modify the whole reservoir model or only given sub-domains (Hoffman and Caers, 2005).

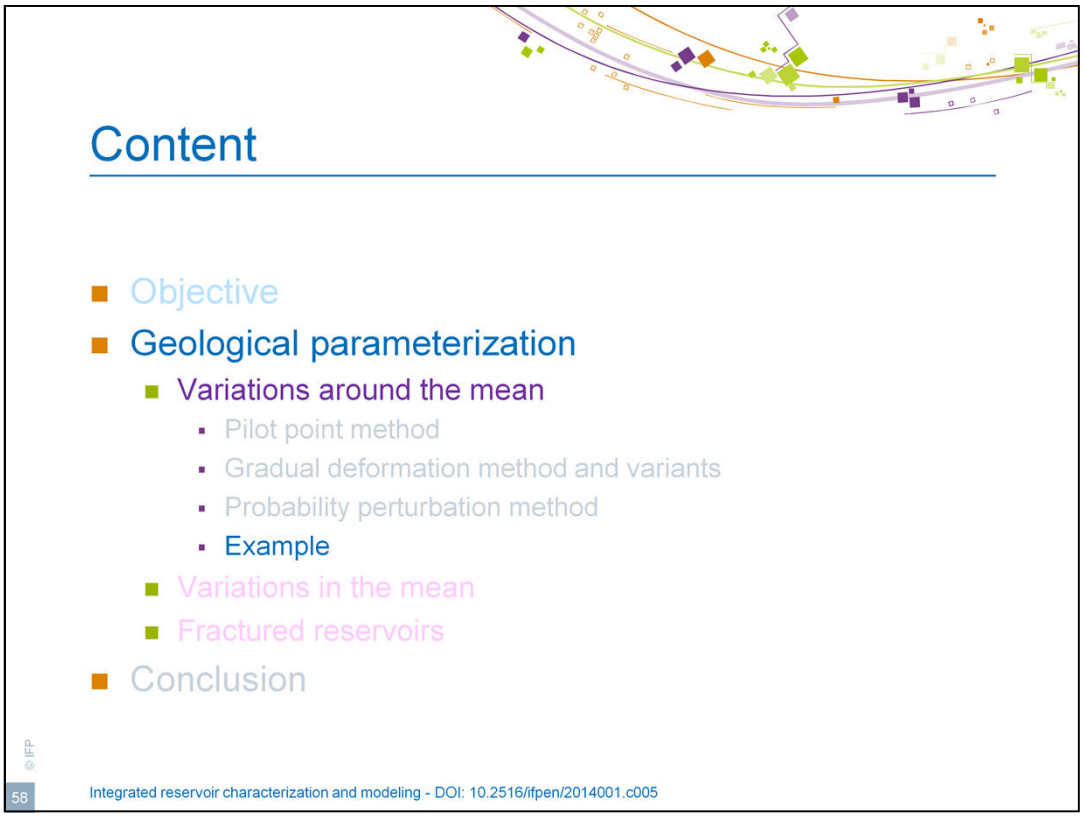

This section presents an example for which the gradual deformation method is used to locally adjust the petrophysical model.

Adjusting the fluctuations around the mean Example

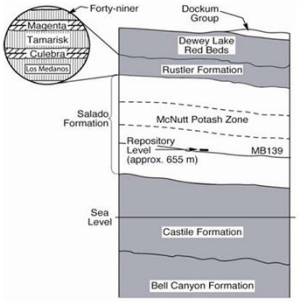

- Objective: modeling transmissivities in the Culebra Dolomite aquifer, the most likely pathway of radionuclide transport from the repository in case of a leak
- Data: transmissivities in 45 wells, heads in 36 wells

Integrated reservoir characterization and modeling - DOI: 10.2516/ifpen/2014001.c005

Again, we come back to the WIPP (Waste Isolation Pilot Plant) case presented in Chapter 2, p. 44.

As already explained, the idea is to model the transmissivities (m^2/s) in the Culebra Dolomite aquifer 450 m above the repository level. This aquifer is the most likely pathway of radionuclide transport from the repository in case of a leak. The available data consist of transmissivity measurements in 45 wells and head measurements in 36 wells.

In Chapter 3, p. 25, we built models consistent with the available transmissivity measurements solely using both estimation and simulation techniques. Given the boundary conditions (constant head values of 950 m and 890 m on the north and south, respectively, and no flow on the east and west, see chapter 4, p. 9), we simulated heads for the simulated transmissivity models (see Chapter 4, p. 11). We observed that heads can behave very differently depending on transmissivity heterogeneity.

We now aim to make these transmissivity models consistent also with the available head measurements.

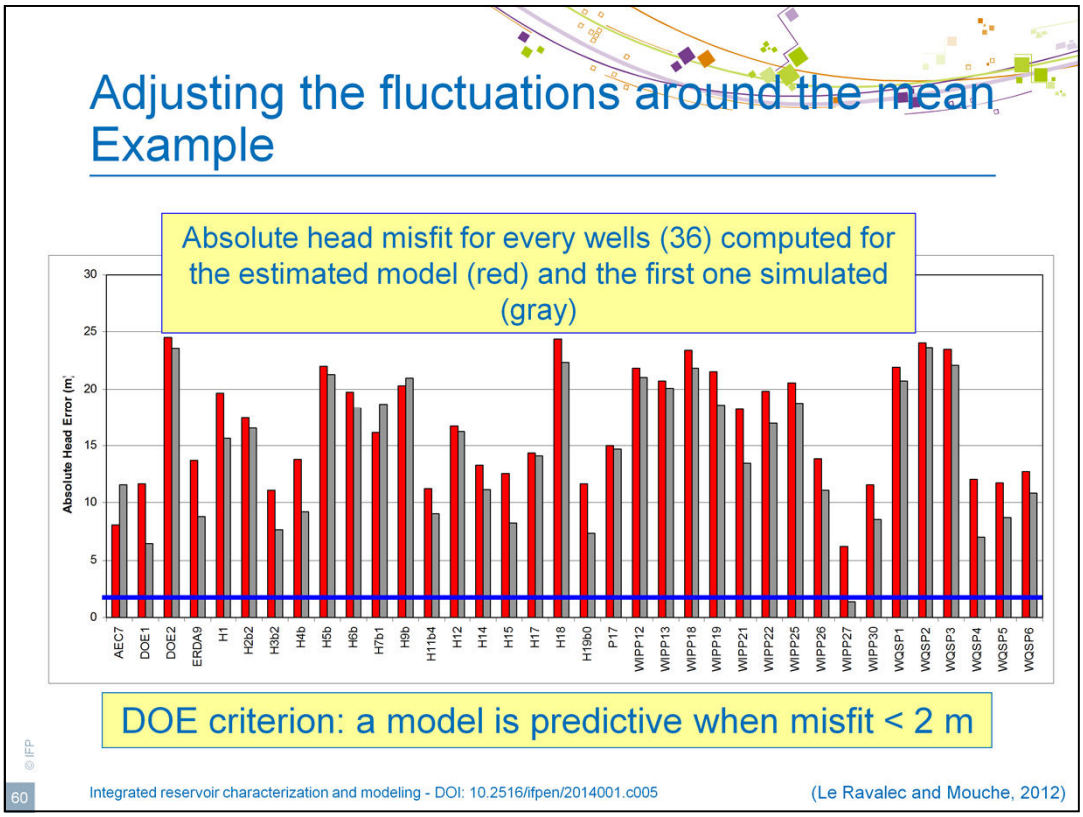

The head error is reported for each well in this figure (Le Ravalec and Mouche, 2012). It was computed for both the estimated model (red bars) and for a randomly simulated one (gray bars). The error is about 15 meters.

However, for this case study, a model is considered as reliable provided the error is less than 2 m (US Department of Energy, 2004). As a result, none of these models is appropriate. This emphasizes the need for history-matching.

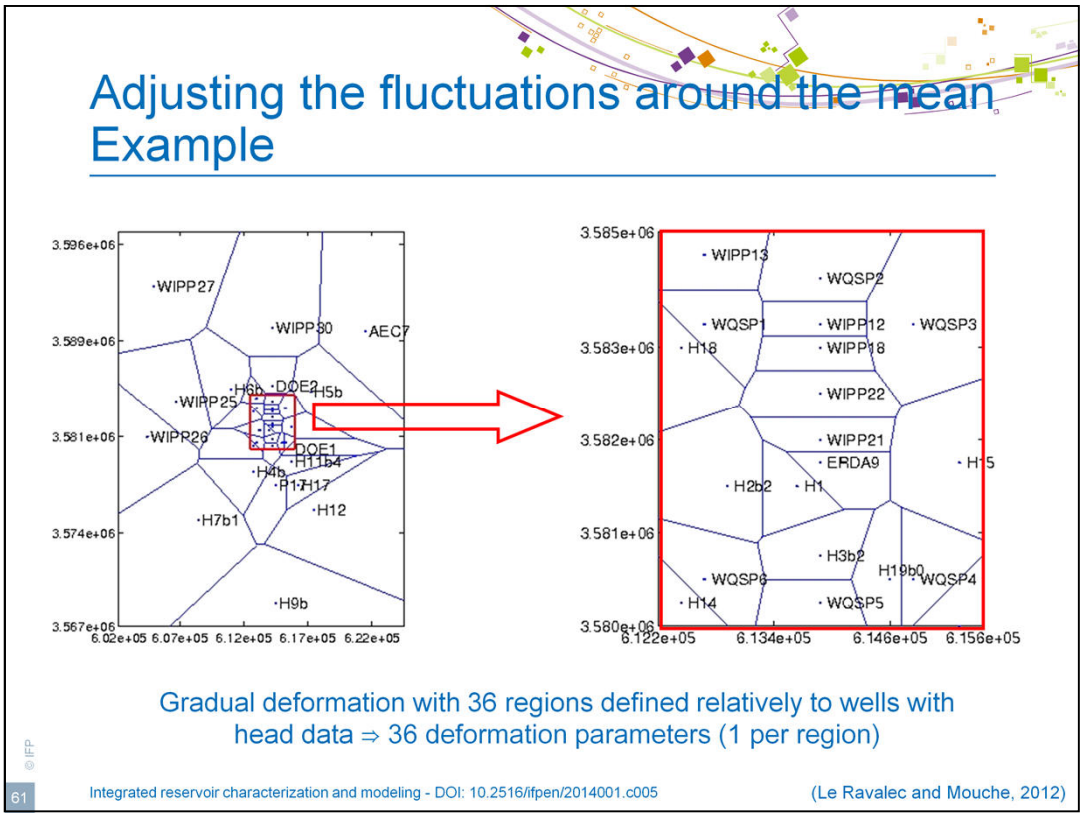

We decided to perform history-matching using the gradual deformation method (GDM) to drive the changes in transmissivities. The local variant of GDM was preferred in order to have more flexibility. Note that the probability perturbation method could have been applied the same way.

The Culebra model was split into 36 regions centered on the wells with head data as shown above. For simplicity, the 36 regions were designed as Voronoï polygons. The figure on the right-hand side is a magnification of the middle red rectangle in the left figure. It corresponds to the area right on the top of the WIPP site.

A region is then linked to a unique well and encloses all the grid blocks lying closer to this well. For performing local deformations, we assigned one deformation parameter to each region, which resulted in 36 parameters.

Adjusting the fluctuations around the mean
Example

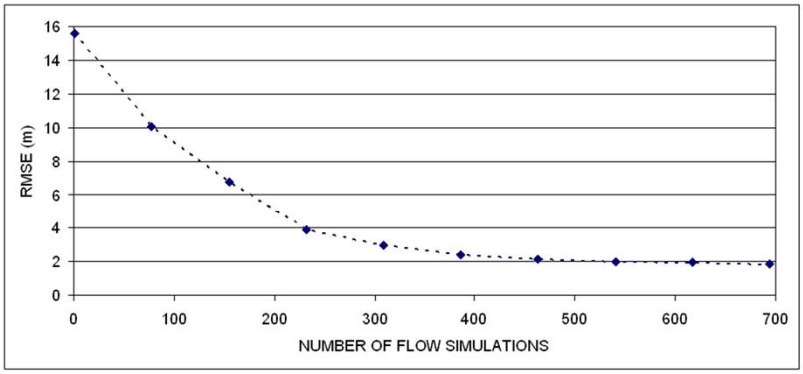

Evolution of the objective function

- 9 successive optimizations
- About 700 flow simulations (650 of them being required for gradient computations)

Integrated reservoir characterization and modeling - DOI: 10.2516/ifpen/2014001.c005

(Le Ravalec and Mouche, 2012)

This figure presents the evolution of the objective function all along the minimization process. It involves the successive investigation of 9 different paths in the search space. The 9 optimization processes were sequentially run, starting each time from the best point obtained right before (indicated by a blue diamond). About 700 flow simulations were required to reduce the objective function down to 2 m. 648 of them were run only for estimating gradients with finite-differences. This could have been clearly avoided with the implementation of an adjoint state (Chavent, 1974).

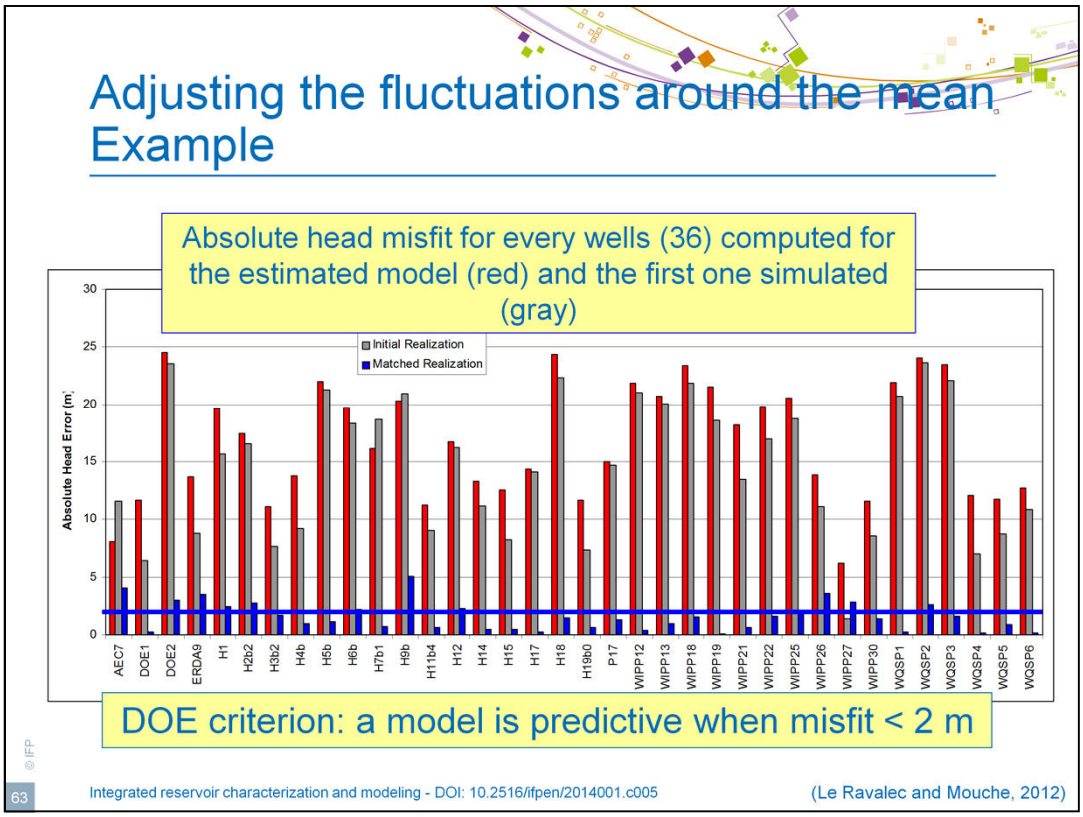

The head error obtained for each well is reported in this figure. It was computed for the estimated model (red bars), the first simulated one (gray bars), and the final matched model obtained starting from the first simulated model.

The head errors are much smaller for the matched model. They are less than 2 m, except for a few wells close to the boundaries (of which well H9b, AEC7 or WIPP26). The head in these wells strongly depend on the specified head boundary conditions, especially in well H9b that is the southernmost well in the domain.

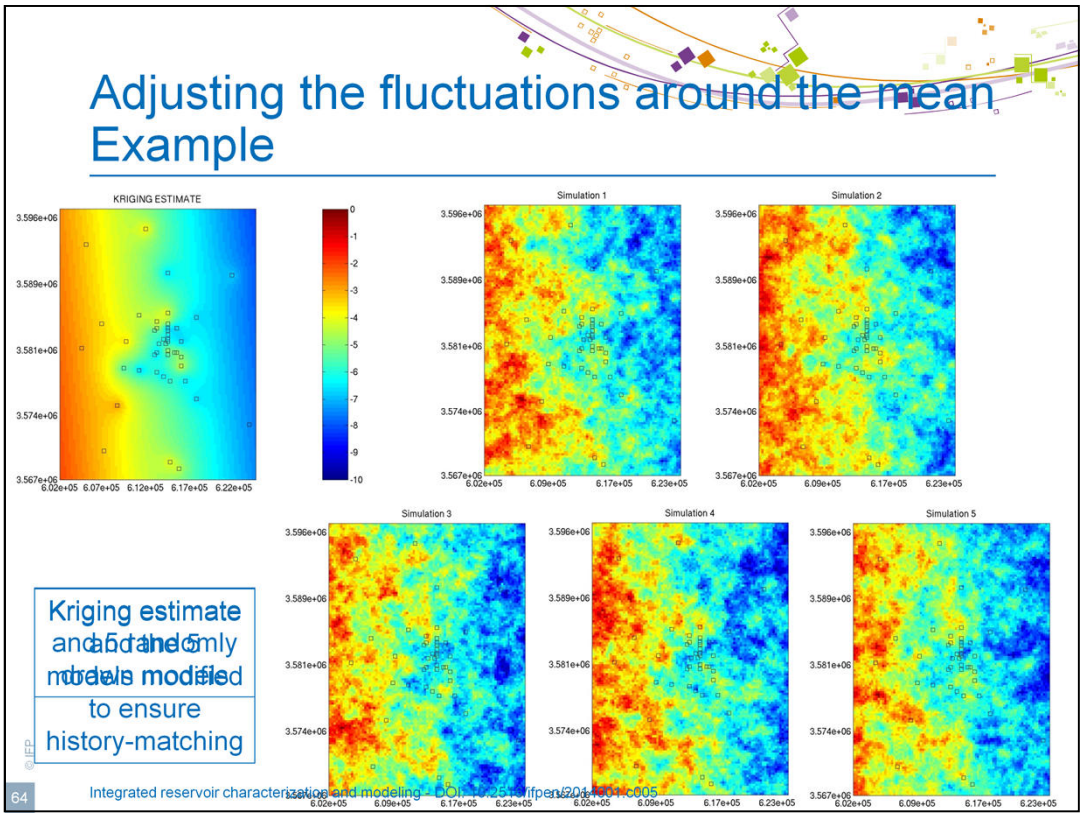

The figure above shows the kriging estimate and the 5 initial simulated models already presented. After applying the GDM-based history-matching process to each of the 5 simulated models, we obtain 5 matched models. The matching processes resulted in significant changes in the transmissivity fields. However, the overall spatial variability is kept.

Adjusting the fluctuations around the mean Example

- Preservation of the variogram

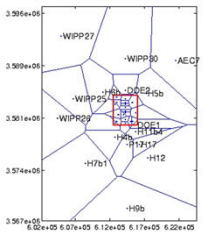

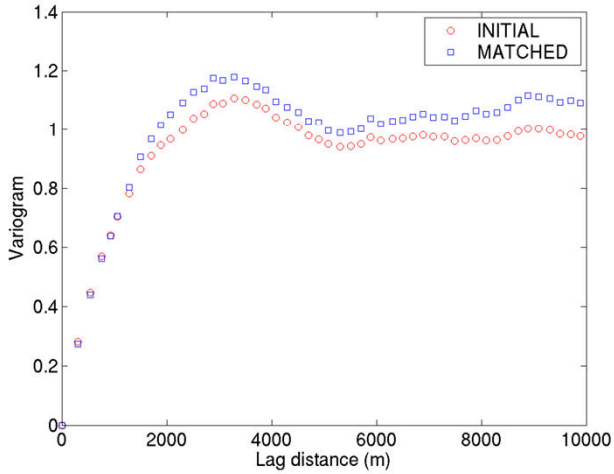

Integrated reservoir characterization and modeling - DOI: 10.2516/ifpen/2014001.c005

We compare the variograms computed for both the initial (red) and final matched (blue) Log transmissivity models. These variograms were determined from the differences between the grid blocks within the WIPP site (middle red rectangle in the area modeled) and all of the others. The two variograms are identical for small distances while the sills are slightly modified. We check that the gradual deformation process ensures the preservation of the spatial structure.

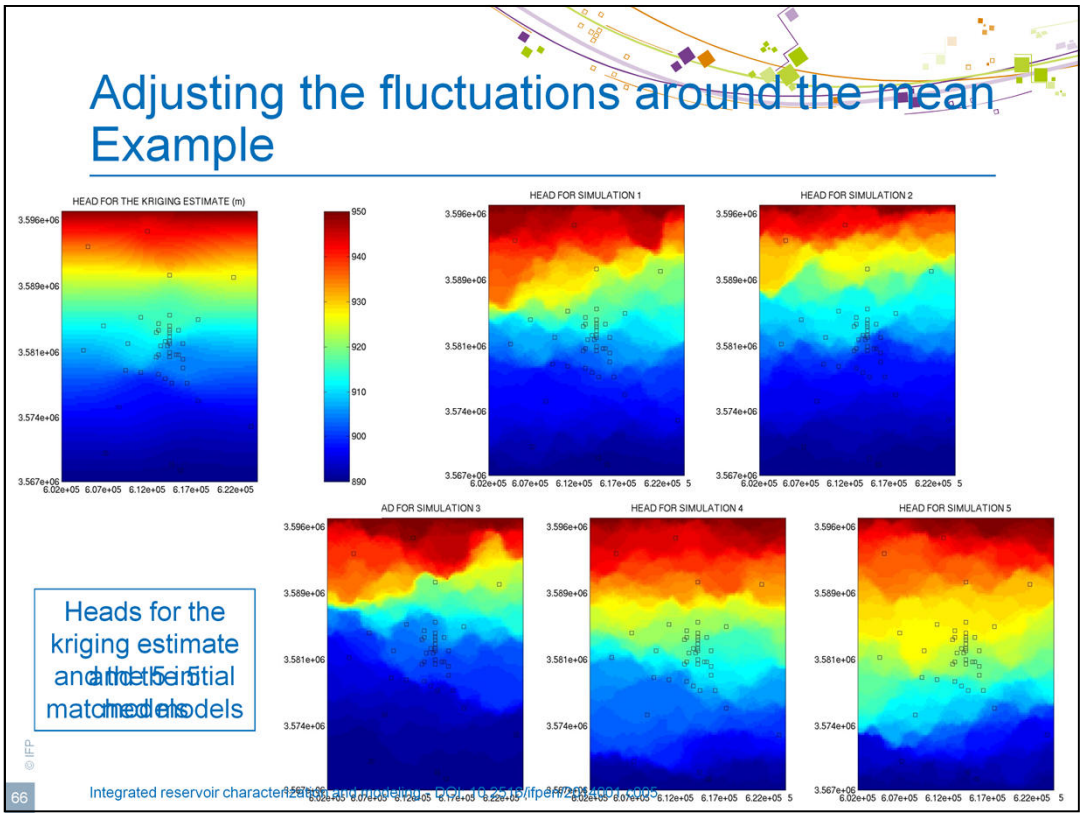

This figure compares the heads simulated for the 5 models initially generated and then, the 5 models obtained at the end of the matching processes starting from the initial ones. The heads computed for the kriging estimate are also shown on the top left. The effect of history-matching on heads is significant. For the models considered, it results in a displacement of the higher head values to the south.

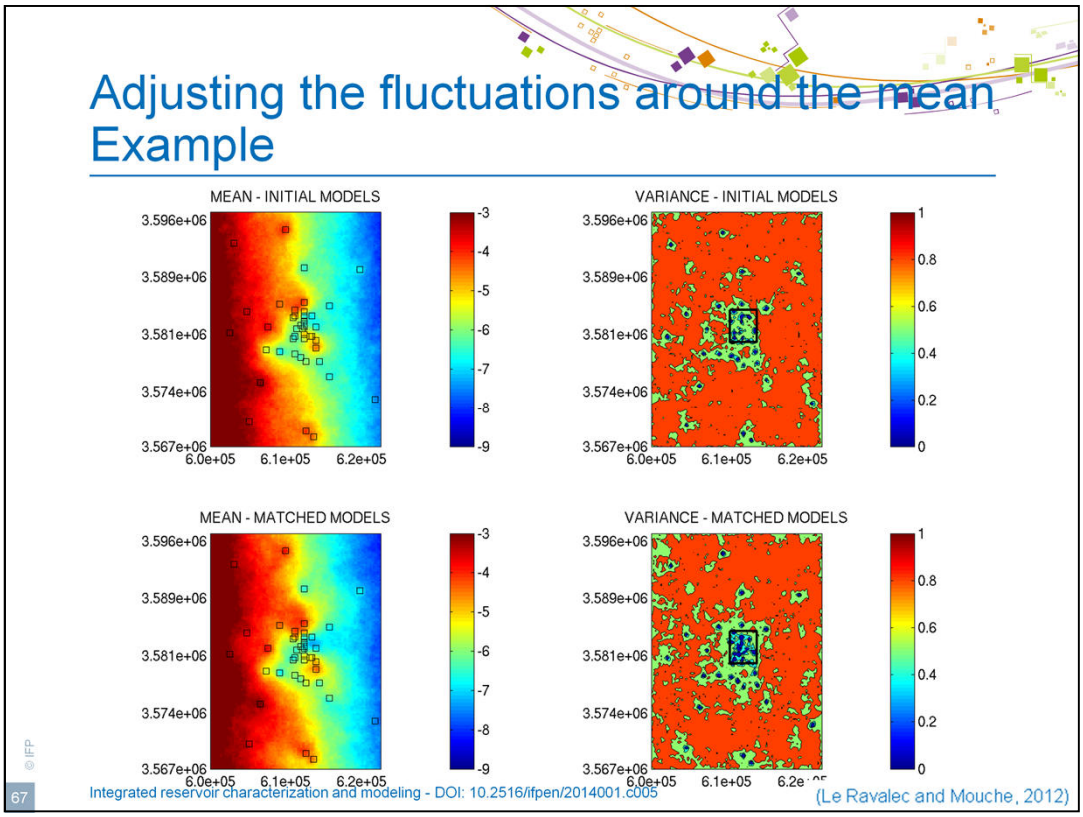

As there is no unique solution, we generated an ensemble of 100 initial equally probable transmissivity realizations constrained to the transmissivity data. Each of these realizations was then calibrated to both transmissivity and head data, resulting in 100 matched transmissivity realizations.

The ensemble mean and variance are displayed above. As expected, the variance goes down to 0 at wells due to the conditioning to transmissivity data and increases to 1 when moving away. However, it is worth focusing on the differences between the two variance maps (top for the initial models and bottom for the matched models) as they stress the informative content of the head measurements. Clearly, the variance decreases for the matched models, particularly in the middle WIPP sub-domain. In other words, there is less uncertainties regarding the model parameters due to data integration.

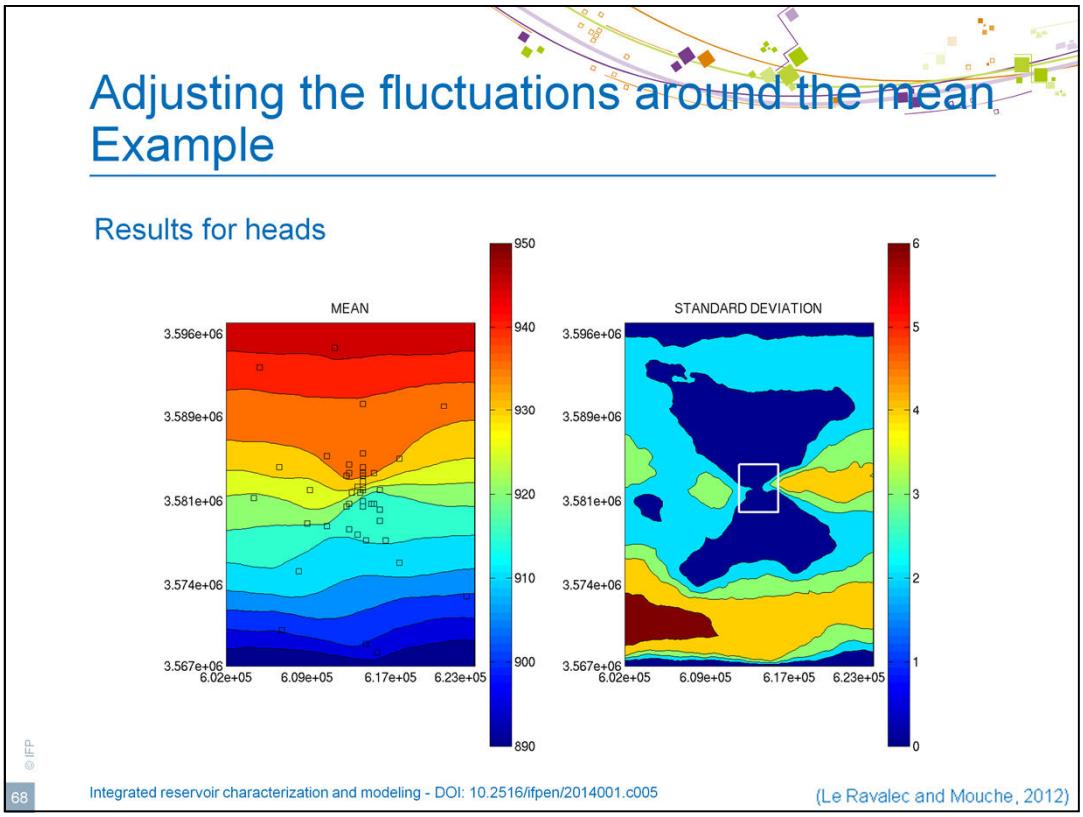

The average and standard deviation of the 100 head realizations computed for the 100 matched LogT realizations are shown on the left and right, respectively. The black squares on the left show the locations of the wells. The large white rectangle on the right indicates the location of the WIPP site.

The head error is reduced mainly in the center of the region studied. There are still uncertainties all around, especially in the south. These results suggest that there are probably uncertainties in the boundary conditions.

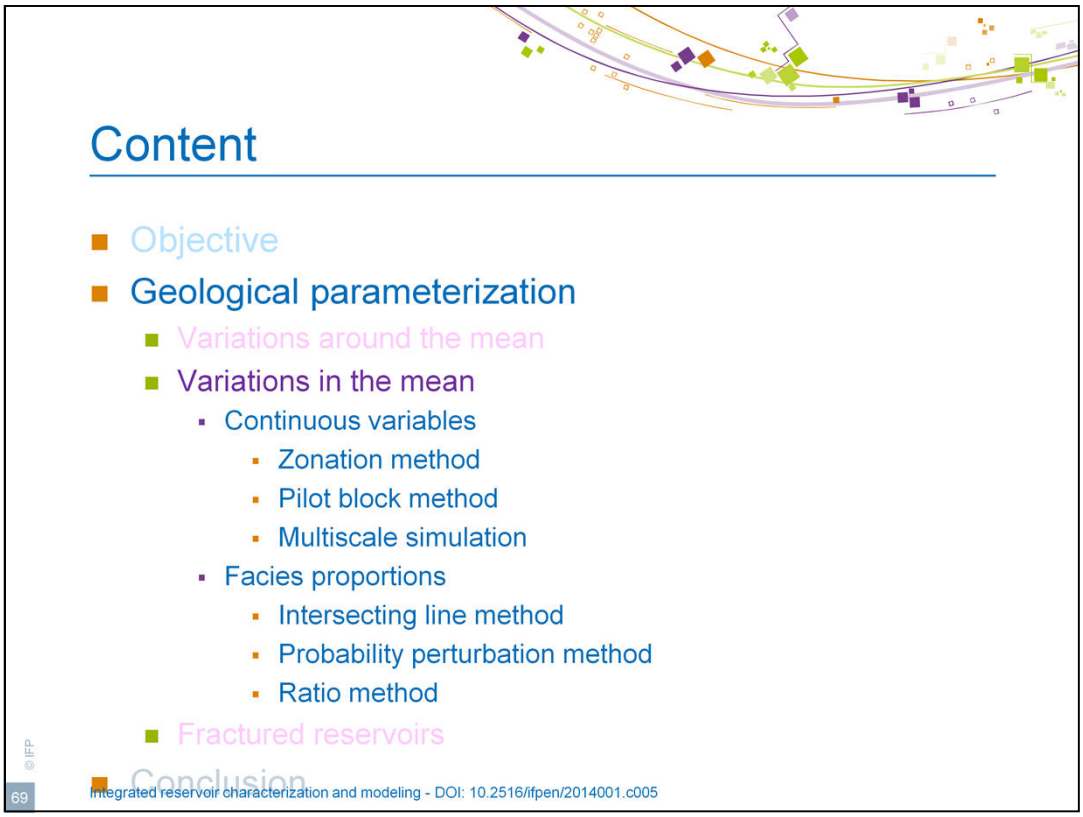

The parameterization techniques previously introduced are applied to vary the spatial distribution of heterogeneities (or the fluctuations around the mean). However, they can be not efficient enough in various cases, especially when significant changes are required in target sub-domains.

In such a case, it may be more appropriate to vary the mean of the target property (*e.g.*, porosity or permeability) over one or several pre-selected sub-domains. Another possible option when dealing with facies realizations consists in adjusting facies proportions.

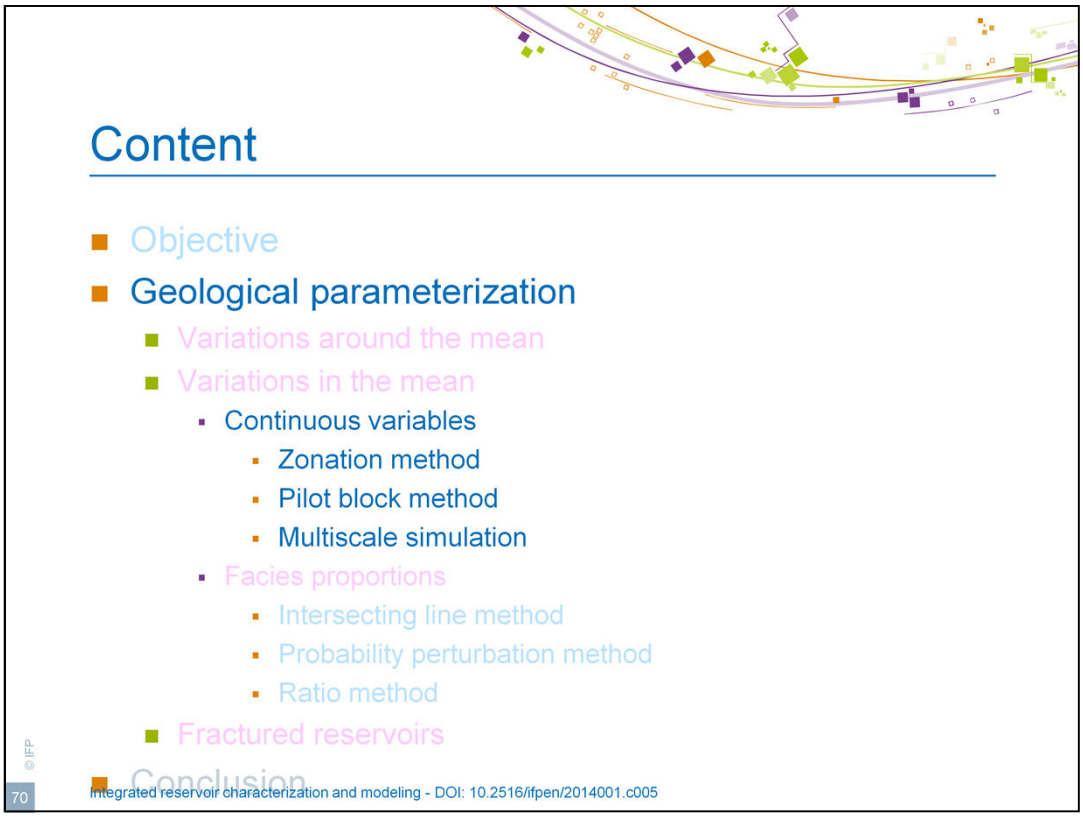

We focus first on a few methods that have been proposed to vary the mean of a given continuous variable over sub-domains.

Zonation method

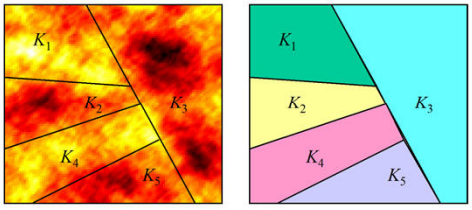

- Definition of sub-domains with constant properties
- These properties = parameters to be adjusted
- Decrease in the number of parameters
- The spatial structure inferred from static data is not accounted for

The zonation method (Stallman, 1956; Jacquard and Jain, 1965) has been traditionally used in history-matching. It consists in grouping grid blocks to create a small number of sub-regions with constant porosity or permeability values. This zonation is performed before history-matching and remains fixed. History-matching is performed in a second step by adjusting the porosity and permeability values assigned to the various zones with the use of multipliers.

The zonation method contributes to decrease the number of parameters (from the number of grid blocks to the number of sub-domains). However, it is not capable of handling the spatial variability model inferred from the static data.

The gradzone method, that permits changes in the zonation along the matching process, was proposed by Bissel (1994) as an improved zonation method.

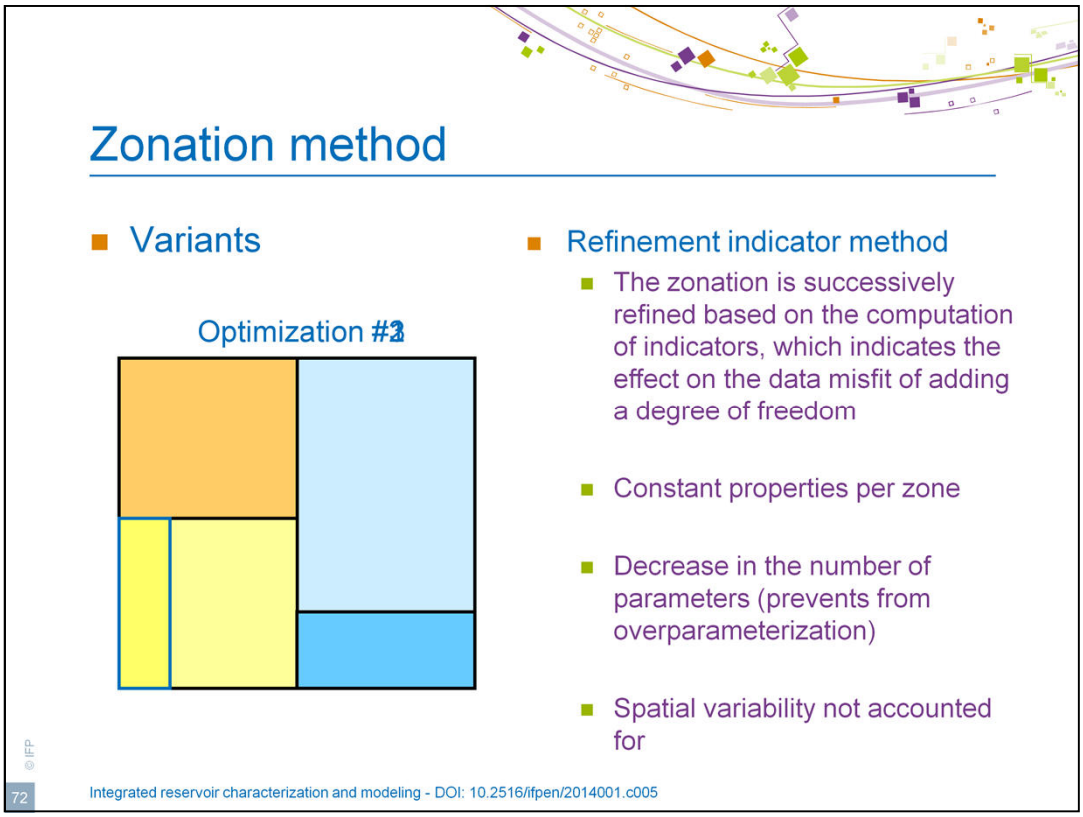

Other methods share some ideas with the zonation method.

The refinement indicator method (Ben Ameur *et al*., 2002; Grimstad *et al*., 2003) provides an adaptive parameterization technique. Following the zonation method, we consider a problem with regions already defined. Constant properties are then assigned to these regions and determined by minimizing the data misfit. Then, the current zonation is refined resulting in smaller sub-domains. This refinement is based upon the computation of refinement indicators, which indicates the effect (at first order) on the data misfit of adding this degree of freedom to the current set of parameters. A new optimization process is run to estimate the constant properties to be attributed to all sub-domains. The procedure is repeated by adding degrees of freedom in an iterative way until a satisfactory match is obtained.

Again, this approach makes it possible to decrease the number of parameters, but does not account for the spatial variability inferred from static data.

It is worth listing the method proposed by Berre *et al*. (2007) who used level-sets to describe the shapes of the sub-domains. This provides even more flexibility, but the pitfall mentioned above (no preservation of the spatial structure) is kept.

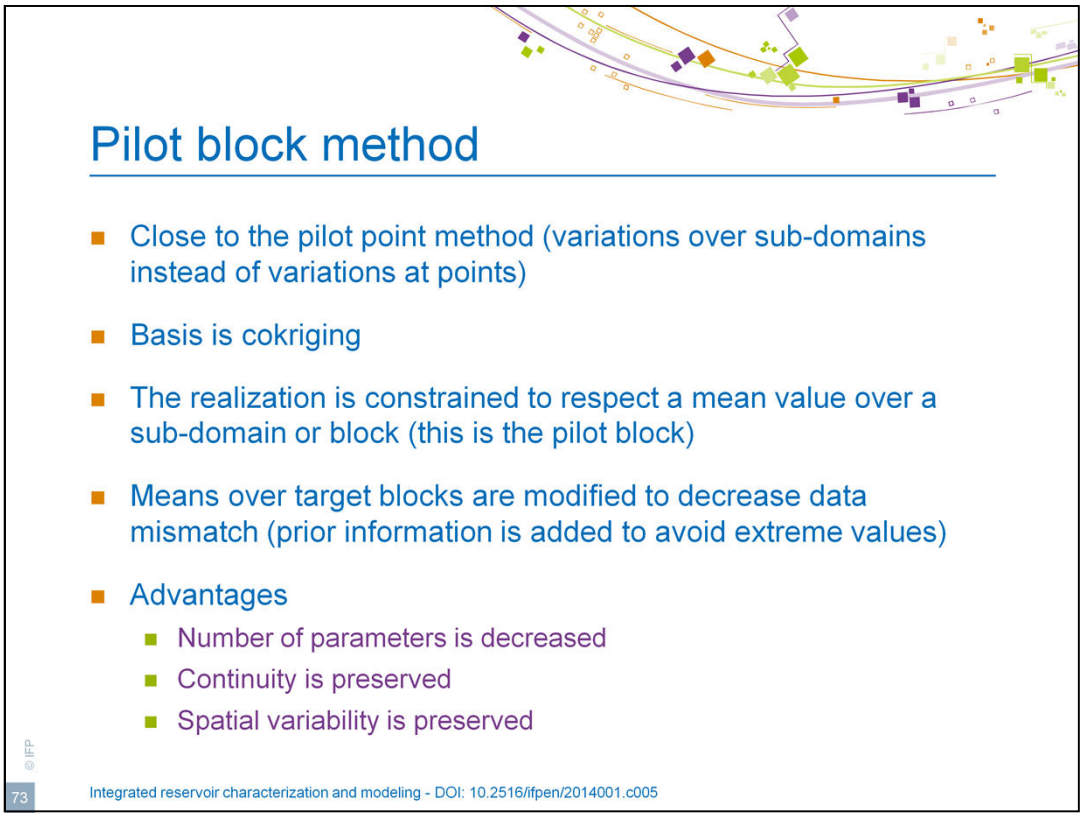

In order to answer the need for preserving spatial variability and continuity between the modified sub-domains and the surrounding areas, Le Ravalec-Dupin (2010) developed a geostatistics-based approach rooted in the pilot point method. As already explained, the pilot point method provides the ability to vary the property under consideration at points in order to minimize the data mismatch. Besides, the pilot block method makes it possible to vary the mean of the property over one or several pre-selected sub-domains. The pilot point method refers to kriging to constrain the realizations to the pilot point values. Likewise, the pilot block method refers to cokriging to constrain the realizations to pilot block means. In this case, the mean (which is arithmetic) is considered as secondary information.

When this parameterization is incorporated into a matching process, it provides the ability to vary the means over the selected blocks in order to decrease the data mismatch. Just as the pilot points, the pilot blocks could be attributed extreme values. This is avoided by adding prior information into the objective function.

The advantages of the pilot block method are the decrease in the number of parameters, and the preservation of both continuity and spatial variability.

A similar approach was presented by Fenwick *et al*. (2005). These authors combined the locally varying mean (LVM) method with the probability perturbation method (PPM). The LVM allows for varying large-scale structures while the PPM perturbs the small-scale variations.

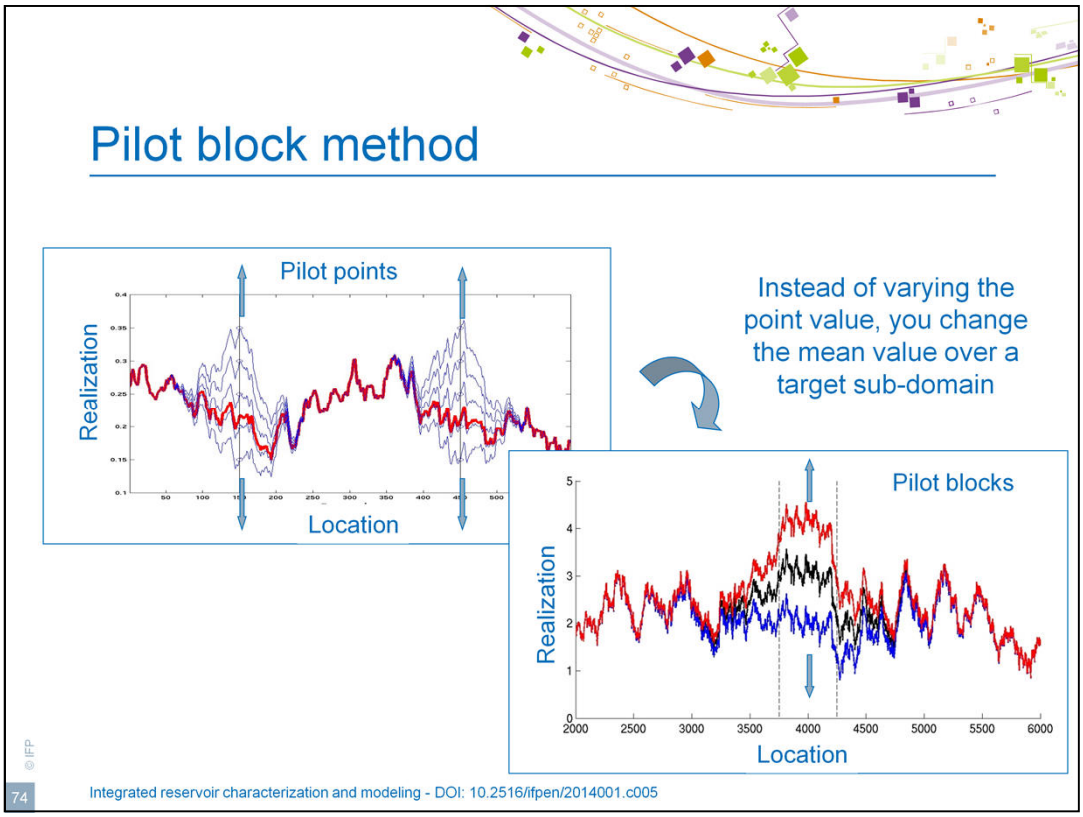

This example presents a one-dimensional realization constrained to a mean value of 2 (blue), 3 (black) and 4 (red) over the block centered at location 4,000 m. The size of the block is 500 m, and the range of the variogram is 1,000 m. Varying the mean strongly impacts the realization. Changes are observed inside the target area, but also around in a transition zone whose size is about the range.

Two features must be pointed out: first, the continuity between the modified zone and the surrounding one; second, the preservation of spatial variability.

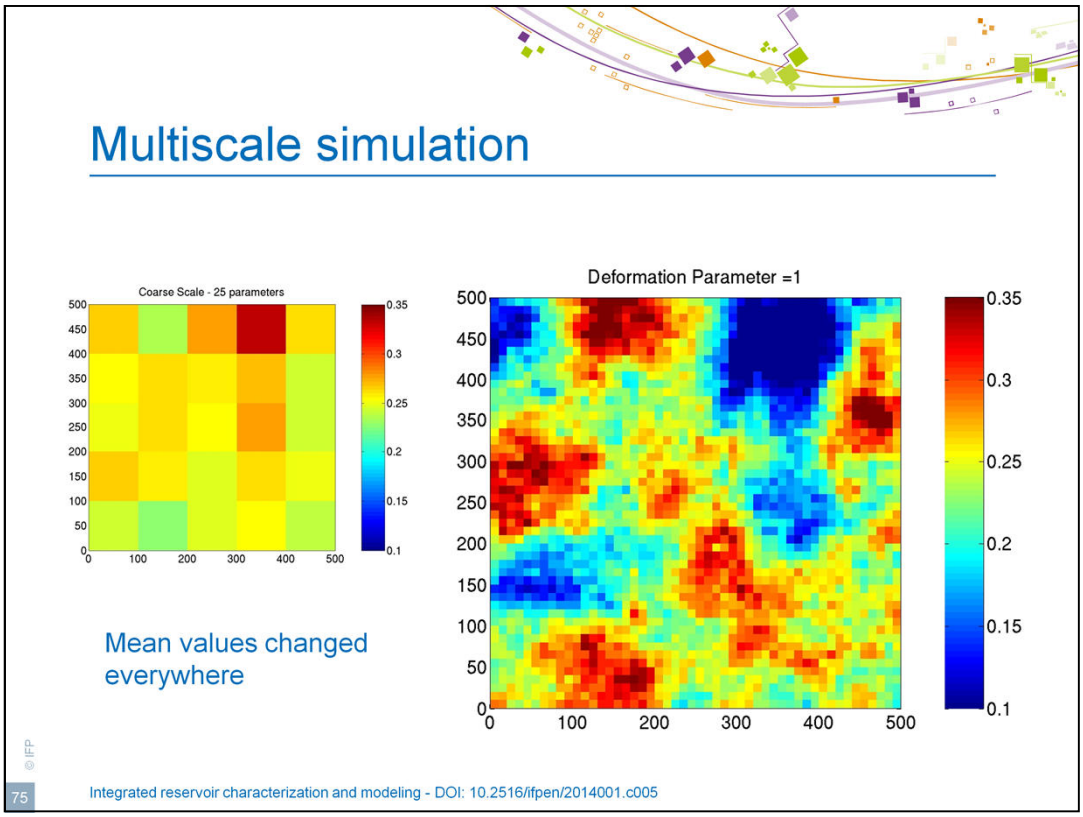

Another emerging approach refers to multiscale simulation (Gardet *et al*., 2014). In this case, a realization is first simulated at the coarse scale. Then, the realization at the fine scale is simulated conditionally to the one already simulated at the coarse scale. The realization at the coarse scale controls the mean variations of the target property. The scheme can be obviously extended to more than two scales.

This multiscale simulation procedure can cope with the geostatistics-based parameterization previously introduced (pilot point method, gradual deformation method, probability perturbation method). The perturbation or deformation can be applied either at the coarse scale, the fine one or both. When applied at the coarse scale, the resulting changes are propagated to the fine scale realization.

An example is displayed above. The realization generated at the coarse scale is shown on the left. The one generated at the fine scale given the realization at the coarse scale is shown on the right. Then, the gradual deformation method is used to vary the deformation at the coarse scale. As expected, this impacts the fine scale realization (figure on the right). We observe strong variations in the coarse trend.

As already pointed out, such an approach makes it possible to significantly vary the property of interest when required. In addition, it induces a strong decrease in the number of uncertain parameters. The number of parameters actually depends on the scale considered. The coarser the scale, the less the grid blocks, hence the less the unknown values. This makes parameterization more adaptive.

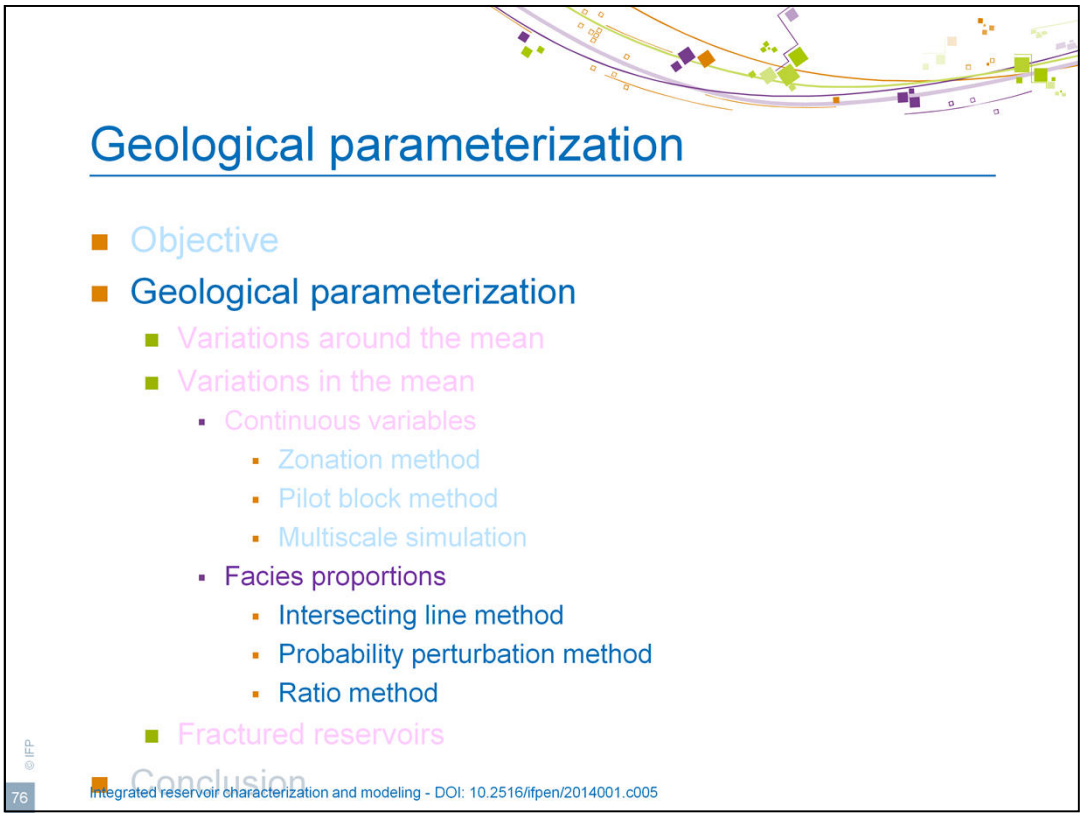

The case of facies realizations is a bit different. Practice has shown that facies proportions strongly control the simulated facies realizations. In addition, there is often a large range of uncertainty about the local proportions of facies due to limited information. This is particularly true when the number of wells is small and facies objects are smaller than seismic resolution.

It is thus essential to investigate the possibility to locally adjust facies proportions when performing history-matching. A few methods have been proposed over the last years to address this issue. A starting point is that facies proportions are equivalent to the probability of occurrence of facies.

We briefly describe three of the proposed methods in the following section. The first one, which is based upon intersecting lines, is appropriate when using the pluriGaussian simulation method. It can be used to adjust facies proportions over sub-domains provided facies proportions are constant per sub-domain. The second approach is more general, but remains closely related to the probability perturbation method whose basics were recapped in the previous section. The last one is very pragmatic, simple, and flexible. It permits to handle facies proportions in very different cases.

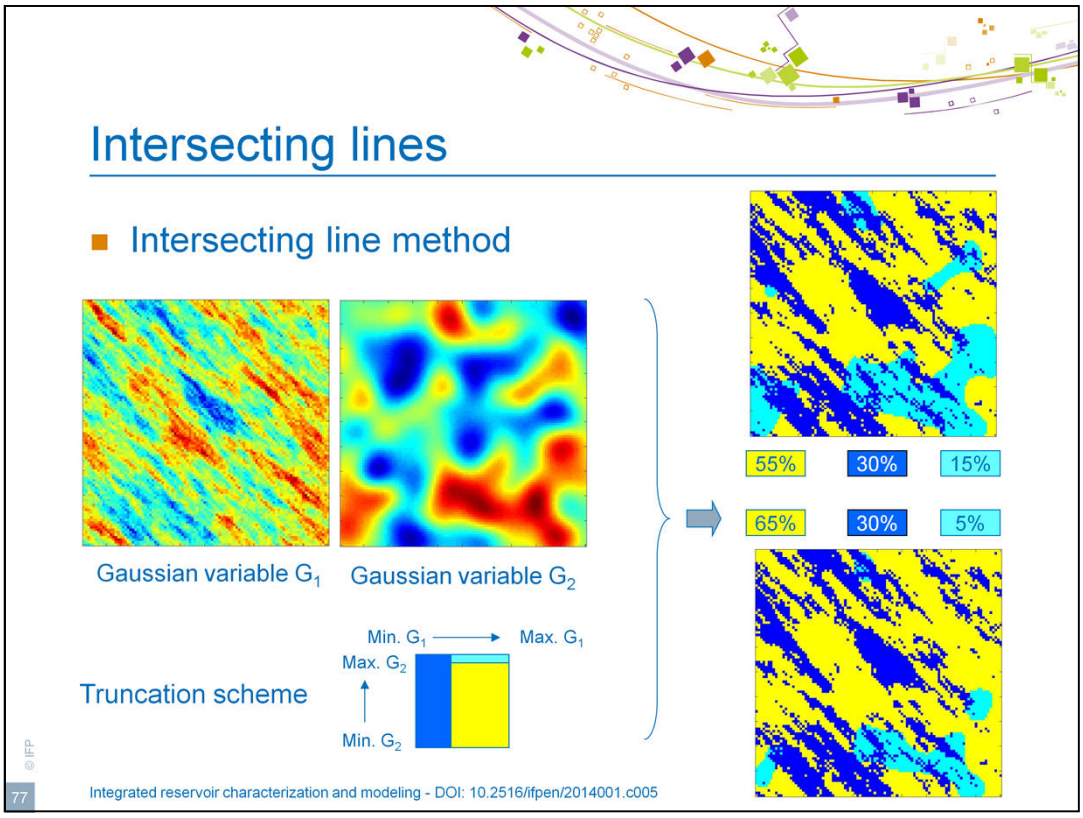

The intersecting line method was proposed by Liu and Oliver (2004) to vary facies proportions within the framework of history-matching. It strongly depends on the simulation technique used to produce the facies realizations, that is the pluriGaussian method (see Chapter 2, p. 71).

In a few words, the pluriGaussian method consists in truncating two continuous Gaussian realizations to obtain a facies realization. The proportions of facies and the contacts between facies are driven by a two-dimensional truncation scheme, the two dimensions being associated to the two Gaussian realizations. Usually, the truncation scheme is defined from rectangles. Each rectangle is associated to a given facies. As facies proportions are related to the surfaces of the rectangles, an increase in the surface induces an increase in the proportion.

In the example presented above, the proportion of the light blue facies are decreased from 15 to 5 % while that of the yellow facies increases from 55 to 65 %. The truncation scheme and the proportion of the dark blue facies being fixed for once, the spatial distribution of this facies on the final realizations is unchanged. The only visible features are a reduction in the size of the light blue facies heterogeneities, which is compensated by the yellow facies.

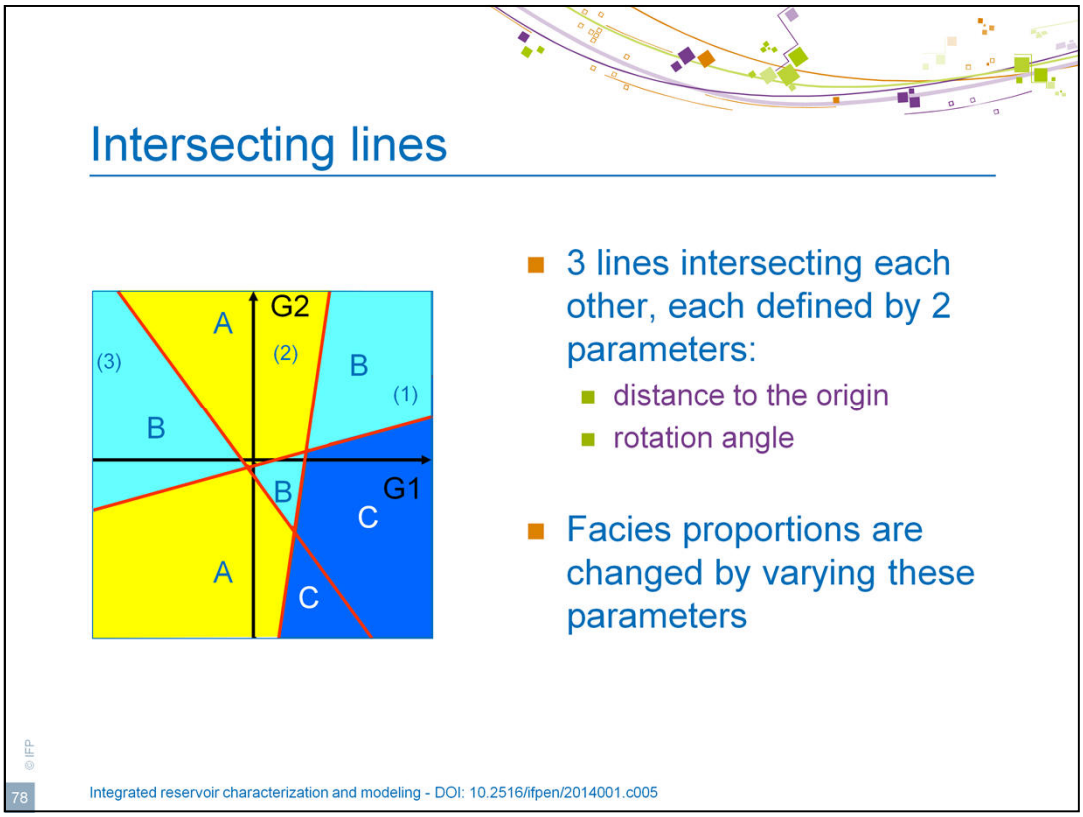

Liu and Oliver (2004) suggested to build the truncation scheme from 3 lines intersecting each other instead of considering rectangles. The locations of the lines are defined from coefficient r and angle θ. r is the distance of the thresholding line to the origin and θ is a rotation angle. There are 2 parameters per line. By varying these parameters, Liu and Oliver (2004) showed that they can adjust facies proportions to match the production data.

On the example shown above, line (1) only is moved. This induces an increase in facies B proportion and a decrease in facies A proportion. That of facies C is unchanged.

This approach can be envisioned as far as facies proportions are stationary over the region where they are optimized. The extension to non stationary proportions is not straightforward. In such a case, the truncation scheme depends on grid blocks meaning that there would be too many parameters to handle.

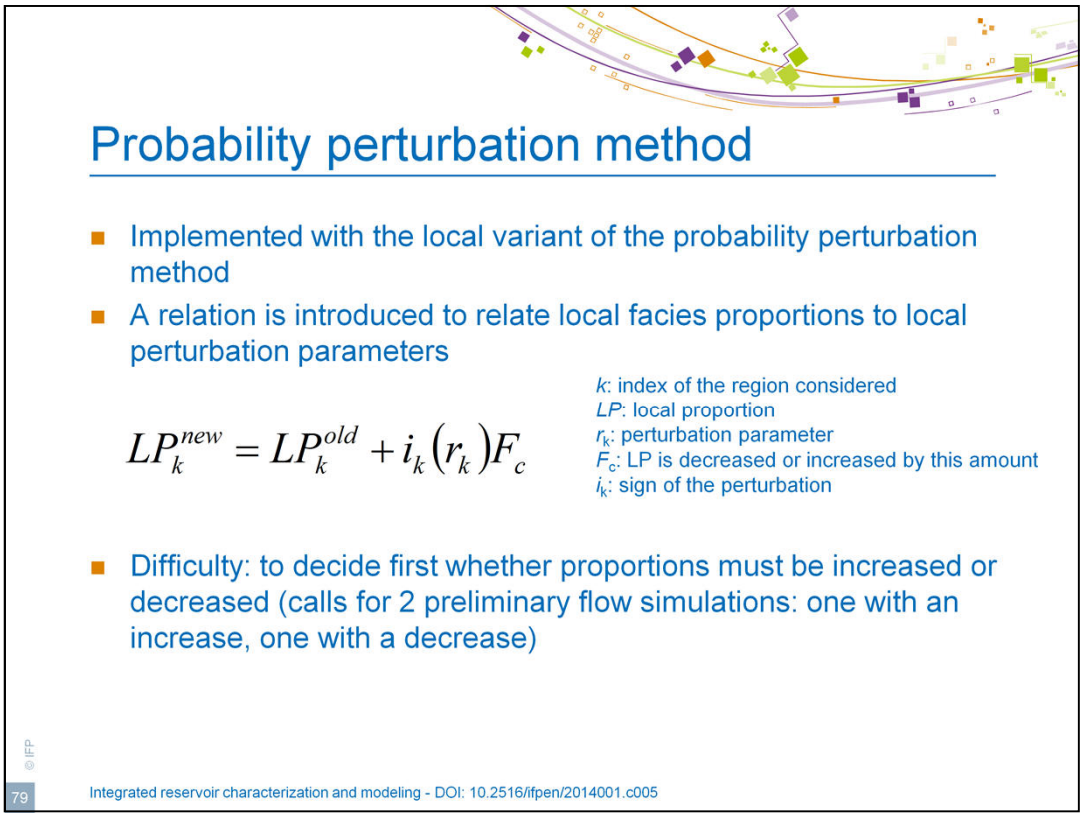

Another possibility to vary facies proportions over given regions was suggested by Hoffman and Caers (2007). This method was implemented within the local variant of the probability perturbation method. It involves a new relation to couple local facies proportions to local perturbation parameters.

A difficulty is that it has to be decided first whether proportions must be increased or decreased. To make a choice, Hoffman and Caers (2007) perform two flow simulations: one with an increase and another with a decrease in facies proportions over all regions. Then, the sign of the perturbation is decided depending on the simulation that decreases the production data mismatch.

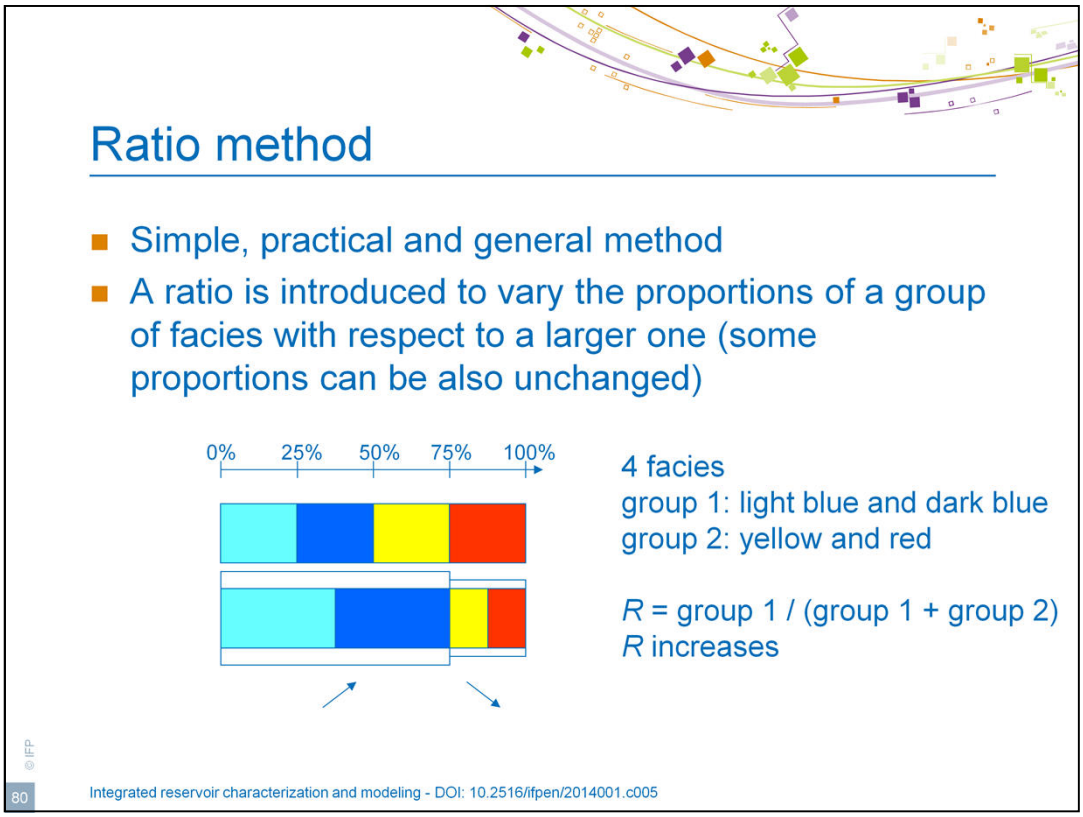

A simple and practical alternative was devised by Ponsot-Jacquin *et al*. (2009). It depends on the ratio of the proportions of a group of facies to the proportions of a larger group of facies, this larger group including the first one.

Distinct ratios can be assigned to distinct regions. They become parameters. When incorporated into history-matching, they can be adjusted to minimize this data mismatch.

To illustrate the method, we consider a case with 4 facies (light blue, dark blue, yellow and red) with initial proportions all equal to 25%. We define the proportion ratio as the ratio of the proportions of the 2 blue facies to the proportions of the 4 facies. As a result, an increase in this ratio leads to an increase of the blue facies to the detriment of the yellow and red facies.

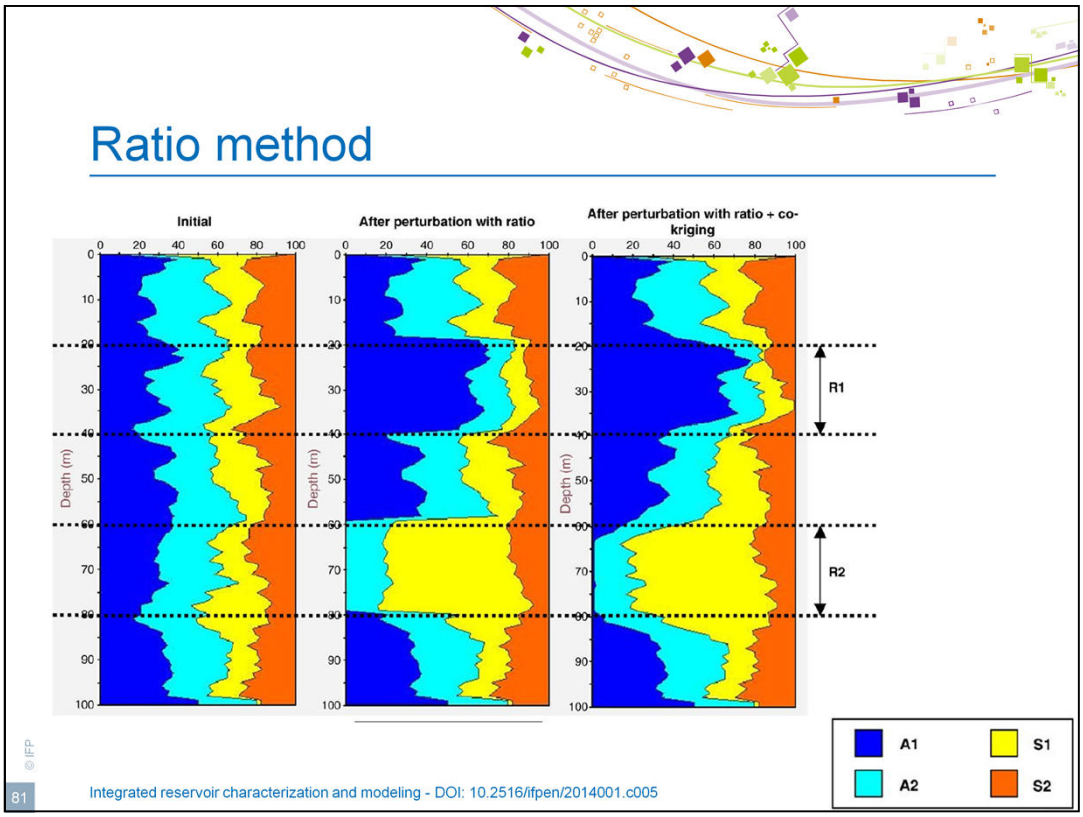

We apply the ratio method to modify the vertical proportion curves (see Chapter 3, p. 29) in two regions, R1 and R2. The vertical proportion curves provide facies proportions against depth. The curves on the left are the initial vertical proportion curves. There are 4 facies: two shales denoted A1 (dark blue) and A2 (light blue), and two sands denoted S1 (yellow) and S2 (orange).

We apply the ratio method to perform the following changes.

In region R1, the ratio of shale is set to 80% and the ratio of shale A1 to shale A2 to 80%.

In region R2, the ratio of sands is set to 80%, the ratio of shale A1 to shale A2 to 0%, and the ratio of sand S1 to sand S2 to 80%.

The resulting vertical proportion curves are displayed in the middle. They satisfy the required variations. However, this method can generate discontinuities at the boundaries of the modified regions.

A variant inspired by the pilot block method was proposed by Tillier *et al*. (2010) who combined the ratio method with cokriging to remove the undesired discontinuities. The resulting variations for the example studied are shown on the right.

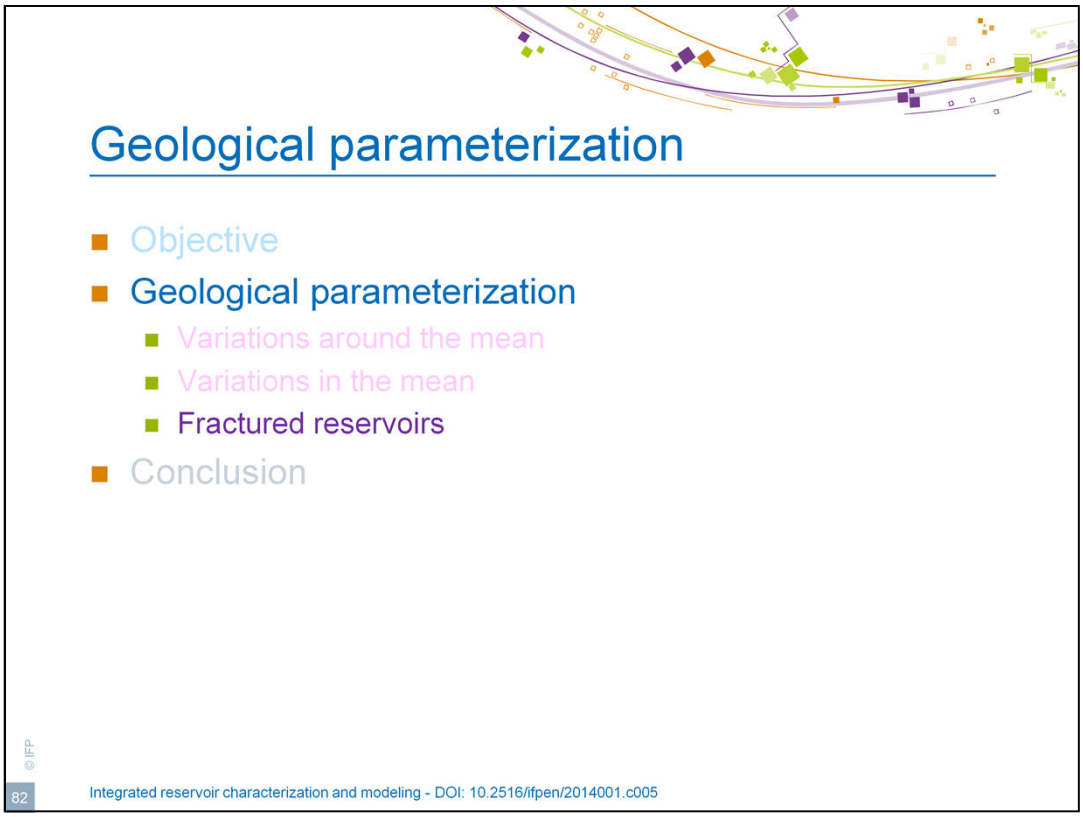

We now move to a slightly different issue, the variations in the spatial distribution of fractures. In this case, fractures are modeled as objects (Chapter 2, p. 82).

The presence of faults seriously affects fluid flows. Conductive faults contribute to create preferential flow paths to the wells and accelerate water breakthrough. On the other hand, sealing faults generate compartmentalization problems. A difficulty is that many faults are not detected because they are below seismic resolution. These undetectable faults are called sub-seismic faults.

Again, the integration of production data helps better describe the network of fractures, especially of sub-seismic faults, provided suitable parameterization techniques are available. The traditional approach consists in varying the parameters characterizing a fault (position, orientation, length) without accounting for the others. When doing so, the number of parameters is very important as faults are individually handled. In addition, such techniques can lead to geologically inconsistent models that cannot be used for predictions.

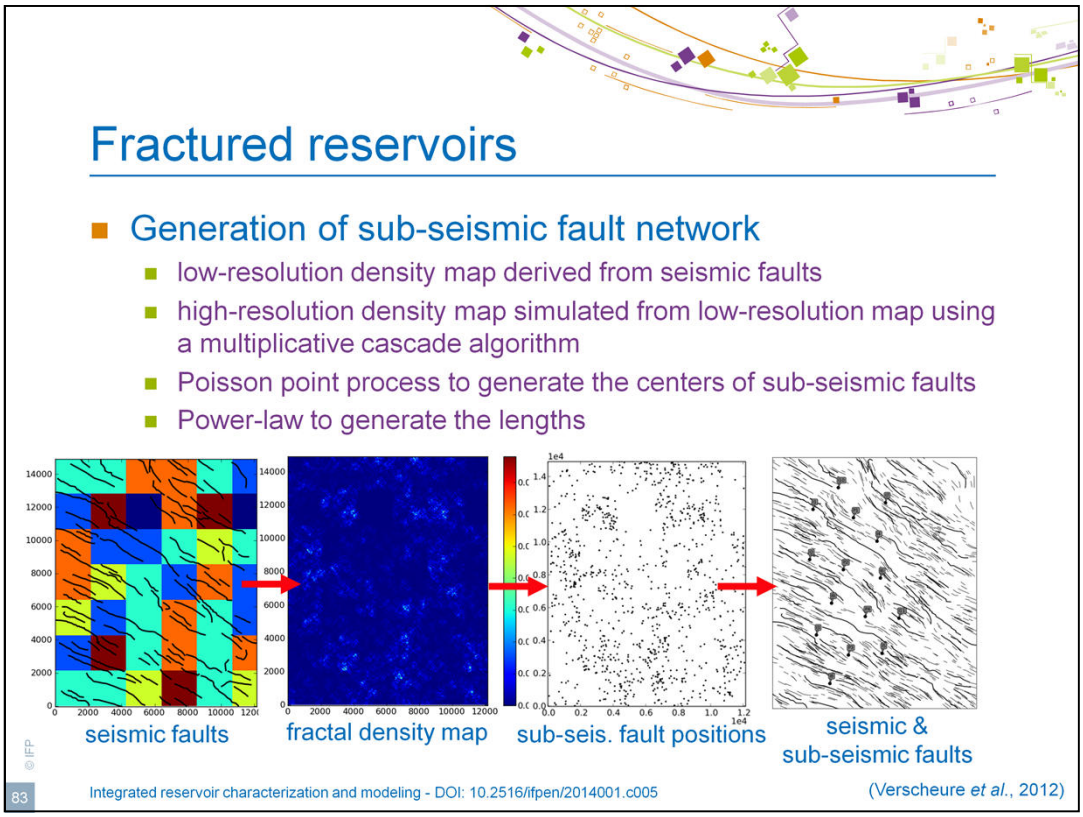

A first method was developed by Hu and Jenni (2005). However, the integration of dynamic data turned out to be difficult within this framework.

This method was then revisited by Verscheure *et al*. (2012). These authors proposed a quite different procedure. First, they derive an initial low-resolution density map from the seismic fault network. The organization of the sub-seismic faults is assumed to be the same as that of the seismic faults. Second, a multiplicative cascade algorithm is used to convert the low-resolution density map into a high-resolution density map. The algorithm generates a scaling structure by recursively replicating a given pattern at different scales. The resulting map is eventually used to draw the population of the centers of the sub-seismic faults following a Poisson point process. Last, fault lineaments are produced from a power-law distribution.

Fractured reservoirs

- Deformation of the spatial distribution of sub-seismic fault centers
  - located at points given by a Poisson point process
  - points are generated sequentially
  - the gradual deformation method is used to vary the coordinates of these points

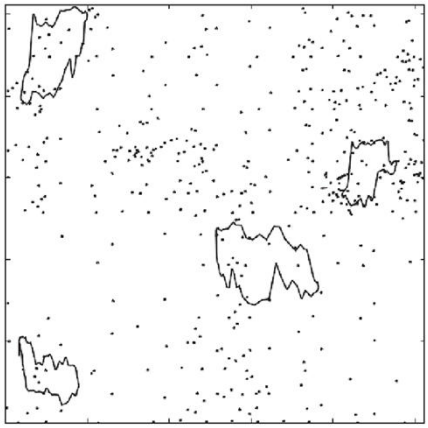

Integrated reservoir characterization and modeling - DOI: 10.2516/ifpen/2014001.c005

(Verscheure *et al.*, 2012)

The centers of the sub-seismic faults are associated to a Poisson point process. Thus, a set of points is first generated and the gradual deformation method (see previous sub-sections) is applied to modify the coordinates of these points.

The figure on the right shows the possible trajectories of sub-seismic faults when varying continuously the deformation parameter. A single parameter can be used to perturb the location of one, several or all sub-seismic faults.

This facility is very useful when integrated into history-matching procedures. The problem boils down to the determination of the deformation parameters that minimize the objective function.

The advantages of this method are twofold: the number of parameters is drastically reduced and the geological consistency of the network of sub-seismic faults is maintained.

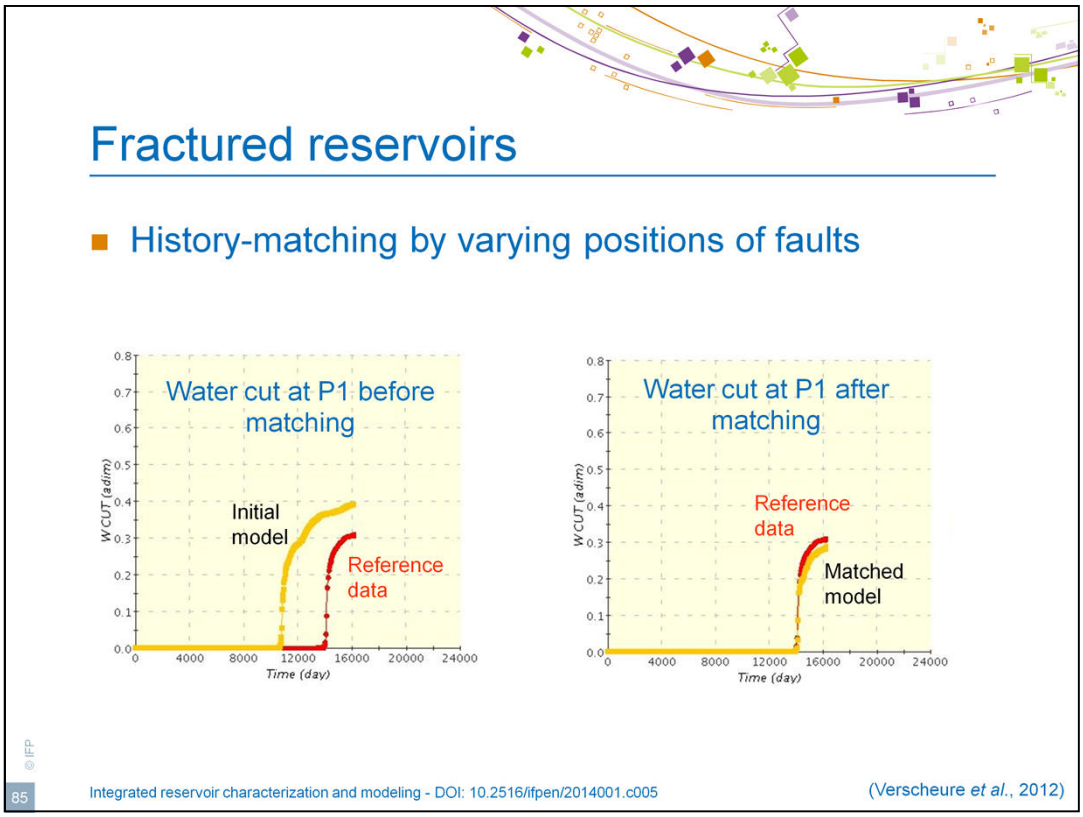

The methodology presented above was applied to match water cuts at several wells by varying fault positions. The results are shown above for well P1. Compared to data, the water breakthrough occurs too early for the initial model. This is improved for the matched model.

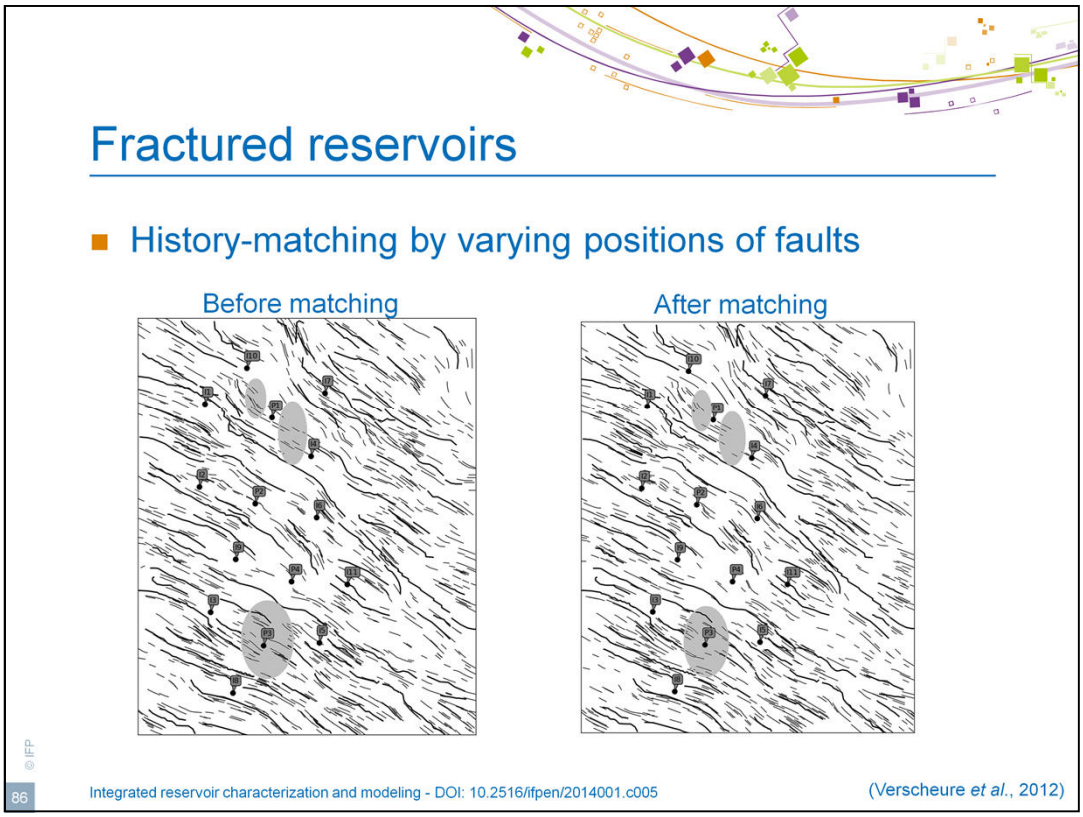

The initial network of sub-seismic fault is displayed on the left and the final one determined from the minimization of the data mismatch on the right. If focusing on well P1, we note that the number of faults has been decreased, which contributes to delay the water breakthrough as desired.

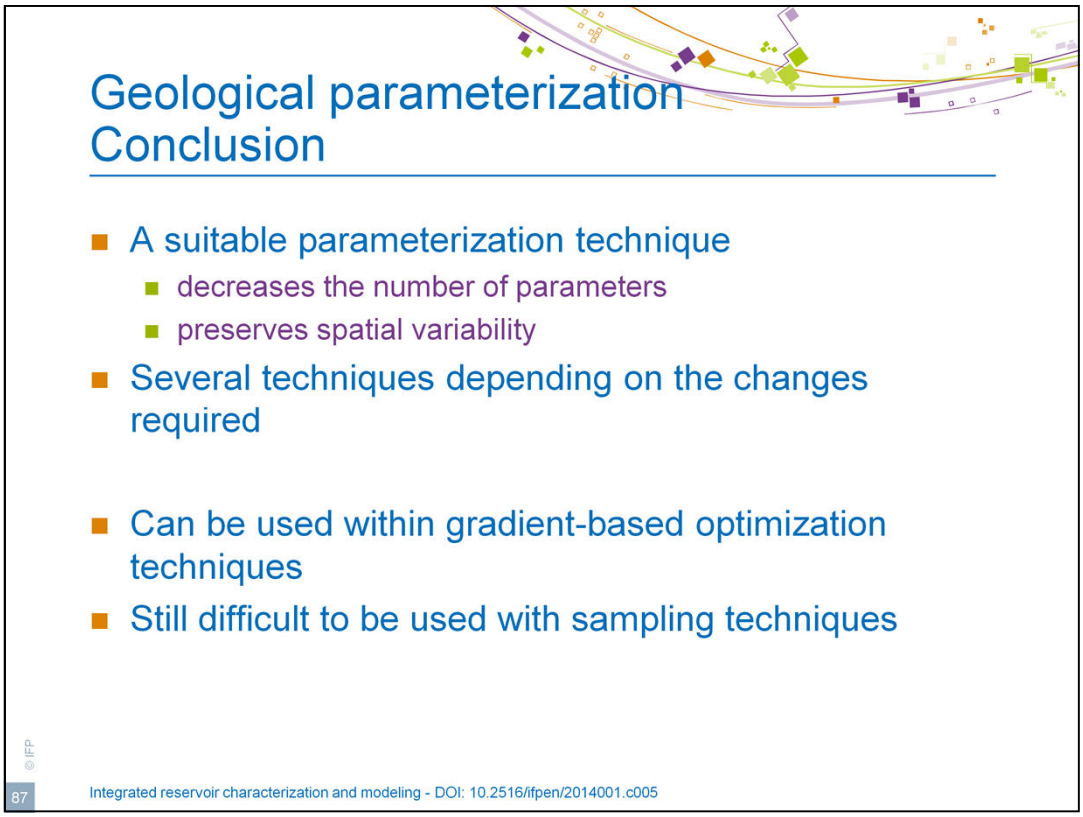

As a conclusion, a suitable parameterization technique when dealing with petrophysical properties has to check at least two features. It must reduce the number of parameters (from millions to dozens) and it must preserve the spatial variability of the property under consideration.

Several techniques have been described in the literature to answer the problem. The one to be selected depends on the problem to be solved. It can even be better to apply two distinct parameterization techniques, simultaneously or not.